# ANALYSIS AND DESIGN OF HELICOPTER ROTOR BLADES FOR REDUCED VIBRATIONAL LEVEL

A THESIS SUBMITTED TO
THE GRADUATE SCHOOL OF NATURAL AND APPLIED SCIENCE
OF
MIDDLE EAST TECHNICAL UNIVERSITY

BY

AYKUT TAMER

IN PARTIAL FULFILLMENT OF THE REQUIREMENTS
FOR
THE DEGREE OF MASTER OF SCIENCE
IN
AEROSPACE ENGINEERING

SEPTEMBER 2011

Approval of the thesis:

**ANALYSIS AND DESIGN OF HELICOPTER ROTOR BLADES FOR REDUCED VIBRATIONAL LEVEL**

submitted by **AYKUT TAMER** in partial fulfillment of the requirements for the degree of **Master of Science in Aerospace Engineering Department, Middle East Technical University** by,

Prof. Dr. Canan Özgen _____
Dean, Graduate School of **Natural and Applied Sciences**

Prof. Dr. Ozan Tekinalp _____
Head of Department, **Aerospace Engineering**

Prof. Dr. Yavuz Yaman _____
Supervisor, **Aerospace Engineering Dept., METU**

**Examining Committee Members:**

Prof. Dr. Serkan Özgen _____
Aerospace Engineering Dept., METU

Prof. Dr. Yavuz Yaman _____
Aerospace Engineering Dept., METU

Asst. Prof. Dr.Melin Şahin _____
Aerospace Engineering Dept., METU

Asst. Prof. Dr. Ercan Gürses _____
Aerospace Engineering Dept., METU

Yüksel Ortakaya, MSc. _____
Turkish Aerospace Industries, TAI

**Date:** 09.09.2009

I hereby declare that all information in this document has been obtained and presented in accordance with academic rules and ethical conduct. I also declare that, as required by these rules and conduct, I have fully cited and referenced all material and results that are not original to this work.

Name, Last Name : Aykut TAMER

Signature :

# ABSTRACT


ANALYSIS AND DESIGN OF HELICOPTER ROTOR BLADES FOR REDUCED VIBRATIONAL LEVEL

Tamer, Aykut

M.S., Department of Aerospace Engineering

Supervisor: Prof. Dr. Yavuz Yaman

September 2011, 103 pages

In this thesis analysis and design of helicopter rotor blades were discussed for reduced vibrational level. For this purpose an optimization procedure was developed which involves coupling of the comprehensive rotorcraft analysis tool CAMRAD JA and the gradient based optimization algorithm. The main goal was to achieve favorable blade structural dynamics characteristics that would lead to reduction in vibrational level. For this purpose blade stiffness and mass distributions were considered as the design variables. In order to avoid likely occurrences of unrealistic results, the analyses were subjected to constraints which were sensitive to the design variables. The optimization procedure was applied on two isolated rotor blades and a full helicopter with main rotor, tail rotor and fuselage by using natural frequency separation and hub load minimization respectively. While the former approach relied on the blade natural frequencies, the latter approach involved higher harmonic aerodynamic and blade motion calculations. For both approaches, the improvement in vibration characteristics and blade mass and stiffness distributions of the initial design and the design after optimization analyses were compared and discussed.



Keywords: Rotor Blade Optimization, Rotorcraft Structural Dynamics and Aeroelasticity

# ÖZ

## HELİKOPTER ROTOR PALALARININ AZALTILMIŞ TİTREŞİM DÜZEYİ İÇİN ANALİZİ VE TASARIMI

Tamer, Aykut

Yüksek Lisans, Havacilik ve Uzay Mühendisliği Bölümü

Tez Yöneticisi: Prof. Dr. Yavuz Yaman

Eylül 2011, 103 sayfa

Bu tezde, helikopter palalarının analiz ve tasarımı azaltılmış titreşim seviyesi için incelenmiştir. Bu amaçla kapsamlı bir döner kanatlı platform çözücüsü olan CAMRAD JA ile gradyan hesaplaması tabanlı bir eniyileme algoritması olan CONMIN'i eşgüdümlü çalıştıracak bir prosedür geliştirilmiştir. Bu prosedürde amaç palaların yapısal karakteristiklerini iyileştirerek titreşim seviyesini azaltmaktır. Bu amaçla palanın kütle ve sertlik dağılımları tasarım değişkenleri olarak seçilmiştir. Uygulaması muhtemel olmayan tasarımları önlemek için eniyileme analizleri sınırlandırılmıştır. Eniyileme prosedürü izole rotor ile birlikte ana rotor, gövde ve kuyruk rotorunu da içeren bütün bir helikopter konfigürasyonuna uygulanmıştır. İzole rotor için palanın vakum durumundaki doğal frekansları tahrik frekanslarından ayrıştırma yaklaşımı, bütün helikopter içinse rotor göbeğindeki aerodinamik ve pala tepkisi kaynaklı titreşim yüklerinin minimize edilmesi yaklaşımı kullanılmıştır. Her iki yaklaşım için titreşim karakteristiğindeki iyileşme ve palaların kütle ve katılık dağılımları karşılaştırılmış ve sonuçlar tartışılmıştır.

Anahtar Kelimeler: Rotor Palası Eniyilemesi, Döner-Kanatlı Araçların Yapısal Dinamiği ve Aeroelastisitesi

Dedicated to my family

# ACKNOWLEDGEMENTS

I would like to thank my supervisor Prof. Dr. Yavuz Yaman for his guidance, support, encouragement and patience throughout the study. The comments of the examining committee members are also greatly acknowledged.

I also would like to thank Turkish Aerospace Ind. for the support and esspecially to Mr. Yüksel Ortakaya, Chief of the Aeromechanics Department in TAI for his technical support, understanding and tolerance.

I specially would like to thank to Ahmet Alper Ezertaş for his helpful comments, Ceren Öztürk for the support in analysis models and also to my TAI colleagues Erdem Ayan, Hakan Aydoğan, Özge Polat, Arda Yücekayalı, Özge Kapulu, Eda Toprakkale, Öznur Yemenici and Taylan Çakıroğlu for their moral support.

Special thanks to Ahmet Usta, for the talks we have made with his delicious tea.

And my friends, Enes, Muris, Mustafa, Akif, Kamil. This is certainly not enough but thanks for supporting me all the time and all the things we have shared.

# TABLE OF CONTENTS

# LIST OF TABLES

TABLES

# LIST OF FIGURES

FIGURES

# LIST OF SYMBOLS

| | |
|---|---|
| AI | : auto-rotational inertia index |
| $EI_F$ | : blade cross section flapwise bending stiffness |
| $EI_C$ | : blade cross section chordwise bending stiffness |
| GJ | : blade cross section torsional stiffness |
| H | : longitudinal hub force |
| $I_b$ | : blade mass moment of inertia with respect to hub |
| $M_{bF}$ | : blade root flapwise bending moment |
| $M_{bI}$ | : blade root in-plane bending moment |
| $M_T$ | : blade root twisting moment |
| $M_X$ | : hub rolling moment |
| $M_Y$ | : hub pitching moment |
| $M_Z$ | : hub yawing moment |
| N | : number of blades |
| R | : blade radius |
| $S_X$ | : blade root radial tension force |
| $S_Y$ | : blade root in-plane shear |
| $S_Z$ | : blade root vertical shear |
| T | : vertical hub force |
| $V_\infty$ | : forward flight speed |
| W | : helicopter gross weight |
| (X,Y,Z) | : hub reference axes |
| Y | : lateral hub force |
| | |
| c | : blade chord length |
| $f_i$ | : $i^{th}$ natural frequency |
| h | : blade box-beam height |
| k | : integer for vibratory hub loads |
| m | : blade cross section mass per unit length |

$m_{NS}$ : blade non-structural mass

n : blade harmonic number

n/rev : excitation frequency at $n^{th}$ harmonic

r : blade radial location

t : blade box beam thickness also time in hub loads equations

w : blade box-beam width

(x,y,z) : blade reference axes

Greek Letters

$\mu$ : advance ratio

$\Omega$ : rotor RPM

$\Omega_0$ : nominal rotor RPM

$\Psi$ : rotor disc azimuth angle

Variables which are used for certain chapters are clearly defined wherever applicable.

# CHAPTER 1

# INTRODUCTION

## 1.1 Rotary Wing vs. Fixed Wing

The powered flight is composed of three main functions of lift, propulsion and control. Powered aerial vehicles are classified into fixed wing and rotary wing categories according to the way of achieving these functions. The first concept of a powered aircraft was the fixed wing which achieves three main functions with independent subsystems. The lifting force is generated by the wings, propulsion from engines overcomes drag and control surfaces adjust the attitude of the aircraft. On the other hand, helicopters or generally rotorcraft, use rotating wings to provide lift, propulsion and control [1]. The rotor is the responsible component for the main functions and composed of rotating wings which are named as blades.

In a fixed wing aircraft the airspeed experienced by the wings is exactly the same speed that aircraft flies with. A difference in airspeed between wings is only possible in some maneuvers and gust conditions which are usually insignificant. The lift generation depends on the square of the airspeed faced by wings, and then at low airspeeds the lift force is not enough to overcome gravity. Aircraft speed must be increased by the propulsive force until a satisfactory airflow is reached over airfoils. Therefore main disadvantage of separated functions of the fixed wing aircraft is that they require a runway depending on their take-off weight in order to accelerate to the required airspeed over wings so that the necessary amount of lift can be generated. Same problem also arises in landing such that in order to maintain the lifting force equal to the aircraft weight, fixed wing aircrafts approach to the ground with a flight speed and could only be slowed down after the landing gears touch down so that the airplane weight is carried by the reactive forces on the landing gears.

Although lift generation with fixed wings is very efficient and fixed wing aircrafts serve in many purposes from transportation to fighting, they cannot manage certain missions including vertical take-off and landing, backward flight, low speed flight and flight within urban areas. This problem restricts the mission capability of the fixed wing aircrafts if there is no suitable runway. Examples to such missions can be given as, rescue from sea or delivery of troops to a mountain [2]. Therefore the solution is to perform such missions by generating lift at stationary conditions or at low flight speeds. The most practical solution of this problem is to rotate the wings so that depending on the angular speed and length of the rotating wings, the aerodynamic surfaces face an airspeed distribution which generates lift without any need to the forward flight speed. That solution provides a great maneuvering capacity to the helicopters at zero, negative and low flight speeds. In addition to its lift function, rotor is also used for propulsion and control. It is possible to fly forward by tilting the rotor disc such that a component of rotor thrust supplies enough propulsive force to overcome the drag force. In the same manner, rotor disc tilt can provide moments around the helicopter center of gravity so that the lateral and backward motions and other maneuvers such as pull-out and roll-over can be performed. As being the main source of flight, the understanding of the rotor and its operational environment which will be discussed in Section 1.2 is essential in understanding the dynamic and vibratory behavior of the helicopters.

## 1.2 The Rotor and its Operational Environment

As previously mentioned, rotor is the main source of lift, propulsion and control in helicopters. The rotor blades rotate at high speeds in a complex unsteady aerodynamic environment and the interaction of blades with this aerodynamic environment is the main source of vibration [2]. Before going into the details of the vibration problem, the rotor with its main components should be discussed so that the reasons of vibration and its solution can be clearly understood.

The major characteristic of a helicopter is its vertical flight capacity which defines the size of the rotor. It is always observed that the blades of the helicopters are long slender structures and most of the time rotor diameter is comparable to the fuselage length. Because of its size, the rotor is the most dominant component of the helicopter in all aspects including

aerodynamics, dynamics, structural dynamics, strength, stability, cost and maintenance of the whole aircraft. The reason of large diameter comes from the disc loading which is the ratio of the thrust to the rotor disc area. For a rotary wing aircraft, in order to overcome gravity forces, the rotor thrust is obtained by accelerating the air downwards which causes induced power loss. This is the cost of vertical flight capacity and proportional to the square root of the rotor disc loading. Therefore increasing rotor diameter reduces disc loading for a given gross weight and induced power loss reduces which in turn increases vertical flight capacity. There are also other structures with rotating wings like airplane propellers but since they operate in high speed axial flow and at a lower thrust level as compared to body weight, their effects are local and their size is very small as compared to that of the helicopter rotor [1].

The outer part of the rotor is composed of the aerodynamic surfaces which are called rotor blades. On any aircraft, whether it is fixed wing or rotary wing, aerodynamic surfaces generate the forces and moments to overcome the resisting force and moments. For the helicopter flight, the necessary forces and moments are sustained by rotating blades which are slender and elastic structures. Figure 1 represents a simplified geometry of blade planform and cross section.

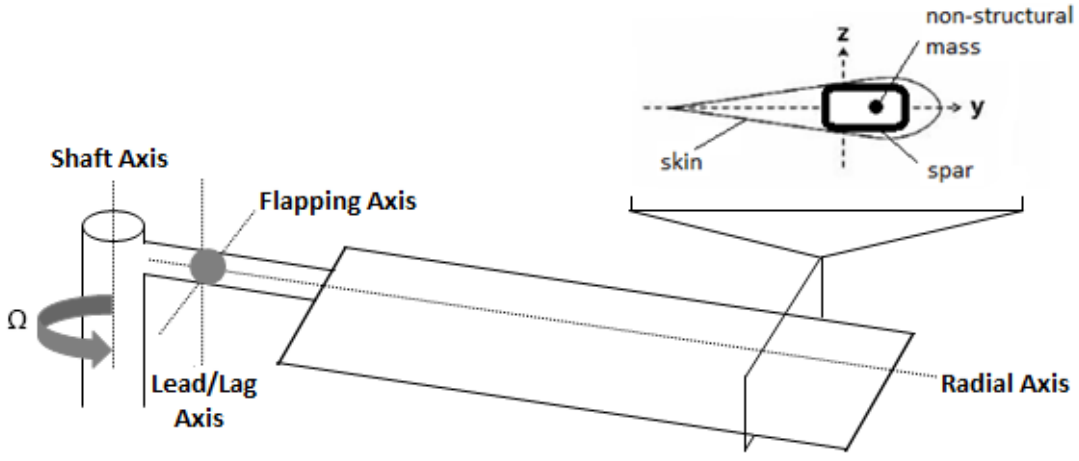


**Figure 1:** A Typical Rotor Blade and its Cross Section

A rotor blade has a free boundary condition at its tip and connected to the rotor hub at its root. Relative motion at the rotor hub is allowed by hinges or elastic supports depending on

the root design and they are called fundamental blade motions. The blade motion which is perpendicular to the rotor plane is called out of plane or flapping motion whereas the motion which occurs in the rotor plane is called in-plane or lead-lag motion. The third motion is the rotation around radial axis and called feathering or pitching. In addition to the fundamental motions governed by the root connections and pitch bearing, there are also elastic motions of the blades because of the blade elasticity. The elastic motion which bends the blade out of the rotor plane is named as out of plane bending or elastic flapping. Similarly, the bending motion occurring in the rotor plane is the in-plane bending or elastic lead-lag. Additionally the deformation around radial axis is called twisting. Axial elongation along the radial axis and cross section warping can also be included but their effects are limited to some special cases [3].

The fundamental and elastic blade motions occur due to the aerodynamic and inertial loads. Lift, drag and pitching loads originate from rotor aerodynamics. From the nature of the rotor, rotation causes centrifugal force on the blade which has important stiffening effect due to high speeds of rotation. Another effect of the rotation is the gyroscopic loads when the rotation axis tilts. In addition to these loads inertial interactions on the blade also exist. The most significant one is the in-plane Coriolis load due the flapping. When blades flap, blade center of gravity moves in radial direction and due to conservation of momentum principle acceleration or deceleration occurs in the rotor plane [2]. Furthermore, there are other sources of coupling due to rotation field, blade external geometry and blade internal geometry.

The representative cross section of the rotor blade in Figure 1 is composed of spar, skin and non-structural mass. The shape of skin defines the airfoil shape. The maximum lift coefficient ($C_{Lmax}$) determines the thrust level and the rotor solidity. Drag divergence Mach number ($M_D$) should be high enough for low drag at higher forward flight speed and low noise. A high lift to drag ratio over a wide range of Mach numbers are required for low power consumption and low autorotation rate of descend. Finally large moment coefficient ($C_m$) should be prevented in order to minimize vibrations around radial axis, twisting moments and prevent high control moments at the blade root [4].

In this particular representative airfoil, the load carrying component is the spar of the cross section. Its distribution over the cross section and the material properties determine the inertial and stiffness properties of the cross section. These properties have primary importance in blade's static and dynamic behavior. On a more detailed rotor blade model, more components like erosion shield, honeycomb filler and other functional parts contribute to the mass and stiffness of the blade but their effects in load resistance are of secondary importance.

From structural dynamics point of view, rotor blades can be analyzed in one dimension for most of the loading conditions. In other words blade's elastic characteristics can be described as functions of radial coordinate. Therefore elastic properties are evaluated by considering the distribution of the blade structure over the cross section at the relevant radial coordinate [3]. When engineering beam theory is applied, the stiffness resisting out of plane and in-plane bending motions are called flapwise bending stiffness ($EI_F$) and chordwise bending stiffness ($EI_C$) respectively and twisting deformation is resisted by torsional rigidity (GJ). The flapwise bending stiffness is calculated around the horizontal principal axis (y-axis of Figure 1), chordwise bending stiffness is evaluated around vertical principal axis (z-axis of Figure 1) and torsional rigidity is evaluated around the blade radial axis. The cross section mass can be evaluated by the contributions from structural load carrying elements and non-structural masses. Non-structural mass is usually implemented for balancing weight or tuning blade natural frequencies which alter the blade mass per unit length [2]. In this respect their effects on the blade stiffness can be neglected as compared to the blade spar.

The rotor blades are connected to the rotor hub which provides the mechanical functions such as load transfer to fuselage, control input transfer, blade relative motion, stabilization of the blades and structural integrity of the whole rotor. A typical rotor hub is represented in Figure 2.

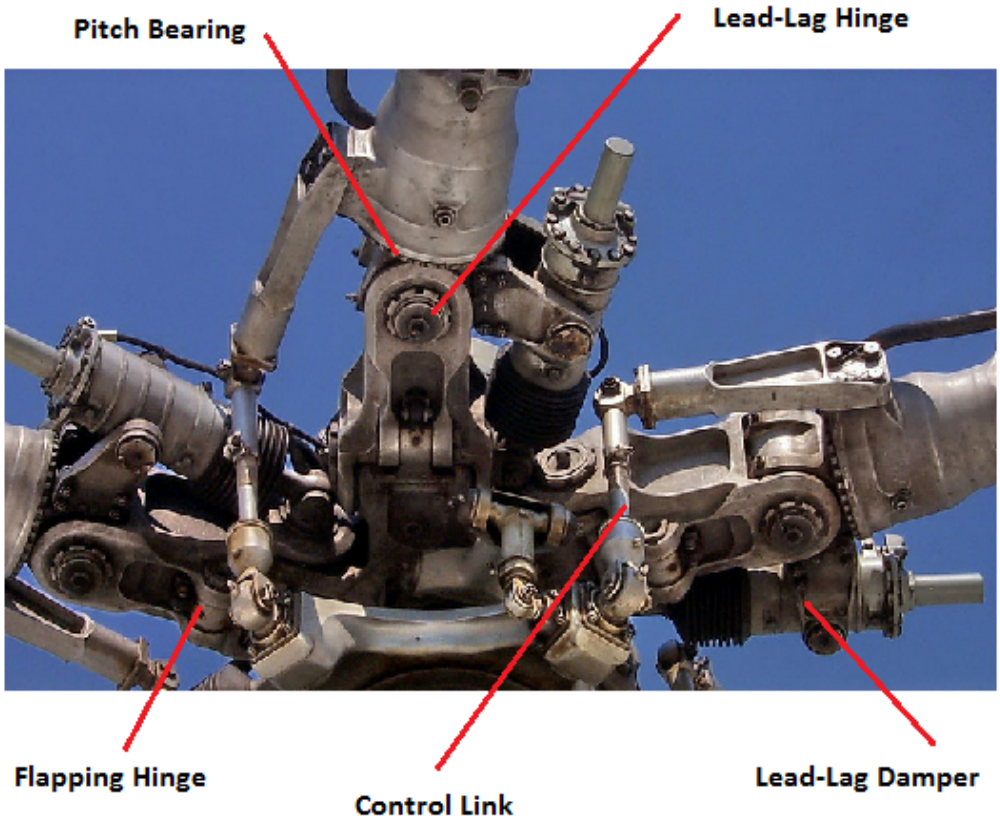


**Figure 2:** Mi-17 Articulated Main Rotor Hub [5]

Inertial and aerodynamic loads acting on the blades are summed at the rotor hub and transferred to the transmission and fuselage. Control links transfer the pilot control inputs to each blade. Lead-lag dampers prevent the possible instable motion of blades in the rotor plane. Hinges or elastic root connections allow blade fundamental motions of flapping and lead-lag and pitch bearing allows blade feathering as previously explained. Blades are classified according to type of the connection since each of them has unique dynamic characters. Rotors with hinged connection are called articulated blades. If there is only one flapping hinge passing through the shaft, then this configuration is called teetering. Another type which is named as hingeless blades eliminate the hinges and use elastic connections in sustaining flapping and lead-lag motions. A special application of hingeless blade is the bearingless blade which also eliminates pitch bearing in addition to the flapping and lead-lag hinges [6].

Control system is required in order to govern the aerodynamic loads acting on the blade so that lift, propulsion and control of the helicopter can be managed. These forces depend on the angle of attack and airflow speed faced by the blades. The blade angle of attack is determined by the blade pitch which is also called feathering. A simple blade control system can be seen in Figure 3.

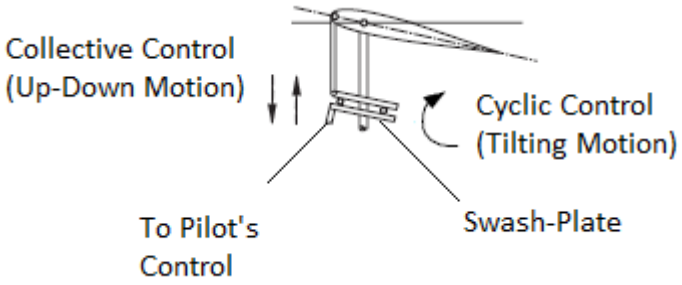


**Figure 3:** Swash Plate Functions

There are two options in pitch control which are collective and cyclic controls and they are applied by swash plate which is linked to pilot controls. This plate is composed of two sections which are connected to each other. Lower plate is stationary and linked to pilot controls whereas upper swash plate is rotating and connected to the blades via control links. When collective lever is moved, then swash plate changes its position up or down and all the blades face the same angle change of attack irrespective of their position on the rotor disc. This vertical motion of swash plate changes thrust output. The other one, cyclic pitch control is used to tilt the rotor disc. Input from the pilot tilts swash-plate in longitudinal and lateral directions. The tilt of swash-plate generates cyclic variation of angle of attack over the rotor disc and thrust vector can be oriented in order to provide propulsion for forward or lateral flight or moment with respect to aircraft center of gravity for the maneuvers.

In addition to complexities arising from blade elastic motion and control system, helicopters also operate in a complex aerodynamic field due to forward flight. Once rotor is tilted, the longitudinal component of rotor thrust accelerates the helicopter. However, forward flight introduces another problem which is the asymmetric distribution of velocity over the rotor disc which can be seen in Figure 4.

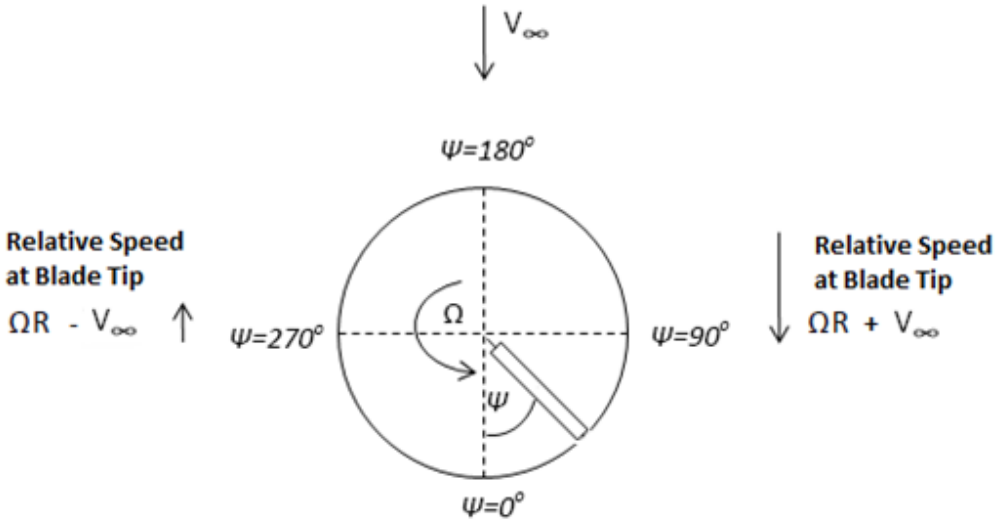


**Figure 4:** A Counter-clockwise Rotor in Forward Flight

For a counterclockwise rotor seen from above, the right hand side faces forward flight speed from blade leading edge and called advancing side whereas left hand side faces forward flight speed from trailing edge and called retreating side. When the angular velocity and forward flight velocity are summed the airspeed distribution in the advancing side is greater in magnitude than that of the retreating side. The differential relative speed distribution on aerodynamic surfaces causes the aerodynamics load on two sides to differ and generate rolling moment on body and large bending moment at root. This in turn causes oscillatory loads on the blades.

In addition to the load asymmetry the aerodynamic environment is more complex. At the advancing side, the compressibility effects increase as forward flight speed increases. Retreating side blade stall is another issue that needs to be considered. As forward flight speed increases the blades at the retreating side faces with lower speed and this reduction must be compensated by increase in blade angle of attack and then blades start stalling which is the major limit for maximum speed [7]. And the final one is the inverse flow region, the blade faces the airflow from leading edge and this area is measured by the circle having the diameter of the advance ratio μ [8]. Blade-blade, main rotor-tail rotor and blade-fuselage interactions are also remarkable [9]. The complex aerodynamic operation of rotor can be seen in Figure 5.

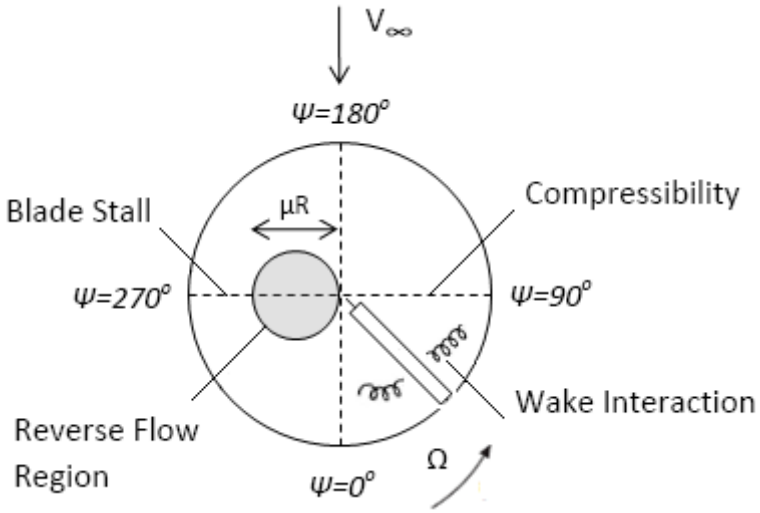


**Figure 5:** Forward Flight Aerodynamic Environment for a Counter-Clockwise Rotor

Since airflow speed, angle of attack, stall effect, reverse flow and compressible flow are non-uniformly distributed over the rotor disc, the aerodynamic loads and blade motion resulting from all the rotational, dynamic and aerodynamic effects are all oscillatory. The oscillations in the load and blade motion are the major sources of helicopter vibration [1].

Although the loads and motion are oscillatory, the periodicity of the rotor simplifies the analyses. In a level flight the orientation of the helicopter body and the rotor rotation axis remain same but rotor still rotates and the time dependent loads and motion still exist on the rotor. In such a case, after transient effects die out the blades face same loads and motion when they are passing through the same azimuthal coordinate (Ψ). In other words there are variations in loads and motion within rotor disc however those variations repeat itself at each revolution. Therefore excluding maneuvers in which there are translational and angular accelerations, the rotor operation is periodic [1]. Using the periodic nature of the rotor, the time domain rotor analysis can be reduced to frequency domain with the period of $2\pi$ and the fundamental frequency of rotor angular speed ($\Omega$). The analysis in frequency domain can be handled by using Fourier Series such that the time dependent variables are represented with a mean component and an infinite sum of harmonics which are the sinusoidal functions of rotor azimuth coordinate at the integral multiples of fundamental rotor frequency. For a

general load variable ($L$) and a general motion variable ($X$), time dependent equations can be represented in frequency domain as [1];

$$L(\psi) = L_0 + \sum_{n=1}^{\infty} \left[ L_{n,C} \cos(n\psi) + L_{n,S} \sin(n\psi) \right] \tag{1}$$

$$X(\psi) = X_0 + \sum_{n=1}^{\infty} \left[ X_{n,C} \cos(n\psi) + X_{n,S} \sin(n\psi) \right] \tag{2}$$

where;

| | | | |
|---|---|---|---|
| $n$ | : Harmonic Number, n=1,2… | $\Psi$ | : Rotor azimuth angle |
| $L_0$ | : Steady Load amplitude | $X_0$ | : Steady Motion amplitude |
| $L_{n,C}$ | : n$^{th}$ cosine Load amplitude | $L_{n,S}$ | : n$^{th}$ sine Load amplitude |
| $X_{n,C}$ | : n$^{th}$ cosine Motion amplitude | $X_{n,S}$ | : n$^{th}$ sine Motion amplitude |

In equations 1 and 2, the time dependent periodic variables ($L$ and $X$) were represented in frequency domain with the amplitude of each harmonic. For a periodic system the sum of all the harmonics and the steady value is exactly equal to the time dependent variable if infinite number of harmonics is used. Luckily, the amplitudes of higher harmonics are usually negligible and a finite number of terms are sufficient for an accurate representation which should be determined according to the complexity of the problem. The Fourier Series representation is very commonly used in rotorcraft industry and simplifies the rotor analysis in understanding and solving the equations of motion since contribution from each harmonic can be analyzed separately and the overall result can be obtained by summing all the harmonics in the range of interest [1].

The dynamics of the rotor is quite complex due to high angular rotation speed, slender elastic blades and unsteady aerodynamic environment. The understanding of the rotor and its operation is critical in understanding the helicopter vibration and solutions of vibration reduction. Although the helicopter vibration requires a lot more knowledge on the rotor and fuselage, the material presented in this section provides the necessary background in understanding the major source of helicopter vibrations which is the main rotor oscillatory loads and motion.

## 1.3 The Vibration Problem of Helicopters

The differences in the operational capacities between the fixed wing and rotary wing aircrafts were introduced in Section 1.1. However in addition to the operational capacities there are more distinctive features. One of the most significant distinctive features is the vibrational levels due to the complex operation of the rotor. The significance of the helicopter vibration problem can be outlined by comparing the vibration induced problems of fixed-wing and rotary wing. Such a comparison on the failure rates of the hydraulic equipment are presented in Figure 6.

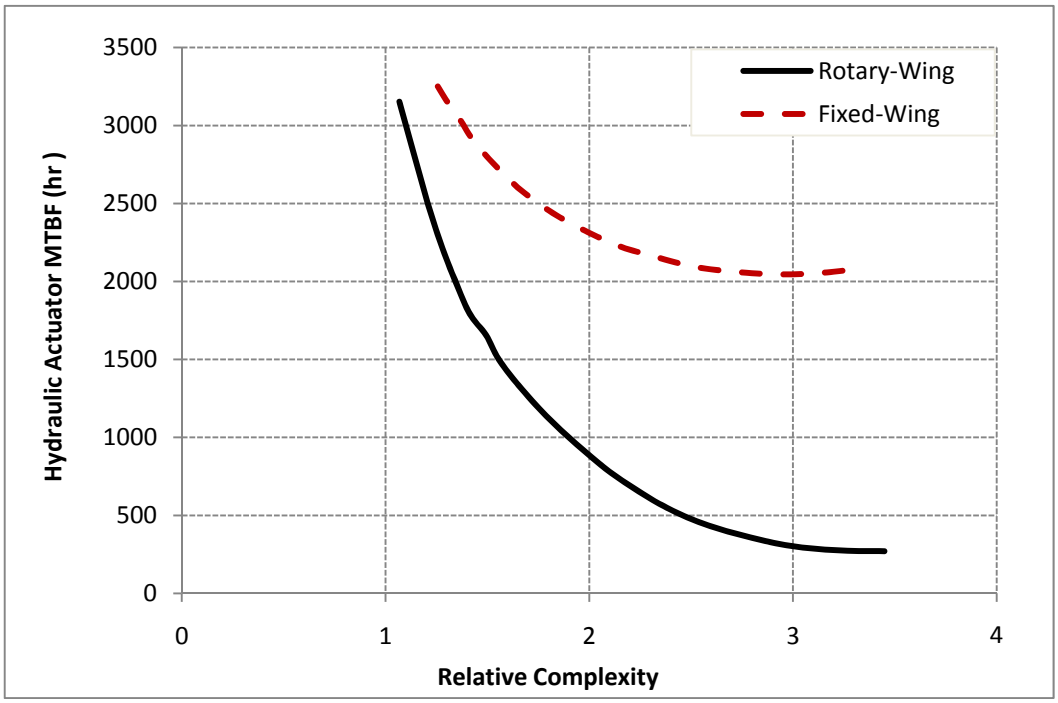


**Figure 6:** Fixed-Wing Reliability vs. Rotary-Wing Reliability (Hydraulic Equipment) [10]

The horizontal axis of Figure 6 represents the relative complexity of the hydraulic equipment whereas the vertical axes represent the mean time between failures. For both fixed-wing and rotary-wing equipment the mean time between failure decreases as the complexity increases. However the reduction in the failure time is remarkable for the rotary wing. This reduction is mainly due to the higher vibration levels in rotary-wing aircraft as compared to fixed wing aircraft.

Vibration is also a critical factor in rotorcraft performance. Maximum flight speed is determined by the available power in fixed wing applications and more powerful engine installation usually results in a higher maximum speed. But in rotorcraft power available is not the only limiting factor. As flight speed increases, retreating side blade stall and advancing side compressibility effects induce high level of vibrations and loads. Because of this reason the design cruise speeds of conventional main rotor tail rotor helicopters usually vary between 150 and 200 knots for modern helicopters [1]. Furthermore maximum flight speed is not the only performance parameter that is degraded because of vibration. Performance at other flight conditions at which rotor operate at its wake such as landing, rolling or autorotation can also suffer from vibrations. More severe vibration levels than those considered do not only decrease performance but also impair flight safety.

Fatigue of the airframe, the rotor blades and other components is another significant result of the helicopter vibrations. The main source of the airframe fatigue loading is the rotor vibratory loads at the integral multiples of the rotor speed frequencies [11]. Rotor blades also operate under oscillatory aerodynamic environment as it was previously mentioned in Section 1.2. The blade response under these loads is quite complex which includes coupled in-plane and out of plane bending, axial elongation and twisting deformations. More or less all the sections of the blade encounter these oscillatory elongations therefore the whole blade should be evaluated for fatigue. In addition to the airframe and blades, the flight equipment also suffer from fatigue loading [11].

Last but not the least, vibration effect on the flight crew and passengers should not be underestimated. High level of vibration cause whole body vibration which occurs when the human body is supported by a surface that is shaking. The vibration from the shaking surface is transmitted through the body of the human in contact with the surface including skeleton, nervous system and spine [12]. In general this whole body vibration reduces flight comfort. Furthermore, the effects are more severe in long term. Especially, back pain is a common complaint for helicopter crew which is mostly related to the whole body vibration [13]. The vibrations cause the stressing of intervertebral discs and paravertebral muscles which serve as the absorber system of the spine [14]. In addition to comfort and health, pilot vision may be blurred and there are cases where pilots are unable to read the flight instruments which is a significant safety problem [2].

A helicopter which is designed without giving the primary importance on vibrations, would suffer from all the aforementioned problems. Therefore at each design phase, possible vibration sources should be handled carefully. The methods of vibration reduction will be discussed in Section 1.4.

## 1.4 Helicopter Vibration Reduction

The discussions on the vibration problem of the helicopters and possible consequences in Section 1.3 prove that, the rotor induced vibrations effect the whole body, crew and payload significantly. Because of these problems, the vibration reduction and control is important in order to improve flight safety, passenger comfort, equipment reliability and material life of components [8]. Therefore the vibration reduction techniques should be clearly understood and implemented into the design in order to achieve safe and competitive designs.

Figure 7 represents the results of a vibration reduction study which was performed on CH-3 helicopter for the failure rates of structure and equipment before and after the application bifilar vibration absorber to the rotor [10]. The failure rates were computed by taking the ratio between the total number of failures and the total flight hours.

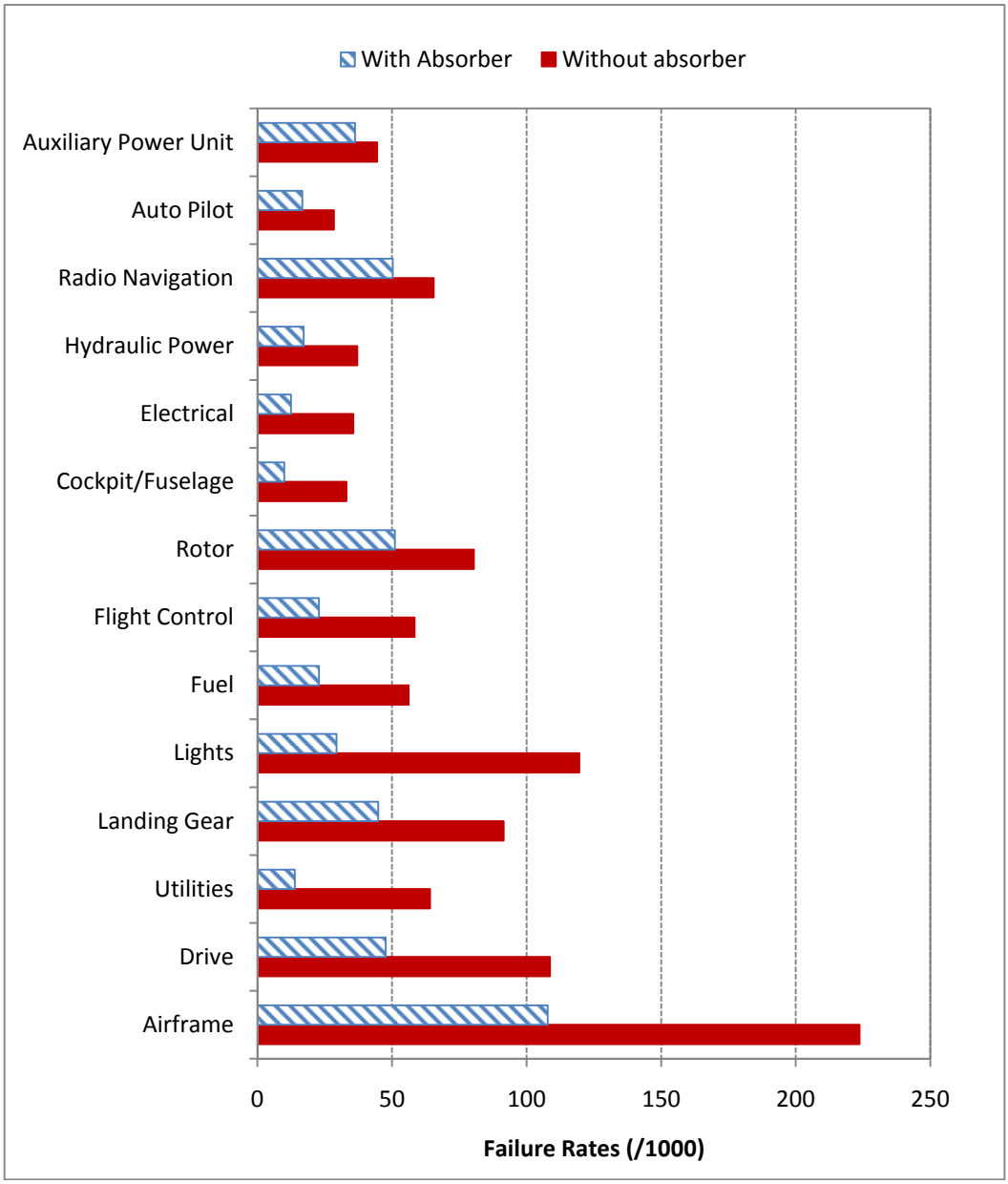


**Figure 7:** Failure Rates of CH-3 Helicopter Components Before and After the Vibration Absorber Installation [10]

According to Figure 7, the failure rates of the components reduced dramatically. The moving masses on the absorber were believed to relieve the vibratory loads so that the most of harmful effects of vibrations were transferred to absorber. The result of the reduction in vibrational levels is not only beneficial in terms of component failure. For the same absorber application the saving analysis was also performed which is outlined in Table 1.

**Table 1:** The Saving Break-Down for CH-3 after the Bifilar Absorber "Application [10]

| | In-the Pocket Savings | | Savings Due to Increased Utility | |
|---|---|---|---|---|
| | Maintenance | Spares | Reliability | Availability |
| Saving | 162064 $ | 134577 $ | 10010 $ | 60662 $ |
| Total Savings | 367313 $ | | | |
| Initial Cost of the Absorber | 11000 $ | | | |
| Operation Cost of Absorber | 4000 $ | | | |
| **NET Saving** | **352313 $** | | | |

The cost saving analysis given in Table 1 was performed on the most sensitive subsystems of the CH-3 helicopter. The savings were categorized under two main sections which were “in-the pocket savings” and “savings due to increased utility”. The former included the reduction in maintenance cost and required spares for maintenance whereas the latter included the decrease in cost due to mission reliability and availability. The total saving was approximately 367000 $ whereas the cost of the absorber was only 15000 $ including the initial cost and operational expenses. Therefore the net savings can be estimated approximately as 352000 $. In addition to total savings, increased safety reduces the possibility of flight accidents which can introduce extra savings on helicopter and more significantly save invaluable human lives and health as well.

## 1.5 Vibration Reduction Techniques

The remarkable benefits of vibration reduction in rotorcraft which were discussed in Section 1.4 have leaded the designers to work on the vibration reduction techniques which achieve vibration reduction by reducing the amplitude and/or alleviating the excitation loads. The techniques can be passive or controlled actively. The passive techniques do not require any actuation and try to reduce vibrations after the vibratory loads are generated. On the other hand active techniques work according to the measured vibration on the helicopter and try to reduce vibratory loads by generating opposing airloads [15]. The passive and active vibration reduction techniques will be discussed briefly in Section 1.5.1 and Section 1.5.2.

The active and passive vibration reduction techniques are effective in controlling the vibrations which exist for a completed design. However, the main source of the rotor induced vibrations is the aeroelastic behavior of the rotor which is directly related to the helicopter design. If the design and modification for reduced vibration level is systematically included in design or modification phase, the level of vibrations can be reduced at the source. Therefore the design and modification for reduced vibration level is also included as a vibration reduction technique which will be introduced in Section 1.5.3, discussed in CHAPTER 2 in detail and implemented in CHAPTER 3.

### 1.5.1 Passive Vibration Reduction Techniques

Passive vibration reduction can be achieved by self-actuated systems which include vibration isolation, absorption and attenuation. The isolators reduce the undesirable effects of vibration by designing the connection between body which is required to be isolated and the foundation which is the source of vibration itself [16]. On the helicopters, they are located between the critical equipment on the fuselage and the supporting structure which transmit the vibration. They are spring mass damper systems and their working principle is represented in Figure 8.

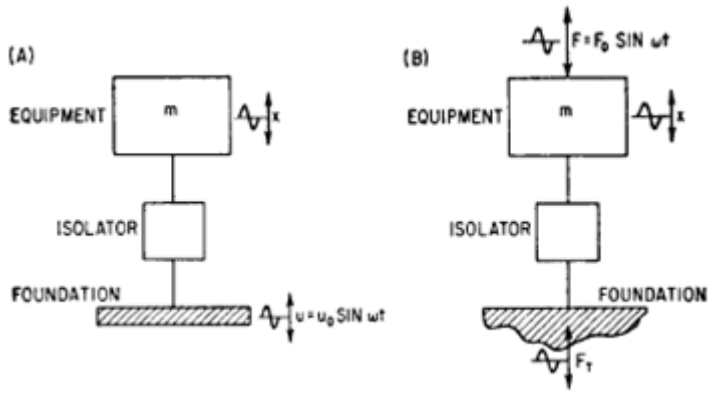


**Figure 8:** Schematic Diagrams of Vibration Isolation Systems [17]:
(A) Vibration Isolation from a Vibrating Foundation;
(B) Vibration Isolation from a Vibratory Excitation Force

According to the Figure 8 the isolators either reduce the magnitude of the vibratory motion transmitted from the vibrating foundation (A) or reduce the magnitude of force transmitted from the foundation (B). The pilot seat, avionics and cockpit instruments can be counted among the critical equipment on a helicopter on which isolators are commonly applied [3]. On helicopters the foundation is the airframe structure which is mainly excited by the vibratory loads coming from the main rotor.

Vibration absorption refers to extra degrees of freedom addition so that the unwanted effects of vibration are transferred to new degree of freedom rather than to the structure [16]. The most popular absorbers in helicopters are pendulum absorbers and bifilar absorbers and can be mounted on the blade in flapwise and in-plane directions. A representative pendulum absorber in flapwise direction is given in Figure 9.

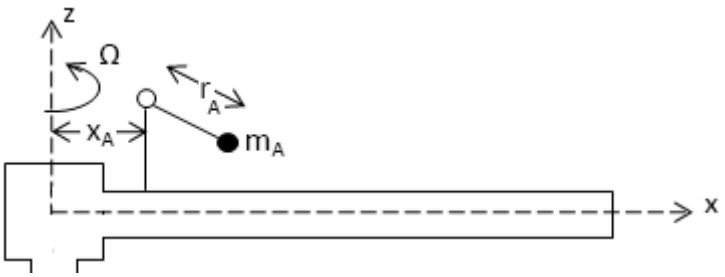


**Figure 9:** Schematic Diagram of Pendulum Absorber Mounted on the Rotor Blade in Flapwise Direction [18]

Significant reductions in blade root loads can be achieved by the pendulums which are mounted in flapwise and chordwise directions [18]. The application of the pendulum modifies the motion of the blades so that favorable blade response reduces vibratory loads. The frequency near which pendulum is effective depends on the natural frequency of the pendulum which is determined by the application point ($x_A$), the length of the pendulum ($r_A$) and the rotor angular velocity ($\Omega$) whereas the load magnitude of reduction depends on the pendulum weight ($m_A$) [3]. This frequency is called the tuning frequency and the pendulum has no effect on vibratory loads at other frequencies. The main disadvantage of these devices is their detrimental effects on performance by weight addition and aerodynamic drag.

Another type of passive vibration reduction systems is the bifilar absorber. This device is mounted on the rotor hub and effective in reducing vibratory in-plane hub shear forces. A representative sketch of a bifilar absorber is presented in Figure 10.

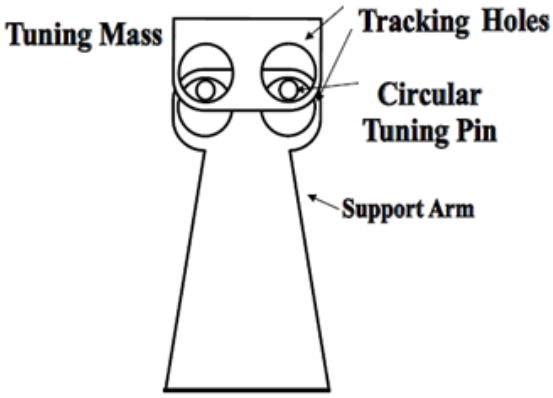


**Figure 10:** Schematic of Bifilar Absorber [19]

The bifilar absorber given in Figure 10 is composed of a support arm, a tuning mass, circular holes and tuning pins. The support arm connects the tuning mass to the hub whereas the tracking holes and tuning pins provide relative motion of the tuning mass. The motion of the tuning mass is governed by the loads acting on it and the natural frequency of the system which is determined by the dimensions of the holes and pins and angular rotor speed. The natural frequency of the system is tuned to the in-plane frequency in the rotating frame at which the vibratory in-plane shear force is supposed to be reduced [19]. The bifilar absorbers are relatively heavier as compared to pendulums and can only reduce in-plane loads.

The attenuators are the non-structural masses which are added to the rotor blade which help in moving blade natural frequencies away from excitation frequencies. They are usually applied at blade tip or mid-span [18]. All three types of the passive vibration reduction techniques are effective at a specific tuning frequency at which the vibratory loads are supposed to be reduced. If vibratory loads exist at any other frequency, the techniques are ineffective and additional vibration reduction systems should be implemented.

### 1.5.2 Active Vibration Reduction Techniques

The active vibration reduction systems are also called excitation reducers which generate opposing aerodynamic loads so that the vibratory loads are cancelled [18]. The most popular active control systems are the higher harmonic control, active flaps and smart structure application on rotor blades.

The swash plate control excites the surrounding air once in every rotor revolution in normal operation as it was discussed in Section 1.2. The idea behind the higher harmonic control (HHC) is to excite the swash plate at a higher frequency in addition to the 1/rev cyclic input so that there is an additional excitation that cancels the vibratory airloads [20]. A sample system is presented in Figure 11.

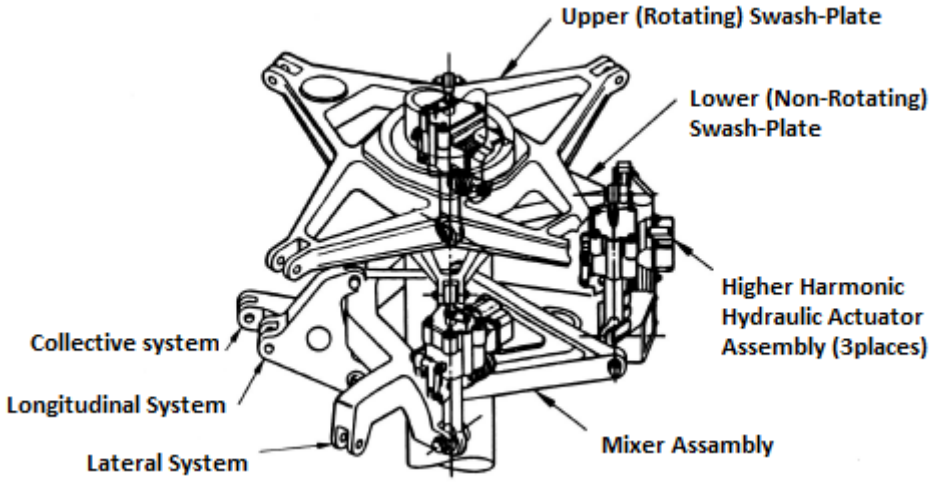


**Figure 11:** Higher Harmonic Application [20]

The system in Figure 11 is a sample HHC application to a helicopter having 4 blades in order to reduce vibrations at the blade passing frequency. The system measures the vibrations by using the accelerometers located at the pilot seat. The measured vibrations which are supposed to be reduced are converted into signals and then fed into the flight computer. The flight computer calculates the necessary motion of the swash plate. The suitable combination of the vertical and tilting motions of the stationary swash plate generate the required canceling loads [20]. Since the canceling loads reduce vibratory loads, which are the sources of the transmitted vibrations to the fuselage, the vibrations on the pilot seat can also be reduced.

An improved method of HHC is called individual blade control (IBC). In this concept the pitch of each blade is excited so that better results can be obtained with the addition of more control degrees of freedom [21]. There are also other ways of exciting blade individually which is the active flap control [22] and smart blade [24]. The flaps located on the rotor blades are actuated such that the resulting airloads cancel the vibratory loads as in the case of HHC. The number of flaps per blade can also be increase. This method consumes less power than IBC with a mechanically simpler system [22]. Smart blade concepts make use of piezoelectric actuators. Depending on the level of vibrations, the elastic twist of the blade is altered by using the actuators and therefore the vibratory loads can be reduced [24].

### 1.5.3 Design and Modification for Reduced Vibration Level

Since the solutions of passive and active vibration reduction systems have the aim of reducing response or loads for a given system, they can be considered as external applications. Depending on the application the external systems introduce extra weight and drag which degrade performance. Furthermore, the effectiveness of the external applications strongly depends on the vibrational level of the clean structure and the application need to be applied after costly flight tests. In addition to performance and cost drawbacks, the local isolation of vibrations solves the problem at the point of application, and then the remaining body may still face significant level of vibrations. Therefore the vibration levels should be carefully considered at the design or modification stages of a rotorcraft so that the vibrations could be reduced before the product is finalized [2].

The design and modification of helicopter structures can be performed depending on the sources of the vibration [25]. The main sources are aerodynamic blade loading, blade dynamic response as it was described in Section 1.2 and fuselage response to the loads transferred through the rotor hub. Therefore a reduced vibration level in helicopters can be achieved by smooth aerodynamic loading, favorable blade dynamics and controlling the response of the fuselage.

The aerodynamic design of the blades has strong contribution on the vibratory loads. Periodic loading in forward flight, compressibility and stall effects and the aerodynamic interaction between blades are responsible for the oscillatory aerodynamic loading. The activities aim to reduce the undesirable effects of these sources. Blade tip geometry can be designed to prevent advancing side shocks, blade twist can be distributed to reduce the retreating side stall loading. The wake of the blades should be considered in order to reduce the level of interference between blades. Furthermore the number of blades has also important effect on the interference of the blades [25].

The other source of vibration which originates from rotor blades is the blade dynamic response. The undesirable effects of blade vibration are the fatigue loading on the blade and the vibratory load amplification on the rotor hub which is transferred to the fuselage. The favorable blade response can be achieved by proper mass and stiffness distribution of the blade. At the same time blade natural frequencies should also be separated from aerodynamic excitation frequencies so that resonant operation is avoided [25].

The vibratory loads that are of rotor origin are transferred to the fuselage and the fuselage responses to these loads. Therefore fuselage dynamic response is significant in terms of the vibration levels acting on the structure, cockpit, crew, equipment and payload. The fundamental solution is to adjust the natural frequencies of the fuselage so that any resonance with the vibrations coming through the rotor hub and/or reduce the level of interference between the rotor and the fuselage [25].

Whatever the source of vibration and its solution are, design and modification for reduced vibrational level involves complex engineering work. The rotor system and operation is very complex and a large number of variables have significant impact on the helicopter vibration.

Furthermore a low vibration design does not necessarily mean that the design is feasible because of the side effects. Therefore the problem can be stated as to reduce the vibrational level of the helicopter as much as possible within a design space which includes a large number of variables and constraints. Optimization algorithms provide effective solutions for such problems when they are coordinated with rotorcraft analysis tools. For this reason, the design and modification activities for reduced vibrational level should be handled as an optimization process and that process is composed of objective function, constraints and design variables. The objective function is defined as the model output which is aimed to be minimized; constraints are selected in order to prevent the unrealistic results and design variables are the proper model inputs which are the most sensitive to the optimization problem. The role of comprehensive model in this process is to provide the values of the objective function and constraints for the assigned design variables.

## 1.6 Objectives

This thesis has two objectives. First objective is to develop a procedure which has the capability of analyzing and designing helicopter rotor blades for reduced main rotor induced vibrational level. The procedure aims to achieve favorable rotor blade structural dynamics characteristics so that the vibrational level can be reduced at the rotor before it was transmitted to the fuselage. For this purpose a rotorcraft comprehensive analysis tool is coupled with an optimization algorithm. The other objective is to implement the coupled program to isolated blades and to a full helicopter configuration which includes main rotor, tail rotor and fuselage. The values of the objective functions and the distributions of the design variables are compared for the initial and final designs while controlling the feasibility of the results by design constraints.

## 1.7 Literature Survey

The studies on the analysis and design of helicopter rotor blades for reduced vibration level by using optimization techniques have become popular after comprehensive analysis gained acceptance in rotorcraft industry. This section outlines the studies in the rotor blade optimization for reduced vibration levels and aims to provide a chronological history.

A thesis on the optimal design of helicopter rotor blades for optimum dynamic characteristics was published by Ko in 1985 [26]. In that articulated rotor blades were optimized for the objective of natural frequency separation and weight reduction by using CONMIN gradient based optimization algorithm. Finite element formulation was used in evaluating the natural frequencies of the blades. The cross section wall thickness and non-structural masses were defined as the design variables. Constraints on the stress, size of non-structural mass and the thickness on the beam were used.

Friedman and Celi conducted a study on the structural optimization of rotor blades with swept tips subject to aeroelastic constraints [27]. The objective function was the vibratory rotor hub shear forces of an isolated rotor which are transmitted to the fuselage. The interaction of the blade natural frequencies with aerodynamic excitation frequencies was limited. An aeroelastic code which included a finite element formulation with trimming capacity evaluated the hub loads and the constraints and CONMIN optimization algorithm performed the optimization task. The cross section wall thickness and width were the design variables for single cell and double cell beams. The effect of tip sweep was investigated also which further reduced vibratory hub shears.

The strategy for the combined structural, inertial, dynamic, aeroelastic, and aerodynamic performance characteristics was discussed by Peters and Cheng [28]. The gradients were provided analytically by a finite element code to optimization algorithm CONMIN. The blade natural frequencies were formulated as the objective function. Two methods were tried in defining the design variables. First one was using cross section dimensions and evaluating cross section inertial and stiffness values from the dimension which had constraints on the dimensions. The second one was directly using the inertial and stiffness distributions and then post-processing for the blade cross section dimensions for the optimum blade which had constraints on the stiffness and inertial quantities. Both methods were successful in the analysis. Furthermore, the stress constraint was not found to be important that when only natural frequencies were considered and no section reached yield stress. However when the blade fatigue life was included in the analysis, the stress constraint became a critical factor.

Lim and Chopra studied the sensitivity analysis and optimization of a helicopter rotor [29]. The design sensitivities of the non-structural mass, the offset of the non-structural mass,

blade center of gravity offset, chordwise and flapwise bending stiffness, torsional stiffness were evaluated with respect to the vibratory vertical shear at the rotor hub which was transmitted to the fuselage. Gradients were calculated analytically which were formulated by using University of Maryland Rotorcraft Analysis Tool which are supplied to CONMIN optimization algorithm. Optimization analyses included two different objective function formulations which were the reduction of the vibratory vertical hub shear and all three vibratory hub shear and moments. The former formulation leaded bigger reduction in vertical shear however increased other shear and moment components. The effects of aeroelastic stability constraints for the initially feasible and infeasible designs were also investigated.

Aditi and Walsh and also Aditi, Walsh and Riley proposed a strategy for the structural optimization of rotor blades with integrated dynamics and aerodynamics [30]-[31]. The former included more details about the strategy while providing results for a weight-stress optimization of a helicopter rotor. The latter implemented the strategy to a Black Hawk Rotor and discussed the results. The optimization analyses included the reduction of vibratory vertical hub shear and blade weight which was subjected to the constraints of the blade natural frequencies, auto-rotational inertia and centrifugal stress. The design variables were the stiffness and nonstructural mass quantities of the cross section and blade taper ratio. The rotorcraft problem was solved by CAMRAD JA which was modeled as an isolated rotor model. Optimization analyses were performed by CONMIN. Additionally, Aditi and Chiu compared the aerodynamic loads and power required of initial and optimum designs and investigated the effect of thrust limit [32].

In 1989, a NASA Technical Memorandum on the integrated multidisciplinary optimization was prepared by NASA Scientists and edited by Adelman and Mantay [33]. The objective function was formulated by the linear combination of power required values at five different flight conditions and vertical vibratory shear. There was a wide range of design variables which include blade radius, radial coordinate of taper initiation, taper ratios for the blade chord and blade thickness, the chord and blade thickness at the blade root, the blade hinge offset and maximum twist, cross section wall and ply thicknesses. The problem was subjected to constraints of rotor power required, airfoil section stall, blade frequencies, blade loads, hub loads, blade response, autorotational inertia, aeroelastic stability, wing box stress,

blade tip deflection, blade twist, blade tip Mach number, blade thickness, lift distribution, ground resonance and rotor airframe coupling. In 1992, the same procedure was also applied to a 4-bladed utility helicopter by Walsh, LaMarch II and Adelman [34].

Non-structural tuning masses were optimized in order to minimize the vertical shear force by Pritchard et al [35]. The locations and mass values of six tuning masses were optimized analytically and compared with test data. CAMRAD JA was used for the rotor solution and CONMIN was used for the optimization.

Lee implemented genetic algorithm to rotorcraft multidisciplinary optimization in 1995 [36]. The purpose of using genetic algorithms is their applicability to parallel computing which is a big advantage in multidisciplinary optimization so that the multidisciplinary problems can be handled by dividing the whole system into subsystems. A finite element based multibody formulation was used to model the blade. A weighted sum of vertical vibratory hub loads was formulated as the objective function which was subjected to the design constraints including power required, autorotational inertia, natural frequencies, rotor thrust, blade weight and buckling stress. The design variables were the tuning masses, blade cross section dimensions, blade twist, blade taper ratio and its initiation point, rotor RPM, and the ply angles of the cross sections.

Surface method approximation has gained acceptance in the last decade. By using response surface approximation the objective function was represented as second order polynomial function of design variables. Ganguli used response surface approximation for optimizing the rotor blades for reduction in vibratory hub loads in 2002 [37]. Design variables were blade flapwise and chordwise bending stiffnesses and torsional stiffness. The optimization was implemented on a hingeless blade with uniform properties. In 2006, Bhadra and Ganguli improved this study by including free wake modeling [38]. In 2008 Murugan et al followed the similar procedure with a robust optimization so that the uncertainties in the design variables were considered [39]. Glaz et al used multiple surrogates together with neural networks in blade vibration reduction in 2009 [40].

In 2004, Viswamurthy and Ganguli optimized the deflection harmonics of the blade multiple trailing edge flaps for the reduction in vibratory hub loads by putting constraints on the deflection of flaps [41]. The university of Maryland Rotorcraft Analysis code was coupled with a gradient based optimization algorithm.

In 2006 NASA Aeroelasticity Handbook, Kvaternik and Murthy discussed the airframe structural dynamic consideration in Rotor Design Optimization [42]. An example design cycle for the helicopter vibration was provided with the role of airframe response. The constraints on the rotor design were addressed. The ground and air resonances which are the two important aeromechanical instability problems were discussed.

Harrison, Stacey and Hansford published the advances in British Experimental Rotor Program including rotor blade optimization for reduced vibration levels in 2008 [43]. An in-house developed optimizer was linked with eigenvalue analysis and load prediction software. The stiffness and inertia properties of the cross section were optimized by changing the dimensions of the cross section. The analyses were subjected to constraints on blade mass, 1$^{st}$ mass moment and composite ply-up restrictions. A tailored blade for minimum vibration and reduced control loads was obtained while significantly reducing the design time.

## 1.8 Scope, Contents and Limitations of the Study

In this study, analysis and design of helicopter rotor blades were performed for reduced vibrational levels. For this purpose the CAMRAD JA comprehensive rotorcraft analysis was coupled with the CONMIN gradient based optimization algorithm.

In CHAPTER 1, the optimization methods for an isolated blade and for a full helicopter composed of main rotor tail rotor and fuselage are defined. The method for an isolated blade includes the natural frequency separation of the blades from aerodynamic excitation frequencies and the method for a full helicopter configuration includes the minimization of the vibratory hub loads. The rotorcraft comprehensive analysis and the optimization program are discussed. The procedure for the analysis and design of helicopter rotor blades for reduced vibrational level is presented.

CHAPTER 2 includes the case studies of the two proposed methods. First, two isolated blades are optimized for the blade natural frequency separation. The natural frequencies of articulated and hingeless rotor blades are aimed to be separated from aerodynamic excitation frequencies by finding the optimum cross section wall thickness and non-structural mass distribution. For the case study of the full helicopter problem, the critical vibratory hub load is minimized by optimizing blade mass and stiffness distributions. The case studies of both methods are subjected to the constraints for the design variables, blade mass, blade auto-rotational inertia and the natural frequencies of the blade.

In CHAPTER 3 conclusions and recommendations for future work are given.

In this study helicopter solution was limited by the analysis capacities of the CAMRAD JA comprehensive analysis [44]-[45]. Engineering beam theory for rotating blades with large pitch and twist is the basis of the rotor structural model which assumes single load path. Blade aerodynamics is evaluated by lifting line theory using steady two dimensional airfoil characteristics and a vortex wake and inflow. For analysis with more detailed models like finite element for structural dynamics and computational fluid dynamics for aerodynamic calculations, other rotorcraft comprehensive analysis tools or general purpose package programs can be preferred which require extra licensing are needed.

The optimization program is a gradient based algorithm which uses the method of feasible directions. The results of the optimization analyses are limited by the capabilities of the optimization algorithm. Better or worse results may be achieved with different optimization methods and programs.

The gradients of the objective function can be evaluated by using numerical or analytical differentiation. The analytical differentiation requires the derivation of the gradients from governing equations of motion which are quite complicated for the helicopter rotor. In this study finite differencing equations of the optimization algorithm was used.

# CHAPTER 2

# ANALYSIS AND DESIGN OF HELICOPTER ROTOR BLADES FOR REDUCED VIBRATIONAL LEVEL

## 2.1 Introduction

Helicopter vibration is defined as the oscillatory response of the helicopter airframe to the rotor hub forces and moments [1]. Although there are other vibration sources like engine and transmission, aerodynamic loads on the fuselage and tail rotor, their effects are mostly local. The vibratory hub loads from the main rotor are the major source of vibration [3]. These loads are transmitted to the fuselage through the rotor hub, and reduction in these loads is expected to reduce the vibrational level on the whole helicopter. Therefore in this thesis, vibrations which are induced by main rotor forces and moments were considered.

Optimization methods are very popular in multi-disciplinary engineering applications. Helicopter operation has strong aerodynamic and structural dynamics interactions therefore optimization algorithms are also used in rotorcraft industry so that lighter, safer, cheaper and high-performance helicopters can be designed. However while algorithms solve the mathematical relations the physical world should also be represented. Rotorcraft comprehensive analysis is the best choice for this purpose which has been very popular in rotorcraft industry due to its fast and reliable solutions for the whole helicopter. Therefore if the coordination between optimization algorithms and rotorcraft comprehensive analysis is ensured, rotorcraft design can benefit from multidisciplinary optimization. For this purpose an optimization procedure that can reduce main rotor induced vibrational level was proposed. Additionally, that procedure was illustrated on the existing isolated blades and full helicopter configuration including main rotor, tail rotor and fuselage.

## 2.2 The Approaches of Rotor Induced Vibratory Load Reduction

The rotor induced vibrations can be handled in two ways which can be identified as direct and indirect approaches. In the direct approach, the blades were designed or modified for the minimized rotor hub vibratory loads. The vibratory loads include inertial and aerodynamic loads which are caused by the complex aerodynamic environment and blade response to oscillatory loads. On the other hand the indirect approach benefits from the relationship between the blade natural frequencies and aerodynamic excitation frequencies instead of direct load calculation. These direct and indirect approaches were referred to as "Hub Loads Minimization" and "Natural Frequency Separation" respectively.

### 2.2.1 Natural Frequency Separation

The calculation of blade natural frequencies is critical in the determination of blade dynamic characteristics. The problem of finding the natural frequencies is a free vibration problem for rotating beams and the knowledge on the blade equations of motion is essential. The helicopter main rotor blades are characterized by slender, elastic beams which are usually subjected to high-speed angular rotation. Generally, the blades are twisted; the mass and stiffness values are variable over the blade. The elastic axis and center of mass are usually separated with an offset and application of non-structural masses is quite common. In addition to the problems arising from the blade geometry, even at usual operating conditions the blades are under a significant centrifugal force field which varies over the blade. This centrifugal force has stiffening effect on the blade and dominates the dynamics of the blade. The dynamic analyses of blades show considerable difficulties because of all these geometric, elastic and inertial effects. In order to achieve a successful blade model these elastic, inertial and coupling effects should be treated carefully.

Important theoretical studies have been conducted on the rotor blade motion by deriving the equation of motion by including the rotor blade characteristics. Due to the slenderness of the blade, most of the studies assume the engineering beam theory. The equations can be derived by using Newtonian approach or energy approaches. Linear analyses of isotropic non-uniform blades with elastic and inertial coupling were performed by Houbolt and Brooks by using Newtonian end energy approaches [46]. The blade was free to bend out of the rotor

plane and in the rotor plane and free to twist under applied loadings. Galerkin and Rayleigh-Ritz methods of solving the equations were discussed and illustrated over examples.

Hodges and Dowell worked on blade equations including non-linear terms [47]. Both Newtonian and energy approaches were used. Application of an ordering scheme in the equations of motion neglected the squares of bending slopes, torsion deformation, c/R (chord over radius) and h/R (blade thickness over radius) with respect to unity. All other non-linear terms were retained which makes the equations exact up to second order. Therefore equations were valid for blades having mass and tension axes offsets from elastic axis, non-uniform cross section mass, inertia and stiffness distributions, variable blade geometry and a small precone angle. Most of the helicopter blade analyses refer to the works of Hodges and Dowell as well as that of Houbolt and Brooks.

The natural frequencies of a rotor blade could be calculated by ignoring the effects of aerodynamic forcing and solving the equations for free harmonic response as the blade was in in-vacuo condition. Even these equations were quite complicated and cannot be solved analytically. Then, several computational tools have been developed. For example, CAMRAD JA solves equations by Galerkin method [44], JANRAD uses lumped parameter method [48], UMARC [49] and CAMRAD II [50] discretize equations by finite element method. FLIGHTLAB [51] and DYMORE [52] follow a different procedure by using finite element based multibody dynamics approach. Among these rotorcraft tools, in this thesis CAMRAD JA has been selected as the analysis tool.

The dynamic analysis of CAMRAD JA follows the work of Houbolt & Brooks [44]. Assuming a high aspect ratio, the coupled flap-lag and torsion of a blade with large pitch and twist were modeled for a single load path, rotating Euler-Bernoulli beam. A concentrated-mass with a chordwise offset was allowed at the blade tip. The natural frequencies were calculated by using Galerkin method. Bending modes, which were composed of flapwise banding and chordwise bending were coupled whereas torsion modes were uncoupled. Hinged and cantilever blade root conditions could be treated.

The knowledge of interaction of natural frequencies with the excitation frequencies is critical. In rotorcraft studies, it is a common practice to identify frequencies in non-

dimensional form. Then the fundamental frequency in non-dimensional form is defined as 1/rev. The aerodynamic excitation occurs at frequencies which are the integer multiples of rotor angular speed (n(1/rev)=n/rev, n=1,2,3…) which are called the rotor harmonics [3]. The main causes of the excitation are the cyclic pitch input, velocity distribution over rotor disc due to forward flight, blade stall, motion induced loads and the vortex interactions between blades and fuselage. Any coincidence of these aerodynamic excitations and the blade natural frequencies causes excessive vibrations and load amplification on the rotor and these rotor vibrations are transferred to the fuselage [1].

Natural frequency separation method is very advantageous if the rotor aerodynamic model is unreliable for high frequency load computations or computationally too expensive. The excitation frequencies are irrespective of the magnitudes of the aerodynamic loads and are always the integer multiples of the rotor angular speed ($\Omega$). Since the natural frequencies of blade should not come close to those excitation frequencies, the blades can be designed for reduced vibrational level by natural frequency separation approach [1]-[2]. Since blade natural frequencies are evaluated for the in-vacuo condition, the solution of the rotor aeroelastic motion is not required.

### 2.2.2 Hub Loads Minimization

Second method of vibration reduction is the direct calculation of hub loads which can be performed with an overall rotor evaluation including aerodynamic and structural dynamic models. The complex dynamic and aerodynamic operation environment of the helicopter rotor was explained in Section 1.2. The blades respond to oscillatory aerodynamic loads which in turn cause oscillatory blade motion. This interaction between excitation and response generates the dynamic loads at the blade root. The dynamic blade loads from each rotor blade root are integrated at the rotor hub and that overall dynamic loads at the rotor hub excite the body and cause helicopter vibration. Figure 12 presents the representative rotating and non-rotating coordinate systems and related force and moments.

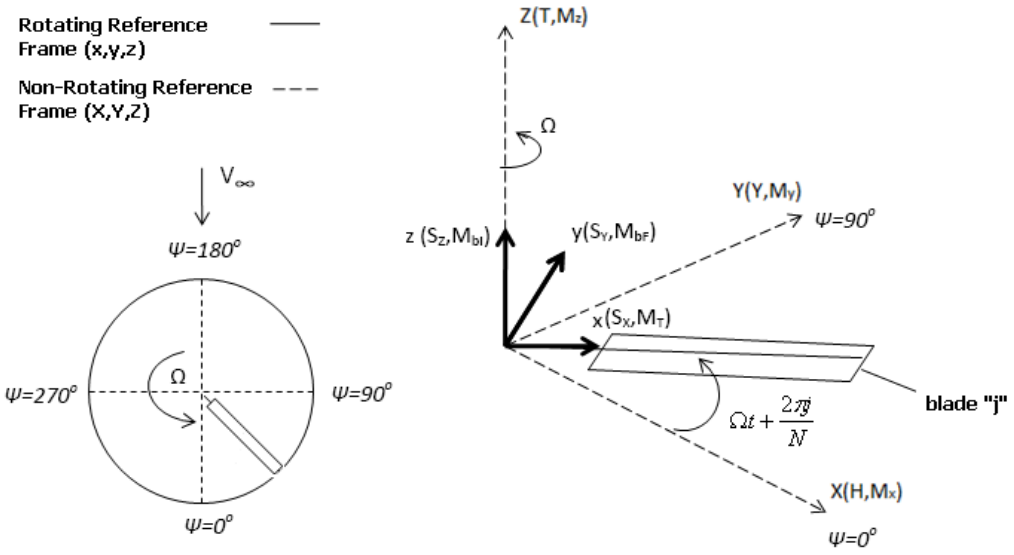


**Figure 12:** Hub and Blade Reference Frames and Vertical Shear Forces

Rotating coordinate system rotates with blade whereas the hub reference frame is fixed on the rotor hub as given in Figure 12. In order to define the loads transferred at the hub, rotating blade loads including three force and moment components should be integrated at the hub origin. H, Y and T represent longitudinal, lateral and vertical hub forces and $M_X$, $M_Y$ and $M_Z$ represent rolling, pitching and yawing hub moments at the non-rotating hub reference system. Force and moment contributions from each blade root in the rotating hub reference frame are identified by $S_X$, $S_Y$, $S_Z$ and $M_X$, $M_{bF}$, $M_{bl}$ respectively. $S_X$, $S_Y$, $S_Z$ represent the shear forces and $M_T$, $M_{bF}$ and,$M_{bl}$ represent the moments in radial, flapwise and chordwise directions. The subscripts *0*, *nc* and *ns* defines the steady, n$^{th}$ cosine and n$^{th}$ sine contributions respectively. Total hub loads are calculated by integrating these blade root loads at the rotor hub. For illustration of the hub loads calculation procedure, if blade vertical root shear and vertical hub forces of Figure 12 is considered[3];

$$T = NS_{Z0} + \sum_{n=1}^{\infty}\left\{\sum_{j=1}^{N}\left[S_{Znc}\cos n\left(\Omega t + \frac{2\pi j}{N}\right) + S_{Zns}\sin n\left(\Omega t + \frac{2\pi j}{N}\right)\right]\right\} \tag{3}$$

By using proper trigonometric summation;

$$T = N\left\{S_{Z0} + \sum_{n=1}^{\infty}\delta_{n(kN)}\left[S_{Znc}\cos n(\Omega t) + S_{Zns}\sin n(\Omega t)\right]\right\} \tag{4}$$

where k is integer, N is number of blades, n is integer harmonics. The Kronecker delta formulation is;

$$\delta_{ij} = \begin{cases} 1; i = j \\ 0; i \neq j \end{cases}$$

Since other force and moment components are also vector quantities, similar integration and trigonometric properties yields the set of hub equations [3];

$$H = \frac{N}{2}\left\{ -S_{Y1s} + \sum_{n=1}^{\infty} \delta_{n(kN)} \left[ \left( S_{Y(n-1)s} - S_{Y(n+1)s} \right) \cos n(\Omega t) + \left( -S_{Y(n-1)c} + S_{Y(n+1)c} \right) \sin n(\Omega t) \right] \right\} \tag{5}$$

$$Y = \frac{N}{2}\left\{ S_{Y1c} + \sum_{n=1}^{\infty} \delta_{n(kN)} \left[ \left( S_{Y(n-1)c} + S_{Y(n+1)c} \right) \cos n(\Omega t) + \left( S_{Y(n-1)s} + S_{Y(n+1)s} \right) \sin n(\Omega t) \right] \right\} \tag{6}$$

$$T = N\left\{ S_{Z0} + \sum_{n=1}^{\infty} \delta_{n(kN)} \left[ S_{Znc} \cos n(\Omega t) + S_{Zns} \sin n(\Omega t) \right] \right\} \tag{7}$$

$$M_X = \frac{N}{2}\left\{ M_{bF1s} + \sum_{n=1}^{\infty} \delta_{n(kN)} \left[ \left( -M_{bF(n-1)s} + M_{bF(n+1)s} \right) \cos n(\Omega t) + \left( M_{bF(n-1)c} - M_{bF(n+1)c} \right) \sin n(\Omega t) \right] \right\} \tag{8}$$

$$M_Y = \frac{N}{2}\left\{ -M_{bF1c} + \sum_{n=1}^{\infty} \left[ \left( -M_{bF(n-1)c} - M_{bF(n+1)c} \right) \cos n(\Omega t) + \left( -M_{bF(n-1)s} - M_{bF(n+1)s} \right) \sin n(\Omega t) \right] \right\} \tag{9}$$

$$M_Z = -N\left\{ M_{bI0} + \sum_{n=1}^{\infty} \delta_{n(kN)} \left[ M_{bInc} \cos n(\Omega t) + M_{bIns} \sin n(\Omega t) \right] \right\} \tag{10}$$

When the blades are uniform and equally spaced, some frequencies of the blade root loads are cancelled at the hub. Direc delta function of *n* and *kN* in Equations 5-10 shows that for equally spaced rotors, the rotor acts as a filter and only harmonic loads at integer multiples of rotor (*kN/rev*) speed are transferred to hub as vibratory loads. For the vertical hub loads, only *kN/rev* harmonics of blade loads contribute to *kN/rev* vertical hub loads whereas for in-plane loads *(kN-1)/rev* and *(kN+1)/rev* harmonics of blade loads contribute to *kN/rev* hub loads. It is also important to observe that the blade root tension force and twisting moment are totally cancelled and has no contribution on the hub loads.

Due to the filtering characteristics of the rotor, engineers consider vibratory loads at *kN/rev* frequency in order to approach a jet-smooth flight. The lower the vibratory loads, the smaller the level of fuselage vibrations. That effectively means the dynamic loads at the frequency of integer multiples of blades per cycle (*kN/rev*) should be decreased. Generally higher frequencies have very small amplitudes therefore it is usually enough to consider *N/rev* loads [42].

Due to the periodic nature of the rotor, it is common practice to represent hub loads by sine and cosine components and functions of rotor angular coordinate ($\Psi$). Therefore the hub load equations in time domain can be formulated in rotor disc angular coordinate domain for a rotor with *N* blades at *N/rev* frequency as;

$$H(\psi)_{N/rev} = H_{N,c}\cos N\psi + H_{N,s}\sin N\psi \tag{11}$$

$$Y(\psi)_{N/rev} = Y_{N,c}\cos N\psi + Y_{N,s}\sin N\psi \tag{12}$$

$$T(\psi)_{N/rev} = T_{N,c}\cos N\psi + T_{N,s}\sin N\psi \tag{13}$$

$$M_X(\psi)_{N/rev} = MX_{N,c}\cos N\psi + MX_{N,s}\sin N\psi \tag{14}$$

$$M_Y(\psi)_{N/rev} = MY_{N,c}\cos N\psi + MY_{N,s}\sin N\psi \tag{15}$$

$$M_Z(\psi)_{N/rev} = MZ_{N,c}\cos N\psi + MZ_{N,s}\sin N\psi \tag{16}$$

The three force and three moment components of vibratory hub loads excite the fuselage at every kN/rev frequency. The fuselage response to these vibratory loads causes the vibration

of the airframe. In addition to airframe structure other components in the non-rotating frame such as avionics, flight crew and passengers and payload are also affected.

As opposed to "Natural Frequency Separation method that was discussed in Section 2.2.1, "Hub Loads Minimization" has the advantage of the contribution of vibratory loads that are of aerodynamic origin. The exact values of the loads to be minimized provide better physical insight into the problem.

## 2.3 Rotorcraft Comprehensive Analysis

Section 1.2 presented that the rotorcraft analysis exhibit difficulties because of the dominancy of main rotor and complex operation environment including high level of dynamic, structural and aerodynamic interactions. Due to this complex behavior of rotorcraft, it is essential to design the rotorcraft by using a single code which is capable of simulating this sophisticated flight environment within reliable accuracy and short computation times [53]. This type of analysis is called comprehensive analysis and widely used in rotorcraft industry. They are specifically written for rotorcraft analysis purposes. To be named as comprehensive, a tool should have the capability of following capabilities;

- Aerodynamics of rotor, inflow modeling, wake modeling
- Structural dynamic modeling of blade, natural frequency calculation, blade response to aerodynamics loads
- Trim model of rotor and fuselage
- Evaluation of static and dynamic loads
- Solution of the equations of motion
- Fast computation
- Reliable results

These items are essential for analysis of rotor dynamics. Additional analysis like flutter, gust response, maneuvering flight, noise analysis and transient analysis have also been included for a wider range of analysis. There are few tools that have comprehensive analysis capacity of rotorcraft. CAMRAD, FLIGHTLAB, DYMORE and UMARC are the most popular ones used in industry and academic studies.

Because of the available license of Turkish Aerospace Industries (TAI), CAMRAD JA was selected as the helicopter analysis platform of this thesis. CAMRAD is the acronym for comprehensive analytical model of rotorcraft aerodynamics and dynamics [44]. Analysis capability includes calculation of rotor performance, loads and noise; helicopter vibration and gust response; flight dynamics and handling qualities and system aeroelastic stability. This capability provides a compound tool for a wide range of rotorcraft configurations at many different flight conditions which makes it a very suitable tool for rotorcraft optimization purposes.

## 2.4 Optimization Program for Minimum Vibration

In a design or modification activity, there are different solutions all of which can meet the requirements. However in terms of performance, safety, comfort, cost and market share considerations any possible design is not enough and tradeoff analyses should be performed between aforementioned factors. The process of performing the tradeoff in the best way is called optimization and very commonly used in engineering [54]. An optimization problem can be stated as in the Equation 17 [55];

Find $X=\{x_1, x_2,\ldots x_n\}$ which maximizes f(X) (17)

subjected to the constraints

$$g_j(X) \le 0,\ j = 1,2,...,m \quad and \quad l_i(X) = 0,\ i = 1,2,...,p \tag{18}$$

where $X$ is termed the design vector which include $n$ design variables, $f(X)$ is called the objective function, $g_j$ and $l_i$ are inequality and equality constraints. The design vector and objective function are essential in an optimization problem whereas constraints are optional depending on the physics of the problem.

An engineering product involves two sets of vectors which are pre-assigned parameters and design variables [55]. The pre-assigned parameters are kept constant during the design activities whereas the parameters which can be altered are termed as the design variables. A predefined function of the design variables is called the objective function which is the criterion of selecting the best design among other possible ones. An optimization problem

can have a single objective function or multiple functions which are required to be minimized at the same time.

In optimization analysis, the design space should be limited in order to avoid the likely occurrences of possible unrealistic results. Limitations can be applied on some specific behavior of the system or on the design variables. Former is called the behavior or functional constraint and the latter is termed as the side or geometric constraint.

Various optimization techniques have been implemented to engineering applications. There are purely mathematical like gradient base algorithms and techniques that inspired from other branches of science such as the genetic algorithm. While the former make use of the derivatives of objective functions with respect to design variables [55], the latter benefit from the "survival of the fittest" principle of evolution theory [54]. The work of Babu and Onwubolu provides detailed information on the new techniques of engineering optimization together with the applications [54].

Gradient based optimization algorithm CONMIN was selected as the optimization algorithm in this thesis [56]-[57]. Linear and non-linear optimization problems can be solved by using method of feasible directions. The code is in subroutine form and any external analysis code can be implemented. The analysis code provides the values of the objective function and the functional constraints whereas CONMIN supplies the design variables to the analysis code. The gradients of the objective function can be explicitly provided or CONMIN can evaluate by using the finite difference method.

## 2.5 Analysis and Design Procedure for Minimum Vibration

The aim of this thesis was to couple an optimization process with a comprehensive analysis tool for reduced vibration levels by using the methods that were discussed in Section 2.2 and implement the procedure on different blades. An optimization procedure was developed which is outlined in Figure 13.

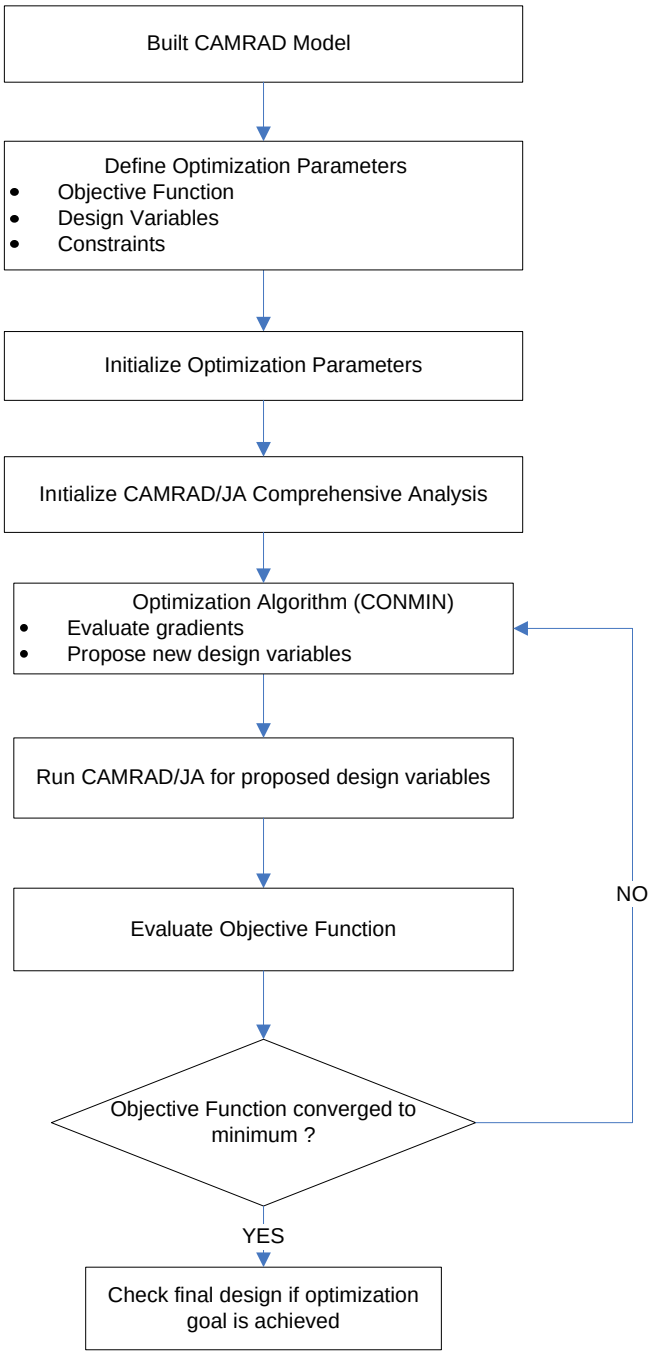


**Figure 13:** Design Procedure for Reduced Vibration Level

According to the procedure given in Figure 13, the CAMRAD comprehensive analysis model of the analysis configuration is built. The analysis model is expected to operate in trimmed condition which is achieved by CAMRAD JA trim analysis and the vibratory loads are evaluated for this trimmed helicopter. For the natural frequency separation approach only blade structural dynamics model is required.

The optimization problem is defined with objective function, constraints and design variables. The objective function is the model output which is aimed to be minimized; constraints are selected in order to prevent the unrealistic results and design variables are the proper model inputs which are the most sensitive to the optimization problem. In this procedure, the objective function and constraints are the analysis outputs of the CAMRAD JA. The design variables are selected among the CAMRAD JA model inputs.

Once the model and analysis parameters are defined, the coupled analysis of CAMRAD JA and CONMIN starts. CONMIN can either evaluate gradients by using finite differences method or in a user provided manner. In this thesis, finite difference equations of CONMIN were used. Optimization algorithm evaluates the gradients of the objective function and functional constraints that are supplied from CAMRAD JA outputs. Based on the evaluated gradients, CONMIN provides new guesses on design variables to CAMRAD JA and the values of objective function and constraints are updated. This process continues until the objective function converges to a stable value within a prescribed limit.

# CHAPTER 3

# CASE STUDIES

The rotor, its operation environment and the helicopter vibration problem were introduced in CHAPTER 1 and the importance of the rotor in helicopter flight and its dominance on helicopter dynamics were discussed. CHAPTER 2 dealt with the analysis and design approaches of reducing the rotor induced rotorcraft vibration problem by the application of CAMRAD JA comprehensive rotorcraft analysis and CONMIN gradient based optimization algorithm. In this chapter, the approaches described in reducing rotor induced vibration were illustrated.

Two methods of vibration reduction were used in order to minimize the vibratory loads transmitted to the fuselage as were described in Section 2.2. As an indirect method, isolated blades were designed by natural frequency separation. This method was applied on two different isolated blades. First blade was articulated blade based on SA349/2 and second one was hingeless blade based on Westland Lynx Blade. Natural frequency calculation did not require any aerodynamic and trim analysis therefore they were excluded from CAMRAD comprehensive models. Direct method in minimizing the vibratory hub loads included aerodynamic, blade response and trim analysis in addition to the blade natural frequency calculation. Full helicopter model of SA349/2 was analyzed which included 6 degrees of freedom free flight trim of fuselage, rigid and elastic rotor dynamics, aerodynamics of the rotor and the fuselage.

Design constraints on the blade mass, auto-rotational inertia and blade natural frequencies were applied to both approaches in order to avoid the likely occurrences of possible unrealistic results. Reduction in vibration can be achieved by designing the blade for proper mass and stiffness properties. Because of this reason parameters which are directly related to

blade mass and stiffness should be limited in order to preserve performance and safety. For aeronautical structures, any increase in structural mass causes reduction in payload and maneuvering capacity. Besides, blade tension load is directly dependent on centrifugal load which is caused by the rotating blade mass. Therefore an upper limit was set for the blade mass so that significant effect of blade mass on helicopter performance can be prevented.

Another critical parameter is the blade mass moment of inertia which determines the rate of deceleration in rotor angular speed in case of an engine failure. Equation 19 presents the autorotative index formulation which is the ratio of rotor kinetic energy divided by the fuselage weight [59];

$$AI = \frac{I_b \Omega^2}{2W} N \tag{19}$$

where;

$AI$ : (Autorotative Index)

$I_b$ : (Blade Mass Moment of Inertia)

$\Omega$ : (Rotor angular Speed)

$W$ : (Helicopter Weight)

$N$ : (Number of Blades)

For a helicopter rotor the larger the autorotative index formula shows that the larger the rotor kinetic energy relative to the aircraft weight therefore the lower the autorotational rate of descend. The optimization analysis focused on the blades and number of blades, rotor angular speed, and helicopter weight were all kept constant. Therefore blade mass moment of inertia of the optimum blade should not be lower than that of initial design in order to preserve autorotation performance.

The third design constraint was applied to blade natural frequencies which should be separated from aerodynamic excitation frequencies. That separation prevents resonant blade operation and load amplification as it was explained in Section 2.2.1. Then, because of these performance and safety considerations, blade mass, mass moment of inertia and natural frequencies were limited so that a feasible design could be achieved.

## 3.1 Helicopter Rotor Blade Design and Modification by Frequency Separation

### 3.1.1 Introduction

The knowledge of interaction of natural frequencies with the excitation frequencies is critical which was discussed in Section 2.2.1. The aerodynamic excitation occurs at frequencies which are the integer multiples of rotor angular speed (n(1/rev)=n/rev, n=1,2,3…) Any coincidence of these aerodynamic excitations and the blade natural frequencies causes excessive vibrations on the rotor and these rotor vibrations are transferred to the fuselage. The critical integer multiples are usually the lower ones because of the low amplitudes of the higher frequencies [8]. For a single main rotor helicopter the resonances up to 5/rev are critical [1]. 6/rev can also be added to be conservative. In this thesis, the higher harmonics of excitation forces after 6/rev were assumed to be negligible.

The blade can be designed in such a way that the blade natural frequencies should not be in spectrum of excitation at normal operating speed which is commonly encountered in rotorcraft industry [1]-[2]. For this purpose, comprehensive analysis and optimization algorithms can provide fast and effective solution. According to the optimization procedure of this thesis, rotating blade natural frequencies were calculated with CAMRAD JA whereas optimization tasks were performed by CONMIN.

The blade natural frequency separation analysis was applied on two blade designs. One of the blades was articulated based on Gazelle SA349/2 Helicopter [60] while the other one was selected as a hingeless one based on Westland Lynx [61]. The dimensions of the blades and the inertial and elastic properties of blade root were remained unchanged. The outer blades were tried to be optimized for separated natural frequencies and the effect of optimization on blade rotational speed range was investigated. The results of the optimization analyses were discussed.

### 3.1.2 Application on an Articulated Blade

Blade articulation is necessary to relieve the bending moment at the root of the blade in forward flight [1]. An articulated blade which was first introduced by Juan de la Cierva in 1920s provides a simple and an effective solution to this problem so that it makes the forward flight possible. The idea was to let the blade freely move up and down so that the bending moments at the blade root can be eliminated which in turn prevents the transfer of rolling moment to the fuselage. Figure 14 provides a typical articulated blade-hub connection.

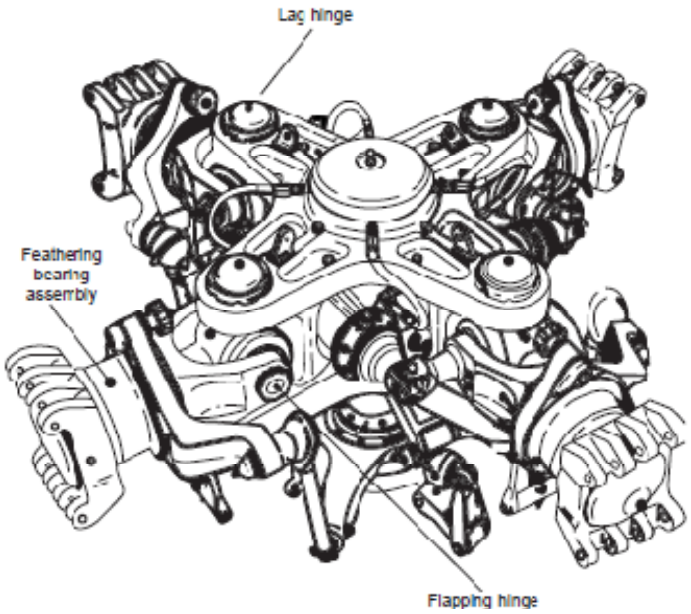


**Figure 14:** A Typical Articulated Blade [8]

The hinges allow the blade to move in flapwise and lagwise directions. The other relative motion is provided by the feathering bearing around which blade pitching motion is performed. In addition to the hinges, a damper in lead-lag direction is always added to the blade root in order to damp Coriolis forces and prevent ground resonance instability [1].

Although the relief of moments at root prevents rolling motion of rotor; the bending moment cannot be transferred to the fuselage because of hinged boundary condition and this in turn decreases the maneuvering capacity. In this case, the maneuvering loads can only be

achieved by increasing thrust and/or tilting rotor disc via cyclic input. Another disadvantage of the articulated blade assembly is the mechanical complexity due to hinges and dampers. Hinges operate under high centrifugal loads causing significant increase in maintenance costs whereas bulky rotor hub generates high parasite drag which is comparable with the drag output of rest of the helicopter [62]. Nevertheless the articulated blades are the most frequently used designs in helicopters.

In this articulated blade analysis, in order to work on a realistic case, the articulated blade of SA349/2 was selected as the basis and the blade radius, rotor angular speed, chord length were directly used. The design of blade root is usually dominated by limit loads and this part is quite stiffer than the outer blade. Hence, SA349/2 blade root was kept same with original design which included original edgewise and flapwise bending stiffness, torsion stiffness and cross section mass. The outside of this part was considered as the design region with a box beam model. Three approaches of blade design were studied. The first was to vary the beam cross section thickness distribution; the second one was non-structural mass addition and third one the combination of both. The blade was tried to be optimized for these three design variables and results were discussed. All three approaches followed the same procedure of blade optimization. Since this analysis included only natural frequency calculations; the aerodynamic calculations and trim iterations were not performed.

#### 3.1.2.1 Objective Function

In order to design a blade for the natural frequency replacement, the blade natural frequencies should be determined for a prescribed number of modes. In many helicopter analyses such as the performance or trim, the fundamental modes which are first flap and lag are usually sufficient; however in vibrational cases; the elastic bending and torsion modes should also be considered [1].

In this thesis, the modes that determine the out of plane and in-plane response are referred to as flap and lag modes respectively, whereas the modes that are related to elastic twist are referred to as torsion modes. Due to the same response characteristics the flap and lag modes are also grouped as bending modes and ranked according to their natural frequency values. In other words, if a blade mode is referred to as a bending mode it can be a flap or lag mode.

Since the higher order modes have little contribution as compared to the lower modes; the modes that have the non-dimensional natural frequency below the prescribed critical limit of 6/rev were included. Because of this criterion, critical blade modes were taken as the first 5 bending modes and the first torsional mode all of which were under 6/rev.

For this articulated rotor blade, first two bending modes are the rigid lag and rigid flapping which are called fundamental modes and the remaining are elastic modes. And the elastic modes that were below the 6/rev include two flap, one lag and one torsion modes. Figure 15 and Figure 16 show the corresponding non-dimensional mode shapes for an articulated rotor blade. According to the changes in blade mass and stiffness distribution, there may be slight local changes in mode shapes, but general trends are expected to be same.

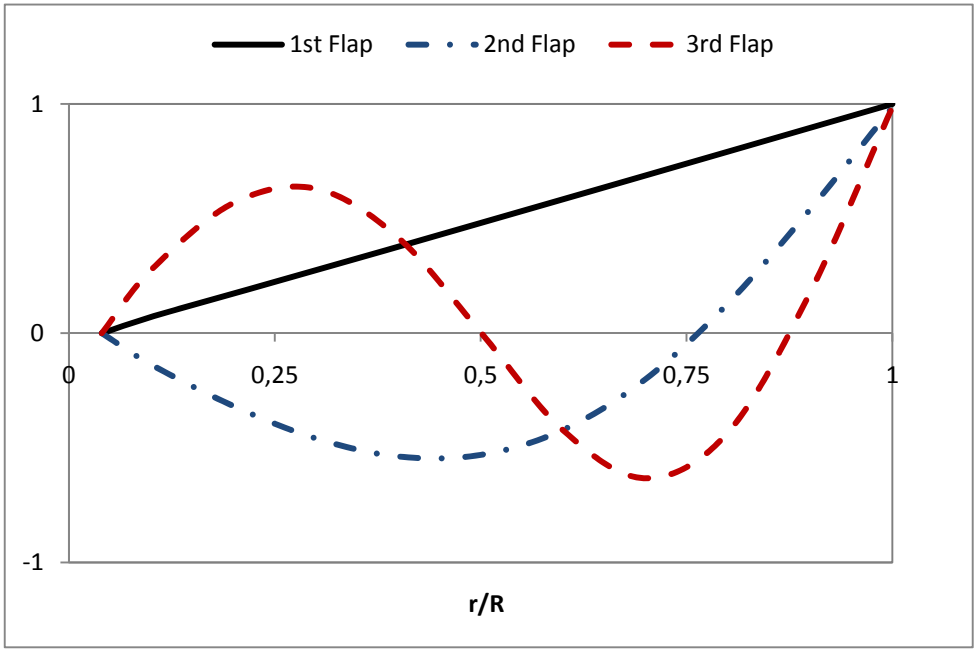


**Figure 15:** Non-Dimensional First 3 Flap Modes of Articulated Helicopter Blade

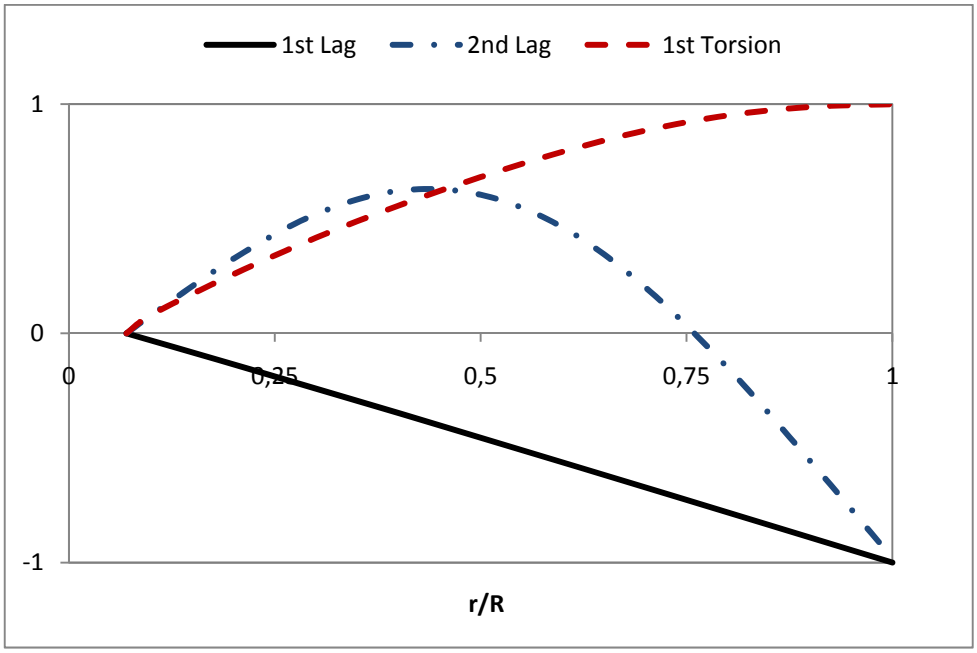


**Figure 16:** Non-Dimensional First 2 Lag and First Torsional Modes of Articulated Helicopter Blade

Between these blade modes given in Figure 15 and Figure 16, only the first flapping mode of Figure 15 which is the 2nd bending mode was excluded from the objective function formulation. This fundamental flap mode is dominated by centrifugal acceleration and very close to 1/rev which is the fundamental rotor frequency [63]. Although the operation near the resonance condition leads to large displacements, this motion is favorable because it relieves lift asymmetry and makes forward flight possible. Besides, rigid flapping motion is aerodynamically damped with a typical damping ratio of $\zeta$=0.4 which makes the mode stable [8]. Rigid lag mode is also dominated by centrifugal force and a significant change after mass and stiffness modification is not expected. However, since the aerodynamic damping is not sufficient and a possible coincidence with aerodynamic excitation is critical, it was added to the modes in the range of interest.

After the modes in the range of interest were defined, the objective function can then be stated. CONMIN can only optimize a single function; therefore the effects of these modes in the range must be formulated into a single function and that must be optimized. This can be achieved by finding the value of the minimum difference between any natural frequency and any aerodynamic excitation frequency and that can be formulated as;

$F_{obj}=Min(f_i\text{-}n/rev)$ for $1 \leq n \leq 6$ and $1 \leq i \leq 6$ (except fundamental flap) (20)

where $f_i$ and *n/rev* represent blade natural frequencies and excitation frequencies respectively for the prescribed range of interest. The optimization algorithm proposed in CHAPTER 1 tried to maximize this difference so that blade natural frequencies are out of the spectrum of aerodynamic excitations and modes are well separated from each other.

#### 3.1.2.2 Design Variables

In terms of CAMRAD files, the governing parameters of natural frequencies are the bending stiffness in flapwise and chordwise directions, torsional stiffness and mass distribution of blade cross section. These parameters can be directly selected as design variables so that the mass and stiffness distributions are directly optimized which requires extra post-processing in matching the desired distributions for the optimum design. Another option is to represent the blade with a cross section model. It is more advantageous to define these parameters with a cross section model which provides a better physical insight to the problem and can be directly implemented to the design. Therefore in order to model the mass and stiffness distributions, a rectangular isotropic cross section was assumed for the outer blade [33]. The dimensions of the blade which were chord, radius and rotor RPM were adopted from the original SA349/2 blade. The mass, inertia and stiffness values of the inner blade was taken as they originally were and the boundary between inner and outer blade was started from r/R=0.15. Figure 17 represents the cross section of the geometry.

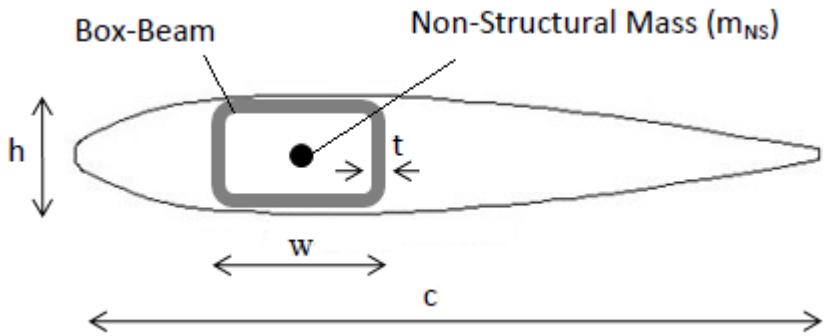


**Figure 17:** Outer Blade Cross Section for Articulated Blade

The cross section geometry of the outer blade which was determined by two constant parameters of the height (h), the width (w) and they were fixed during optimization analysis. Two variable parameters were defined as the cross section wall thickness (t) and non-structural mass ($m_{NS}$). These variable parameters were determined as the design variables of the optimization analysis were tried to be optimized in order to achieve a design having low vibration. The parameters for an aluminum blade are presented in Table 2.

**Table 2:** Outer Blade Cross Section Material and Size Properties for Aluminum Articulated Blade

| | |
|---|---|
| Young's Modulus (GPa) | 69 |
| Density (kg/m$^3$) | 2700 |
| Width-w (m) - Constant | 0.3c |
| Height-h (m) – Constant | 0.1c |
| t (cm) - Initial | 1.4 |
| Non-Structural Mass (kg/m) - Initial | 0.0 |

The blade model was defined with first 5 bending modes and 1 torsional mode for an articulated blade. Among 5 bending modes, fundamental flap mode was excluded from the objective function formulation but calculated in order to check the argument of its insensitivity to the optimization. The optimization procedure was applied on three different design variables which were cross section wall thickness distribution, non-structural mass addition and considering both of them together. The failed and successful optimization analyses were discussed.

The design variables were distributed over 6 points from radial coordinate r/R=0.15 to the blade tip. Side constraints were applied to thickness and non-structural mass values in order to avoid the likely occurrences of possible unrealistic design variables. Based on the initial design of Table 1, side constraints were applied as follows:

[0.80 cm < t < 1.80 cm] (Outer Blade Thickness)

[0.0 kg/m < $m_{NS}$ < 2.4 kg/m] (Outer Blade Non-Structural Mass)

For CAMRAD JA which solves equations of motion by using modal equations, the nodal points of the modes are an important guide in deciding the number of design variable stations. By definition, nodal points do not move in the motion of that mode. Therefore modifying the mass and stiffness parameters at the nodal points does not affect the natural frequency of the related mode. For example, it can be observed from Figure 15 and Figure 16 that the highest mode that was considered was the 3rd flap mode. Among five flap and lag bending modes, this mode was referred to as the 5th bending mode of the blade and it has three node points which does not move. If the design variable stations are determined only at these three nodal points, any improvement cannot be obtained in case of a resonant operation at 3rd flap mode. Because of this reason, a large station number should be used in order to cover all the modes in the range of interest. In order to be conservative, at least two times the number of nodal points of the highest blade mode should be selected. In this particular case, considering the highest mode has 3 nodal points, the mass and stiffness parameters were distributed over 6 points starting from radial coordinate r/R=0.15 to the blade tip.

#### 3.1.2.3 Constraints

Blade mass, blade mass moment of inertia with respect to blade root and natural frequencies were applied as the constraints for the problem. Starting design was proposed a blade mass of 45 kg and the limit was set as 60 kg for performance considerations. Blade mass moment of inertia was taken by considering auto-rotation and inertia of the blade was limited such that the final blade inertia was not lower than the initial value.

The minimum difference between the blade natural frequencies and the aerodynamic excitation frequencies was already defined in the objective function. Additionally, 0.20/rev was set as the interval such that the any two frequencies cannot be closer than that. This interval was defined as the criterion of the success while evaluating the optimization analysis. The modes of the objective formulation which were the rigid lag, 3rd, 4th and 5th bending and 1st torsion modes were taken into consideration. Table 3 presents the design constraints of the optimization problem.

**Table 3:** Design Constraints of the Optimization Problem for Articulated Blade

| Parameter | Constraint |
|---|---|
| Blade Mass (kg) | Blade Mass< 60 kg |
| Blade Inertia ($Nm^2$) | Inertia > Initial Value |
| Fundamental Lag Frequency (/rev) | 0.20/rev away from n/rev |
| $3^{rd}$ Bending Frequency (/rev) | 0.20/rev away from n/rev |
| $4^{th}$ Bending Frequency (/rev) | 0.20/rev away from n/rev |
| $5^{th}$ Bending Frequency (/rev) | 0.20/rev away from n/rev |
| $1^{st}$ Torsion Frequency (/rev) | 0.20/rev away from n/rev |

#### 3.1.2.4 Results

Optimization analyses were performed for three different design variable distribution approaches. Table 4 gives the initial and final blade mass and inertia and achieved minimum difference between the blade natural frequencies and aerodynamic excitation frequencies.

**Table 4:** Initial and Final Blade Mass, Inertia and Minimum Difference Between Modes for Articulated Blade

| | Initial | Thickness Optimization | Non-Structural Mass Optimization | Thickness & Non-Structural Mass Optimization |
|---|---|---|---|---|
| Blade Mass (kg) | 45 | 45 | 49 | 54 |
| Blade Inertia ($kgm^2$) | 410 | 410 | 425 | 458 |
| $F_{obj}$=Min($f_i$-n/rev) (/rev) | 0.01 | 0.01 | 0.20 | 0.33 |

Initial design had a mode near resonance with a 0.01/rev therefore it needed to be improved. Due to the requirement of 0.2/rev minimum difference between the modes, the optimization by using thickness distribution approach failed in solving this problem. However optimization by non-structural mass addition and thickness modification with non-structural mass addition separated the natural frequencies as required. The latter one showed better

improvement although with a heavier blade and had 0.33/rev lowest difference between any excitation frequency and any natural frequency. However when the mass increase was considered, non-structural mass optimization could be a better choice with approximately 5kg lighter blade.

Figure 18 shows a more detailed explanation of the initial and final frequencies after each optimization analysis. The horizontal lines drawn about the vertical integer values define the frequency intervals that the blade natural frequencies were limited. The frequencies of initial design and final designs of thickness optimization, non-structural mass optimization and combined thickness and non-structural mass optimization were given in that order for each mode considered.

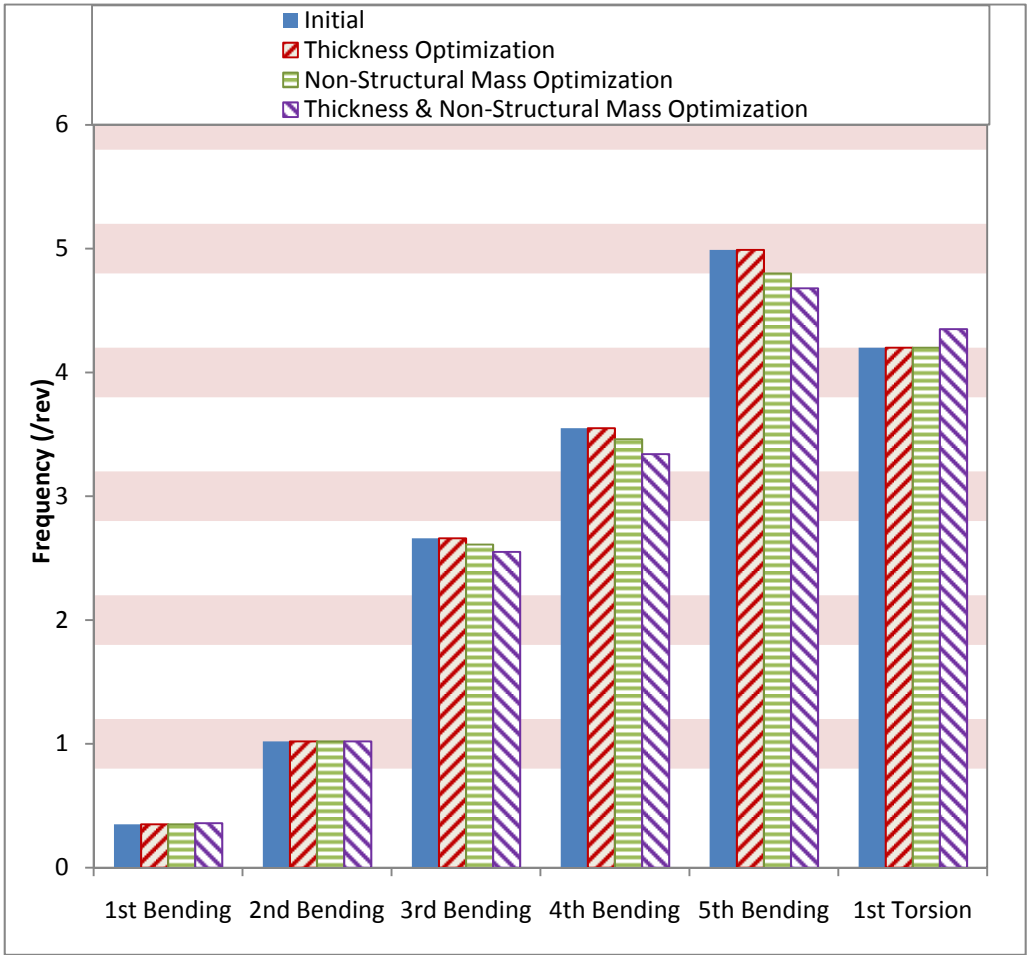


**Figure 18:** Blade Natural Frequency Spectrum of Initial and Final Designs for the Articulated Blade

It can be seen from Figure 18 that the 5th bending mode of initial design is in resonance with 5/rev aerodynamic excitation. The thickness optimization could not remove the coincidence between the 5th bending and 5/rev frequencies. However, the non-structural mass addition reduced this 5th bending natural frequency below the critical limit. The non-structural mass addition was also found to reduce the 3rd and 4th bending natural frequencies. Since non-structural mass was assumed to be added on the center of gravity of the blade, the inclusion did not affect the torsional natural frequency. The combined thickness and non-structural mass optimization caused further reduction in third, fourth and fifth bending frequencies, which were elastic bending modes; however the torsional frequency was found to increase.

As expected the 2nd bending mode which was the fundamental flap mode is near 1/rev and since could not be improved for all three approaches. This proved the dominancy of centrifugal force field on this frequency. However as stated before due to high level of aerodynamic damping this mode is highly damped preventing the mode to respond in large amplitudes. Furthermore, rigid lag mode was also dominated by centrifugal force and its initial value remained constant during the optimization analyses. However this mode was initially far from excitation frequencies therefore cannot be considered as critical in terms of rotor induced vibrations. Figure 19 gives the initial and final cross section wall thickness distributions of the blade in the range of design variable stations.

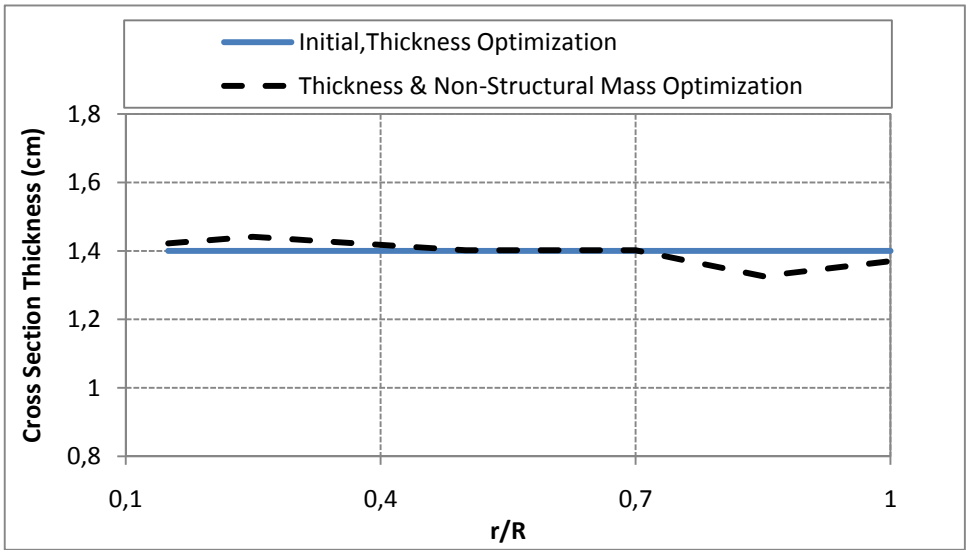


**Figure 19:** Cross Section Thickness Distribution of Initial and Final Designs for the Articulated Blade

Since the cross section wall thickness was not defined as a design parameter for the non-structural mass optimization it was excluded from Figure 19. The thickness distribution remained the same after the thickness optimization analysis. As previously mentioned, the thickness optimization failed in separating 5$^{th}$ bending and 5/rev aerodynamic excitation. This means, for this particular blade design and within the prescribed design constraints, blade natural frequencies were not sensitive to the thickness variation which caused them to stay same. Therefore the thickness distribution remained constant and the results of thickness optimization cannot be considered as optimum.

Again considering the combined thickness and non-structural mass optimization in Figure 19, there is an increase in thickness in the region where r/R varies between 0.15 and 0.5 and decrease at the tip. It should be noted that while the thickness optimization failed, the combined thickness and non-structural mass optimization became rather successful.

Figure 20 shows the blade cross section mass distribution in the radial range of design variable stations.

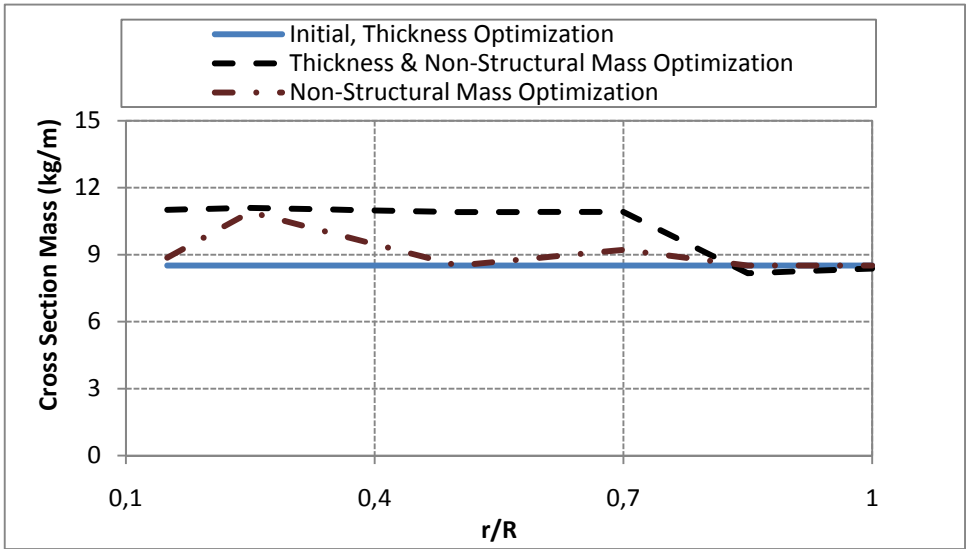


**Figure 20:** Cross Section Mass Distribution of Initial and Final Designs for the Articulated Blade

The change in mass distribution given in Figure 20 was related to the change in cross section wall thickness and the non-structural mass addition. The mass distribution did not change for the thickness optimization and consequently the thickness optimization did not yield satisfactory answers. For the combined thickness and non-structural mass optimization, the mass distribution was affected which remained constant up to r/R=0.7 and then decreased. The mass addition in the non-structural mass optimization can also be observed near r/R=0.3 and r/R=0.7.

If the mass distribution of non-structural mass addition in Figure 20 is carefully examined, the mass addition at r/R=0.5 and r/R=0.85 is zero. These points were exactly the node points of the fifth bending mode which was the third flap mode given in Figure 15. When the optimization algorithm perturbed mass addition at node points and evaluated the sensitivity of objective function, the $5^{th}$ bending natural frequency did not change and the algorithm started trying other points. This proves the efficient coupling between optimization program CONMIN and CAMRAD JA. This observation is also critical in determining the design variable stations. In this particular case if these stations were selected as the node points of the $5^{th}$ bending mode, then the optimization program would fail to improve the required design although it was possible to optimize the blade. Therefore it is essential to use a number of stations which is large enough to cover the necessary modes in the range of interest.

The optimization analyses were conducted at the normal rotor RPM. In order to see the effect of optimization over the whole main rotor RPM range Figure 21 and Figure 22 were plotted. These are Fan-Plot diagrams of initial design and final design of combined thickness and non-structural mass optimization. Solid lines represent blade natural frequencies and dashed ones are from the lowest 1/rev to the highest 6/rev excitation frequencies in increasing slope. The vertical line is the normal operation RPM at which the blade was optimized.

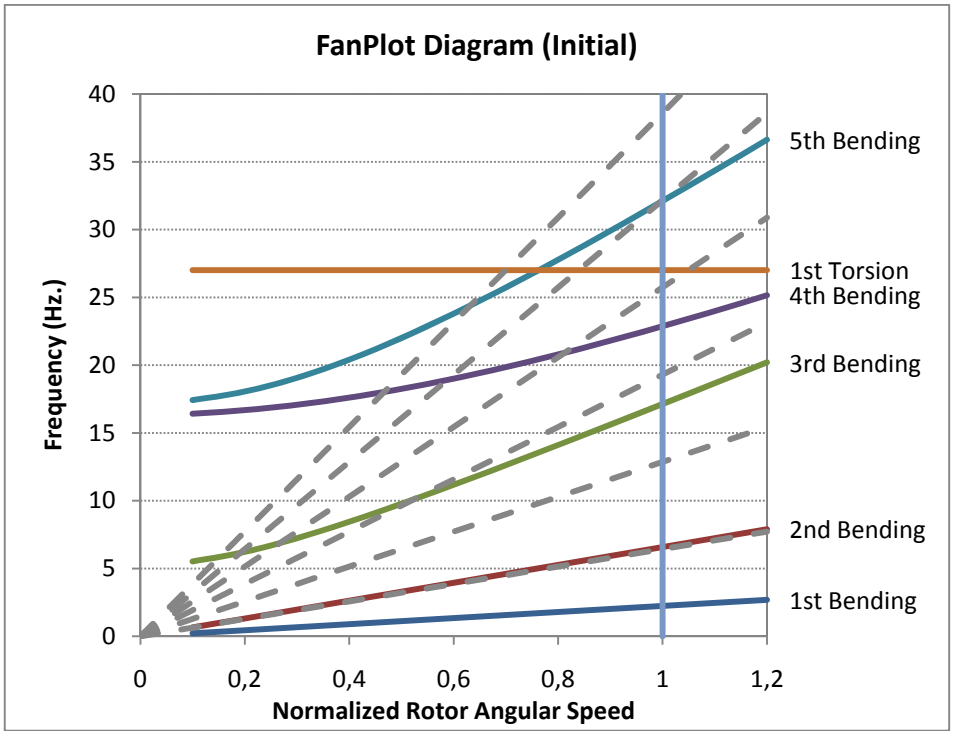


**Figure 21:** Fan-Plot Diagram of Initial Design for the Articulated Blade

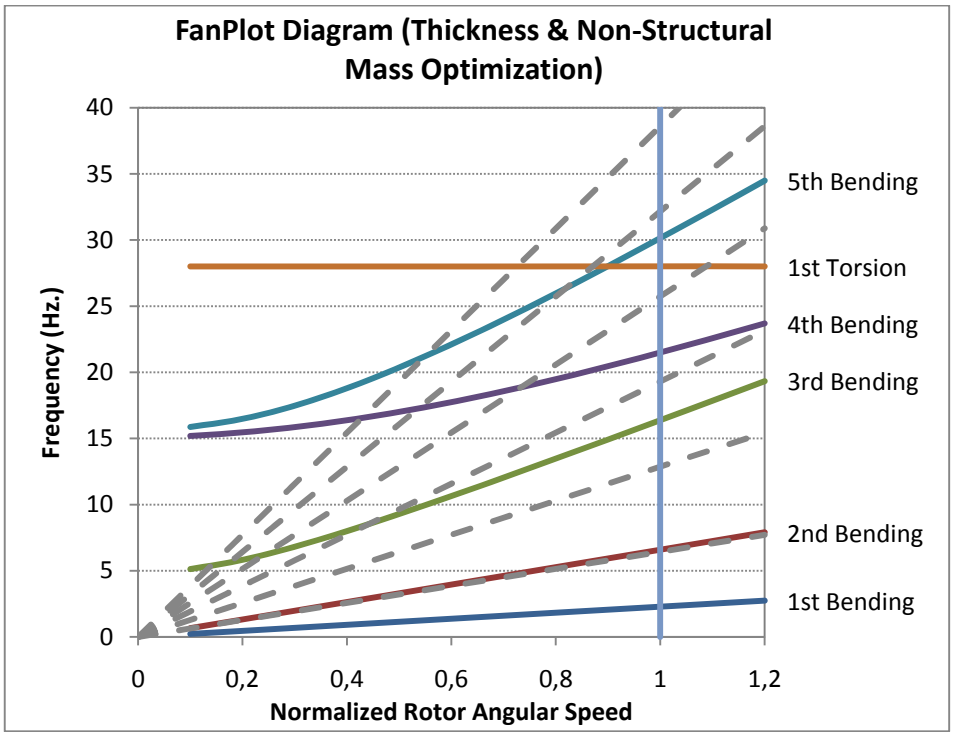


**Figure 22:** Fan-Plot Diagram of Thickness and Non-Structural Mass Optimization for the Articulated Blade

The coincidence of 5th bending mode with aerodynamic excitation line at normal RPM and its separation from 5/rev excitation frequency can be observed from the 5th mode curves of the Figure 21 and Figure 22. Both graphs have the same trends over to whole RPM range in terms of the response of natural frequency values with respect to rotor angular speed and the coincidence of natural frequencies with excitation frequencies.

Table 5 provides detailed information on the coincidence points. Real numbers represent the non-dimensional blade natural frequency whereas the integers within parenthesis represent the relevant coincident excitation frequency.

**Table 5:** Overlapping Frequencies for the Articulated Blade

| | Initial Design- Frequency ($\Omega/\Omega_0$) | Optimum Design-Frequency ($\Omega/\Omega_0$) |
|---|---|---|
| 1st Bending | - | - |
| 2nd Bending | All Range | All Range |
| 3rd Bending | 0.15(6)/0.20(5)/0.27(4)/0.55(3) | 0.14(6)/0.17(5)/0.24(4)/0.45(4) |
| 4th Bending | 0.46(6)/0.58(5)/0.80(4) | 0.44(6)/0.55(5)/0.74(4) |
| 5th Bending | 0.63(6)/1.00(5) | 0.54(6)/0.83(5) |
| 1st Torsion | 0.70(6)/0.84(5)/1.05(4) | 0.72(6)/0.87(5)/1.09(4) |

According to the similar coincident frequencies of Table 5 there is no significant difference in natural frequency characteristics except the 5th bending frequency near normal rotor speed at which the optimization was performed. This shows that the optimization at normal rotor RPM has no detrimental effect on the rest of RPM range for this particular case.

### 3.1.3 Application on Hingeless Blade

In Section 3.1.2, an articulated blade was investigated and the disadvantages of mechanical complexity and loss of control power of these rotors were briefly discussed. In order to reduce maintenance and manufacturing costs and achieve an aerodynamically clear

configuration with higher control power, hinges are replaced by flexible elements. Many modern designs have made use of this concept and Westland Lynx and Bo105 were the first two produced hingeless helicopters [63]. Figure 23 illustrates a typical hingeless blade-hub connection.

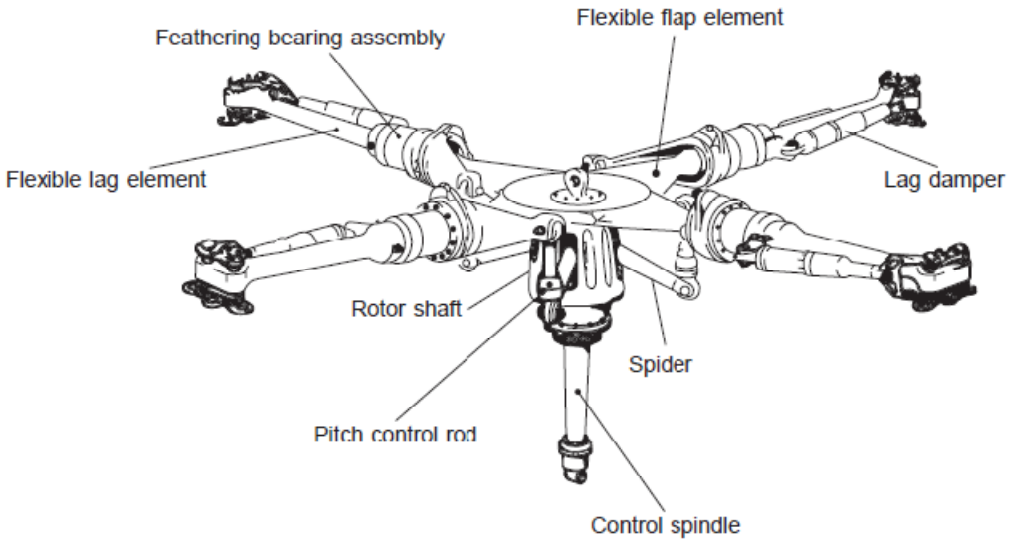


**Figure 23:** A Typical Hingeless Blade [8]

The flexible elements perform the same function of hinges but this time flapwise and edgewise bending moments are generated at the blade root. Flapwise bending moment increases the maneuvering capability of the helicopter since extra maneuvering load component in addition to the rotor thrust tilt exist. However, these flexible elements should be designed such that the moments at the blade root do not cause rolling of the fuselage and the root stresses remain under critical levels. Furthermore, as in the case of articulated blade, there is still a necessity of lead-lag damper for stability issues and a feathering bearing for blade pitching motion. Although rare yet, some designs also try to eliminate feathering bearing by torsional flexible elements which are still rare [64].

In this analysis, in order to work on a realistic case, the hingeless blade of Westland Lynx was selected as the basis and the blade radius, rotor angular speed and chord length values were directly used [61]. Additionally, the Lynx blade root was originally taken which included edgewise and flapwise bending stiffness, torsion stiffness and section mass. Like in

the analysis of the articulated blade, the outer part of the blade was considered as the design region with a box beam model. The blade was tried to be optimized for the same three design variables of articulated blade analysis, namely the cross section wall thickness distribution, non-structural mass addition and consideration of both together and results were discussed. Since this analysis included only natural frequency calculations; the aerodynamic calculations and trim iterations were excluded.

#### 3.1.3.1 Objective Function

This analysis followed the same procedure of the articulated blade and the critical blade modes were same as those of fundamental flap and lag modes; 3rd, 4th and 5th modes of bending and first torsional mode. Figure 24 and Figure 25 show the corresponding mode shapes of hingeless blade. According to the mass and stiffness distribution, there may be slight changes, but general trends would remain same.

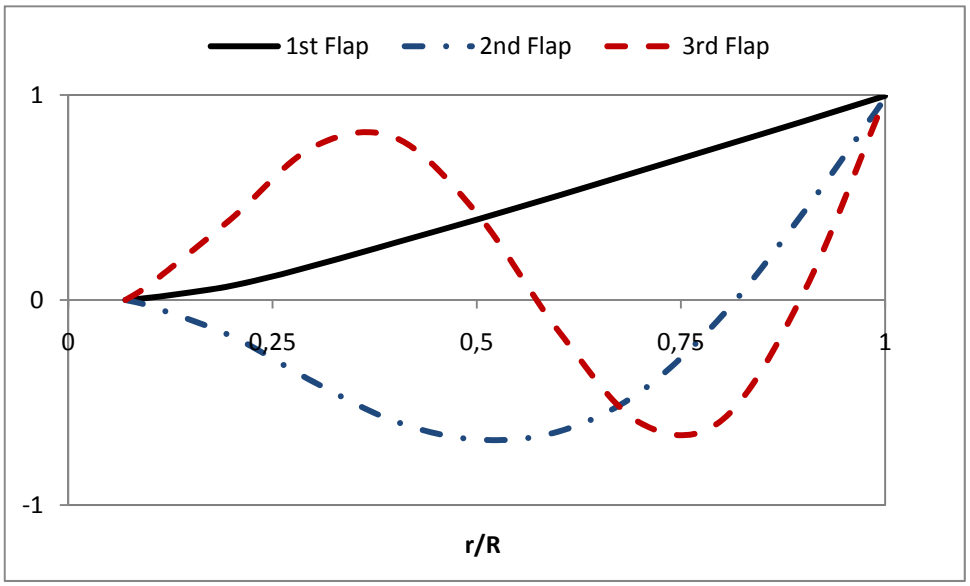


**Figure 24:** Non-Dimensional First Three Flap Modes of Hingeless Helicopter Blade

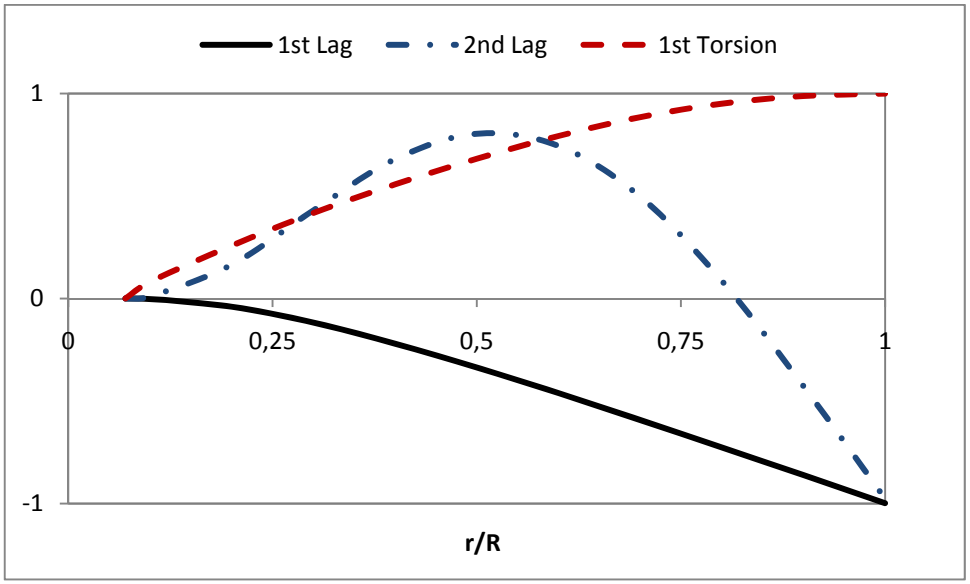


**Figure 25:** Non-Dimensional First Two Lag and First Torsion Modes of Hingeless Helicopter Blade

The difference from the articulated blade mode shapes is the zero slopes of bending modes at root so that the fundamental flap and lag modes are also elastic. This is the effect of elastic connections in providing the blade articulation which act as hinges at the blade root. Furthermore, although the fundamental modes given in Figure 24 and Figure 25 are elastic near blade root both follow rigid motion after r/R=0.15. This shows the fundamental flap mode is also critical for a hingeless blade assembly and dominated by centrifugal acceleration which makes it very close to 1/rev [63]. The discussions about the fundamental flap and lag modes of an articulated blade are also valid for a hingeless blade and therefore first flapping mode was excluded from the objective function while first lag mode was remained in the range of interest. The same objective function was used again and revisited as;

$$F_{obj}=\text{Min}(f_i\text{-n/rev}) \qquad \text{for } 1 \leq n \leq 6 \text{ and } 1 \leq i \leq 6 \text{ (except fundamental flap)} \qquad (21)$$

where $f_i$ again *n/rev* represent blade natural frequencies and excitation frequencies for the prescribed range of interest respectively.

### 3.1.3.2 Design Variables

The same outer blade cross section geometry with articulated blade analysis was selected but this time titanium was selected as the beam material. The dimensions of the blade which were chord, radius and rotor RPM were adopted from the original Lynx blade. The mass, inertia and stiffness values of the inner blade was taken as they originally were and the boundary between inner and outer blade was started from r/R=0.15. The same cross section of Figure 17 was used with different dimensions and material, it is represented in Figure 26.

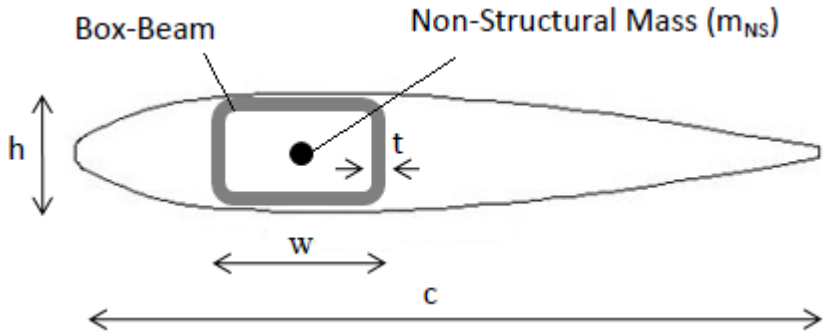


**Figure 26:** Outer Blade Cross Section for the Hingeless Blade

The cross section geometry given in Figure 26 was determined by two constant parameters which are the height (h), the width (x) and two variable parameters which are the cross section wall thickness (t) and non-structural mass ($m_{NS}$). The variable parameters were defined as the design variables of the optimization analysis were tried to be optimized in order to achieve a design having low vibration. These parameters for a titanium blade are presented in Table 6.

**Table 6:** Outer Blade Cross Section Material and Size Properties for the Titanium Hingeless Blade

| | |
|---|---|
| Young's Modulus (GPa) | 110 |
| Density (kg/m$^3$) | 4450 |
| Width-x (m) - Constant | 0.3c |
| Height-h (m) – Constant | 0.1c |
| t (cm) - Initial | 0.6 |
| Non-Structural Mass (kg/m) - Initial | 0.0 |

The blade model was defined with five bending modes and one torsion mode for an articulated blade. Among five bending modes, fundamental flap mode was excluded from the objective function formulation but calculated in order to check the argument of its insensitivity to the optimization. The optimization was performed for three different design variables which were cross section wall thickness distribution, non-structural mass addition and considering both of them together.

The design variables were distributed over six points from radial coordinate r/R=0.15 to the blade tip. Side constraints were applied to thickness and non-structural mass values in order to avoid the likely occurrences of possible unrealistic design variables. Based on the initial design of Table 6, side constraints were applied as follows:

| | |
|---|---|
| [0.40 cm < t < 1.20 cm] | (Thickness) |
| [0.0 kg/m < $m_{NS}$ < 2.4 kg/m] | (Non-Structural Mass) |

#### 3.1.3.3 Constraints

Blade mass, inertia, natural frequencies were applied as the constraints for the problem. Blade mass was chosen by considering the performance considerations. Starting design proposed a mass of 58 kg and the limit was set to 70 kg. Blade mass moment of inertia was taken by considering auto-rotation. The inertia of the blade was limited such that the final blade inertia was not lower than the initial value.

The minimum difference between the blade natural frequencies and the aerodynamic excitation frequencies was already defined as the objective function. Additionally, 0.20/rev was set as the interval such that the any two frequencies cannot be closer than that. The modes of the objective formulation which were the fundamental lag, $3^{rd}$, $4^{th}$ and $5^{th}$ bending and $1^{st}$ torsion modes were taken into consideration. Table 7 presents the design constraints of the optimization problem.

**Table 7:** Design Constraints of the Optimization Problem for the Hingeless Blade

| Parameter | Constraint |
|---|---|
| Blade Mass (kg) | Blade Mass< 70 kg |
| Blade Inertia ($Nm^2$) | Inertia > Initial Value |
| Rigid Lag Frequency (/rev) | 0.20/rev away from n/rev |
| Third Bending Frequency (/rev) | 0.20/rev away from n/rev |
| Forth Bending Frequency (/rev) | 0.20/rev away from n/rev |
| Fifth Bending Frequency (/rev) | 0.20/rev away from n/rev |
| First Torsion Frequency (/rev) | 0.20/rev away from n/rev |

#### 3.1.3.4 Results

Optimization analyses with the same objective function and same constraints were performed for three different design variable distributions. Table 8 gives the initial and final minimum difference between the modes, blade mass and inertia.

**Table 8:** Initial and Final Blade Mass, Inertia and Minimum Difference Between Modes for Hingeless Blade

| | Initial | Thickness Optimization | Non-Structural Mass Optimization | Thickness & Non-Structural Mass Optimization |
|---|---|---|---|---|
| Blade Mass (kg) | 58 | 58 | 62 | 59 |
| Blade Inertia ($kgm^2$) | 683 | 683 | 793 | 792 |
| $F_{obj}$=Min($f_i$-n/rev) | 0.02 | 0.02 | 0.05 | 0.26 |

Initial design had a mode near resonance with a 0.02/rev lowest difference between modes therefore it needed to be improved. Due to the requirement of 0.2/rev minimum difference between the modes, the analysis of the thickness distribution and non-structural mass addition could not solve this problem and their results were not considered as optimum. However thickness modification together with non-structural mass addition separated the

natural frequencies from excitation frequencies as required and an improvement were achieved with a 0.26/rev lowest separated natural frequencies from excitation and other natural frequencies. The increase in mass though was only less than 1kg.

Figure 27 shows a more detailed explanation of the initial and final frequencies after the optimization analyses. The horizontal lines drawn about the vertical integer values define the frequency interval that the blade natural frequencies were limited. The frequencies of initial design and final designs of thickness optimization, non-structural mass optimization and combined thickness and non-structural mass optimization were given in that order for each mode considered.

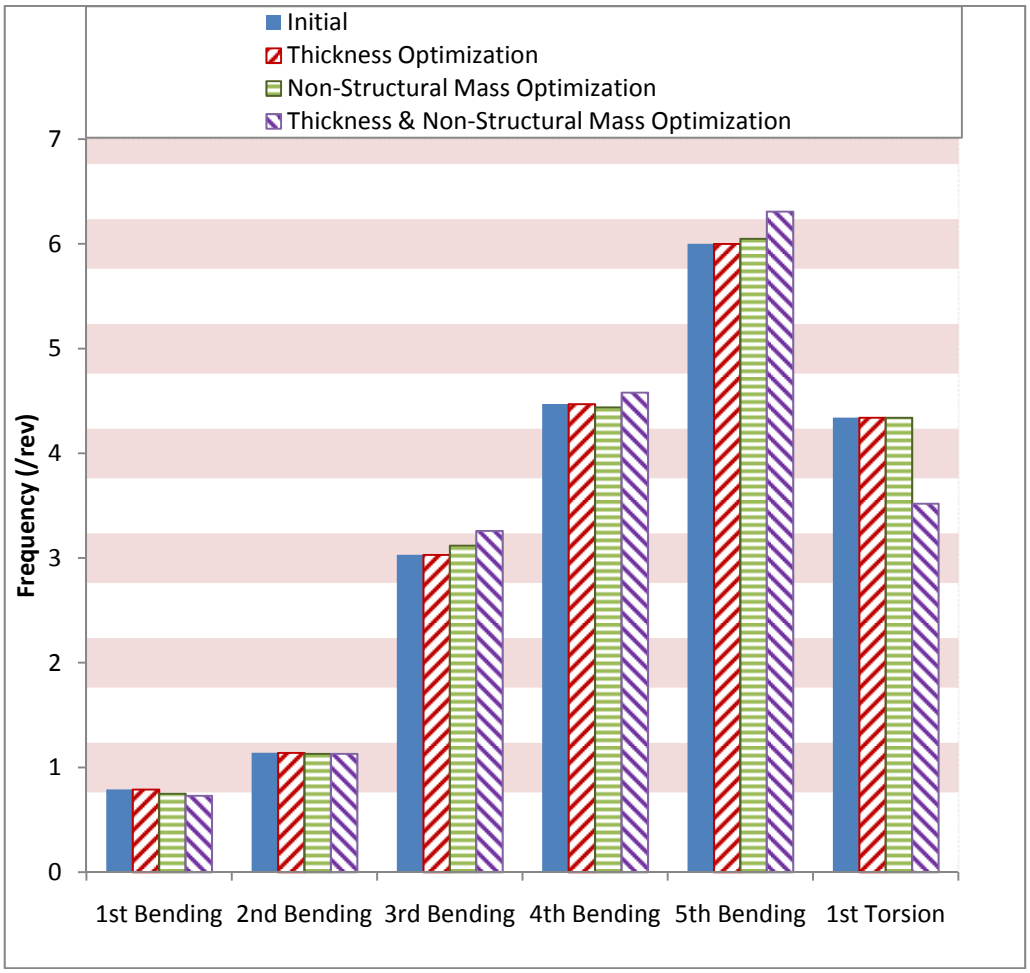


**Figure 27:** Blade Natural Frequency Spectrum of Initial and Final Designs for the Hingeless Blade

It can be seen from Figure 27 that the 3rd and 5th bending modes of initial design were within critical limits of 3/rev and 6/rev aerodynamic excitations respectively. The thickness optimization and non-structural mass optimization which failed in meeting the 0.2/rev lowest difference between modes requirement could not move these frequencies out of the critical regions. Combined thickness with non-structural mass optimization was the only successful one and this analysis increased these modes outside the critical regions while increasing 4th bending and decreasing torsional mode. Since non-structural mass was assumed to be added on the center of gravity of the blade, the inclusion did not affect the torsional natural frequency. The reduction in torsional natural frequency was believed to be due to the thickness modification. As previously mentioned and expected, the optimization could not change the fundamental flap mode.

Figure 28 gives the initial and final cross section wall thickness distributions of the blade for the radial range of design variable stations.

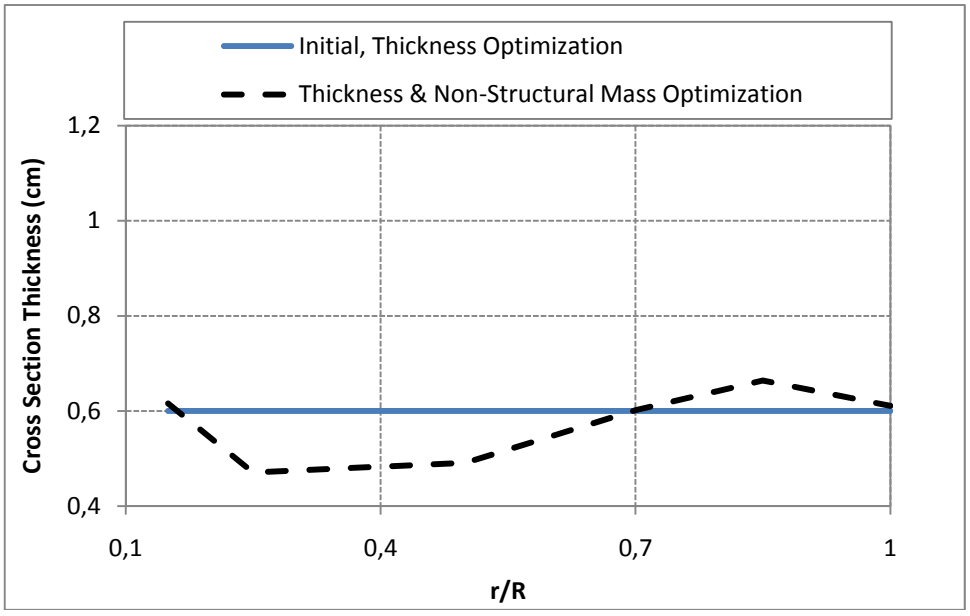


**Figure 28:** Cross Section Thickness Distribution of Initial and Final Designs for the Hingeless Blade

Since cross section wall thickness was not defined as a design parameter for the non-structural mass optimization it was excluded from Figure 28. The thickness distribution remained same after the thickness optimization. As previously mentioned, the thickness optimization failed in separating 3rd and 5th bending modes from critical limits. That means, for this particular blade design and within the prescribed design constraints, blade natural frequencies were not sensitive to the thickness optimization. Therefore the thickness distribution remained constant and the results cannot were considered as optimum. For the only successful optimization attempt, at which thickness and non-structural mass was optimized together, thickness reduced between r/R=0.15 and r/R= 0.7 and increased at the tip. The reduction at mid-points is the reason of reduced torsional rigidity and therefore reduced torsional frequency.

Figure 29 shows the blade cross section mass distribution in the radial range of design variable stations.

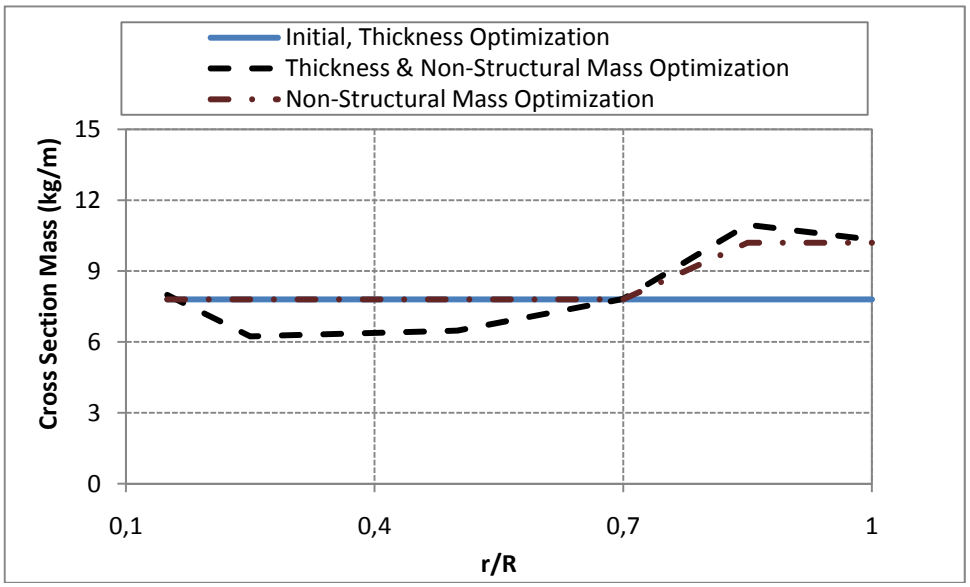


**Figure 29:** Cross Section Mass Distribution of Initial and Final Designs for the Hingeless Blade

The change in mass distribution given in Figure 29 was relevant to the change in cross section wall thickness and the non-structural mass addition. For the previously mentioned

reasons, the mass distribution did not change for the thickness optimization in Figure 29. The non-structural mass optimization remained same until r/R=0.7 and then decreased but this optimization analysis was not successful in meeting the design requirement of minimum 0.2/rev minimum difference between modes. The combined thickness and non-structural mass optimization decreased up to r/R=0.7 and then increased.

The optimization analysis were conducted at the normal rotor RPM. In order to see the effect of optimization over the whole main rotor RPM range Figure 30 and Figure 31 were plotted. These are Fan-Plot diagrams of initial design and the final design of combined thickness and non-structural mass optimization respectively. Solid lines represent blade natural frequencies; dashed ones are from the lowest 1/rev to the highest 6/rev excitation frequencies in increasing slope. The vertical line is the normal operation RPM at which blade is optimized.

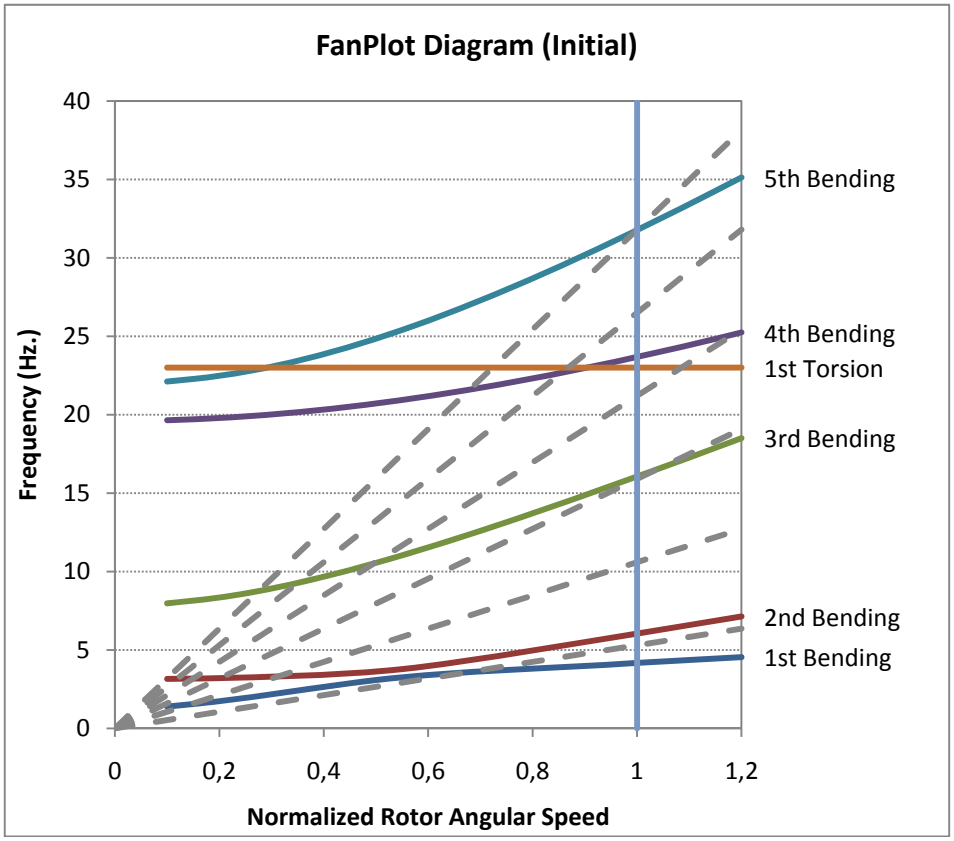


**Figure 30:** Fan-Plot Diagram of Initial Design for the Hingeless Blade

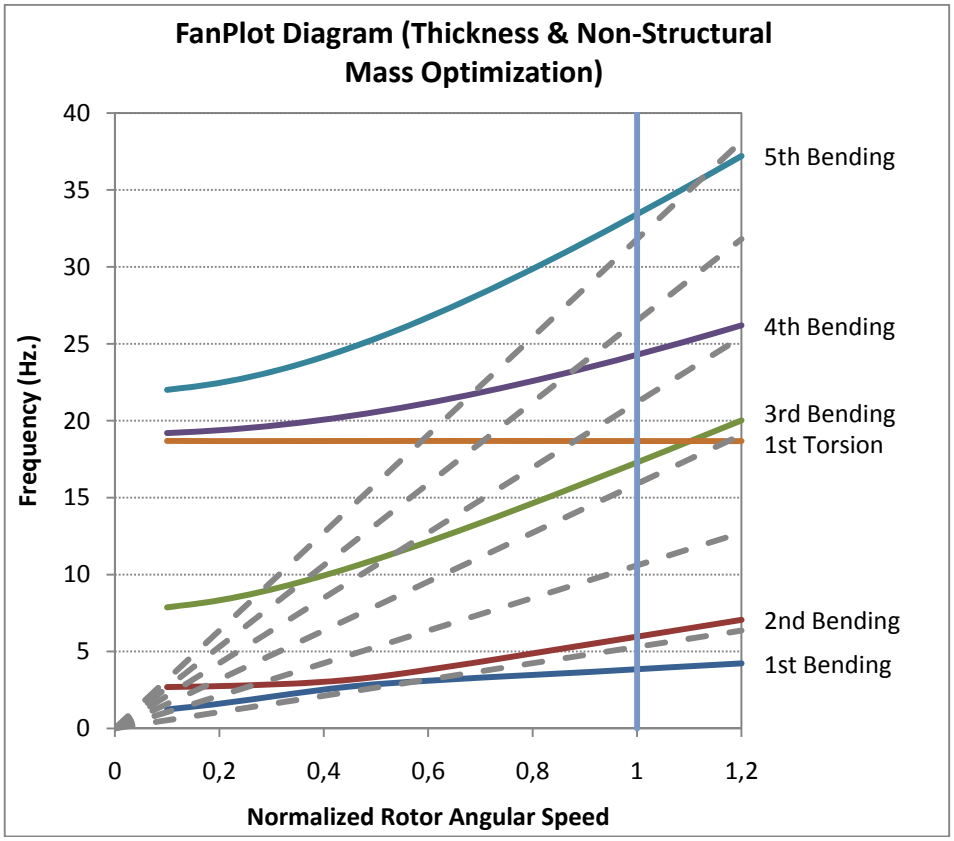


**Figure 31:** Fan-Plot Diagram of Thickness & Non-Structural Mass Optimization for the Hingeless Blade

The coincidences of 3rd and 5th bending mode curves with aerodynamic excitation lines at normal RPM can be observed in Figure 30; however the modes are separated in Figure 31 as a result of the optimization. Both graphs have the same trends over to whole RPM range in terms of the response of natural frequency values to the rotor angular speed and the coincidence of natural frequencies with aerodynamic excitation while rotor is accelerating to its normal RPM.

Table 9 provides detailed information on the coincidence points of natural frequencies. Real numbers represent the non-dimensional blade natural frequency whereas the integers within parenthesis represent the relevant coincident excitation frequency.

**Table 9:** Overlapping Frequencies for the Hingeless Blade

| | Initial Design- Frequency ($\Omega/\Omega_0$) | Optimum Design-Frequency ($\Omega/\Omega_0$) |
|---|---|---|
| 1st Bending | 0.1(3)/0.15(2)/0.69(1) | 0.13(2)/0.57(1) |
| 2nd Bending | All Range | All Range |
| 3rd Bending | 0.28(6)/0.35(5)/0.50(4)/1.00(3) | 0.28(6)/0.37(5)/0.53(4) |
| 4th Bending | 0.68(6)/0.85(5)/1.19(4) | 0.68(6)/0.88(5) |
| 5th Bending | 1.00(6) | 1.14(6) |
| 1st Torsion | 0.72(6)/0.87(5)/1.09(4) | 0.71(6)/0.88(5)/1.18(4) |

According to the similar coincident frequencies of Table 9 there is no significant difference in natural frequency characteristics except the 3rd and 5th bending frequency near normal rotor speed at which the optimization was performed. This shows that the optimization at normal rotor RPM has no detrimental effect on the rest of RPM range for this particular case.

### 3.1.4 Conclusions

In this section, the blade dynamic design by using natural frequency separation was analyzed on articulated and hingeless blades. In the study, the wall thickness of a simple box beam cross section and non-structural mass addition to the blade were the design variables. Both articulated and hingeless blades converged to an optimum design for combined wall thickness together with the addition of non-structural mass optimization. For both type of the blades, the thickness optimization alone failed whereas the non-structural mass optimization was only successful for the articulated blade. As being the objective function; the minimum difference between any natural frequency and any excitation frequency was tried to be maximized while the blade mass, inertia and natural frequencies were limited. 0.2/rev minimum offset between natural frequencies and excitation frequencies were defined as the criterion of success. The models using the natural frequency evaluation did not require neither aerodynamic nor trim analysis. The blade natural frequencies were directly evaluated for the first five bending modes and the first torsion mode. Among these modes fundamental flapping was excluded from the objective function formulation however its value was calculated in order to check the argument of centrifugal load effect on that mode. The

excitation harmonics were taken into consideration up to 6/rev and the higher harmonics were omitted from the study because of their possible negligible amplitudes.

The effects of optimization over the whole RPM range of the rotor were investigated by using fan-plot diagrams of the initial and optimum designs. The optimization analyses were successful in separating natural frequencies at normal RPM but general behavior of blade natural frequencies over the whole RPM range did not change. In other words there were still coincident blade natural frequencies and excitation frequencies at non-operational RPM values. However, it is impossible to design a blade without resonant condition over the whole RPM range. Although these resonant conditions cause load amplification at rotor run-up, it is not necessary to consider the natural frequencies at the non-operational RPM range because rotor run-up is performed on the ground [1]. It is sufficient if the natural frequencies are well separated at normal RPM of the rotor.

It is quite clear that, in addition to the blade spar and non-structural tuning mass, a blade model has more components which contribute to the dynamics of that specific blade. Two of these can be stated as the skin and honeycomb which can be taken into account in the cross section mass and stiffness calculations. Besides the cross section model can be a composite section which is also quite common. Although current analyses ignored these parameters, future models can accommodate those by using the proposed optimization scheme. For example the fly angles of a composite beam can be optimized in order to improve the aeroelastic performance.

Finally, it should be noted that, although the maximum effort was put in order to deal with the logical values; the values in the analyses were the estimations based on other optimization analyses those were examined in literature survey. In a real design process the critical loads should be determined by considering all the maneuvering loads within the flight envelope and then the cross section design limits should be determined accordingly. Besides, the manufacturing capability is another important contributor to be considered and optimized. This is actually a very lengthy process involving design standards, maneuver load analysis and computer aided design. These steps are beyond the scope of this thesis. However, once the limits are provided that aspect can also be studied for the helicopter blade optimization.

## 3.2 Blade Design and Modification for Minimum Vibratory Loads

### 3.2.1 Introduction

When the vibrations transferred to the fuselage are concerned, the consideration of the integrated effects of all blades with aerodynamic loads is more effective then considering only the effects of the blade natural frequencies. Hence the natural frequency separation method of Section 3.1 can be improved one step further by analyzing the whole rotor operation.

Due to the rotating blades at forward flight there is always harmonic excitation on the rotor as it was explained in Sections 1.2. Besides the relationship between the hub loads from blade loads was explained in Section 2.2.2. Hence the total elimination of the vibrations is virtually impossible [8]. However the blades can be designed in such a way to minimize the source of vibration. Since the vibratory loads at the rotor are the major source of helicopter vibrations, the helicopter vibratory response can be reduced by reducing the vibrations at their source.

In this section in order to decrease the vibratory loads at the main rotor, the optimization analysis described in Section 2.5 was applied to Aerospatiale Gazelle SA349/2 helicopter which was chosen because of available flight test data and detailed information about the helicopter [60]-[65]. SA349/2 analysis model included main rotor, tail rotor and fuselage together with body trim, aerodynamic loads and dynamic response calculations. During the analysis, first the validation of the analysis model was performed then the optimization analysis was conducted.

Two analyses were conducted on Aerospatiale Gazelle SA349/2 for the purpose of vibratory load minimization. In the first analysis, all design variables including the cross sectional mass, flapwise bending, chordwise bending and torsional stiffness distributions were optimized for minimum critical vibratory loads. This approach took the design of the whole cross section into account with structural components like cross section dimensions, blade material properties and non-structural mass. As opposed to the blade natural frequency separation that was performed in Section 3.1 in which a blade cross section model was used,

this approach requires post-processing in matching the proposed optimum distribution in a real blade design. This process is not within the scope of the thesis however a sample model for the way of matching the blade stiffness was discussed. In the second analysis, critical vibratory loads were tried to be minimized by the addition of non-structural mass. The effect of non-structural mass on blade stiffness was assumed to be negligible; therefore this approach does need post-processing for stiffness matching. Because of this reason the addition of non-structural mass is far easier to implement on a design than full cross section analysis. Results of the two approaches were compared and discussions were made on the effectiveness and feasibility of two methods.

Aerospatiale Gazelle is French-Design helicopter which was first flown in 1967 and then became a part of the joint program between Aerospatiale and Westland [66]. As can be seen on Figure 32, Aerospatiale Gazelle has a classical main rotor and tail rotor configuration. Main rotor has 3 blades whereas tail rotor is a fenestron. Helicopter is driven by a Turbomecca turbo-shaft engine and can perform utility and attack missions. A large number of, over 800, Aerospatiale Gazelle was produced.


**Figure 32:** Aerospatiale Gazelle [67]

Both in first and second optimization analyses, SA349/2 variant of Gazelle were used. This configuration has an extensive test data that so that the analysis model can be compared with test results. Additionally detailed helicopter parameters are available which make comprehensive analysis possible. Table 10 shows the general aspects of the SA349/2 analyzed.

**Table 10:** General Aspects of SA349/2 [60]

| | |
|---|---|
| Main Rotor Radius (m) | 5.25 |
| Number of Blades | 3 |
| Blade-Hub Connection | Articulated |
| Main Rotor RPM | 387 |
| Mean Chord (cm) | 33.6 |
| Helicopter Mass (kg) | 1972.35 |
| Maximum Speed (knots) | 167 |

SA349/2 variant of Gazelle was analyzed for the purpose of reduction in vibratory hub loads. The vibration level in helicopters is relatively low at hover and increases with forward flight velocity to high levels with maximum flight velocity [1]. There are high-level of vibration at some specific conditions such as the transition flight (near $\mu$=0.1) but since the helicopter operates most of its time at cruise conditions, these specific conditions were excluded and in this thesis only vibrations caused by cruise flight was analyzed. Because of this reason analyses focused on high-speed cruise flight. 145 knots flight speed was selected for the analysis which was high enough to see the significant vibratory loads.

Before the analysis was conducted, the reliability of the analysis model was tested. This is especially important because the vibratory loads at the rotor hub were directly used as the objective function. Therefore a reliable model is necessary in the evaluation of the vibratory load gradients with respect to design variables which are directly related to the results of the optimization analyses. For this purpose a CAMRAD model was developed for the helicopter and compared with flight test data at 145 knots level flight. In the flight test, the hub loads were calculated from the data that were measured by the strain gauges on the rotor shaft [65].

Since, the aim of this study was to minimize the vibratory hub loads for a 3-bladed rotor; third multiple of rotor speed (3/rev) was the critical frequency as it was explained in Section 2.2.2. Hence CAMRAD model output for SA349/2 was compared with 3/rev hub loads of flight test data. Figure 33 and Figure 34 show the comparison of 3/rev loads between model and flight test results. In the figures, peak values of 3/rev loads were taken into account.

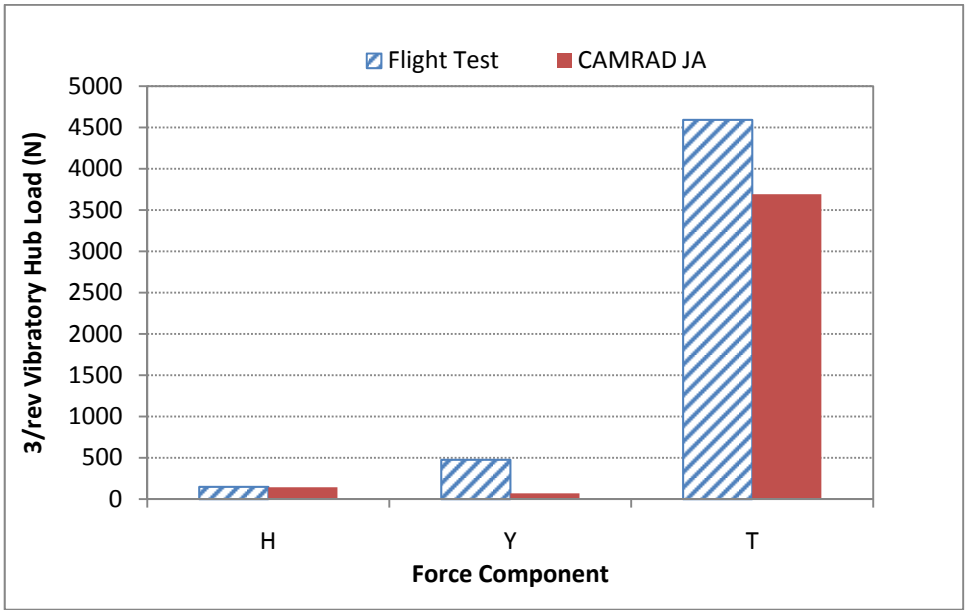


**Figure 33:** Comparison of CAMRAD and Experimental Hub Forces of SA349/2 Helicopter at 3/rev Peak Values

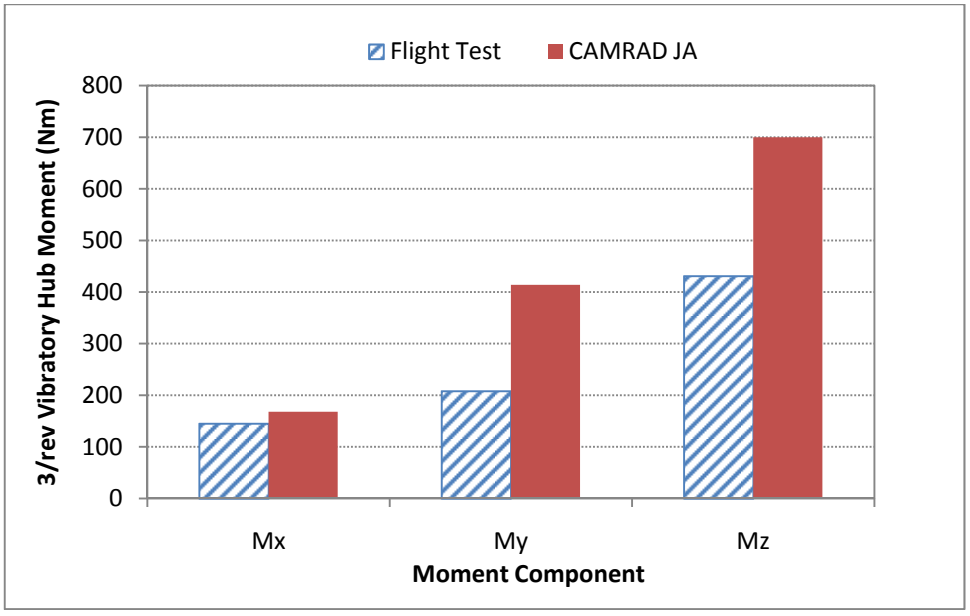


**Figure 34:** Comparison of CAMRAD and Experimental Hub Moments of SA349/2 Helicopter at 3/rev Peak Values

In this model, the 3/rev vertical hub force T was critical between force components whereas longitudinal and lateral components are negligible with respect to vertical load. The

longitudinal 3/rev hub force H is almost same with experimental results and vertical 3/rev hub force can be considered as close. Between vibratory hub forces, lateral hub force Y deviates from experimental data significantly but it can be ignored since it is very small compared to vertical hub force. The CAMRAD 3/rev hub moment calculations show overestimation with respect to flight test results but still remains within the same order of magnitude. Good correlation in the critical load component and the ability of capturing non-critical load components within the same order of magnitude provided satisfactory knowledge on the vibratory loads for the optimization purposes.

In fact, dynamic load calculation is a very complicated task which includes aerodynamic loads, inertial loads, elastic restoring forces, rotor-hub connection, blade dynamic stall, rotor wake, inflow, blade vortex interactions and rotor fuselage aerodynamic and dynamic interactions that are mostly of aerodynamic origin. In helicopter analysis, the steady integrated parameters like thrust or power can be perfectly correlated against flight test but spatial and time dependent distribution parameters are more difficult to predict because of huge number of unknowns in a specific design. Besides the understanding of rotor loads especially those of aerodynamic origin need to be improved [3] and even with sophisticated dynamic, structural and aerodynamic models, the analysis cannot be entirely successful [1]. It should also be noted that, since the design variables are directly related to the structural dynamics of the blade, the effect of aerodynamic uncertainties are expected to be on the same level for the initial and optimum results. When the difficulties in dynamic load calculations and design variables are considered the CAMRAD JA model provides the required knowledge on the level of the 3/rev vibratory loads for the purpose of blade structural dynamics optimization. Therefore within the scope of this thesis, a reliable model is sufficient and hence the developed model can be used for the purpose of vibratory hub loads calculation.

### 3.2.2 SA349/2 Vibratory Hub Loads Minimization by Full Cross section Optimization

The analysis was about the optimization of rotor blade in order to achieve the reduced critical vibratory loads. Blade flapwise and lagwise bending stiffness, torsional rigidity and mass distributions were considered as design variables. Vibratory hub loads of CAMRAD

JA model at 3/rev frequency was considered as the objective function. The results of the optimization analysis were discussed for the reduction in 3/rev vibratory loads.

#### 3.2.2.1 Objective Function

In this optimization study, it was aimed to reduce the helicopter fuselage vibrations by decreasing the level of vibratory loads at the main rotor. The main rotor is the main source of helicopter vibrations. Since all load components do not have the same level of importance, it is not practical to try to minimize all the force and moment components. Generally vertical hub shear is critical as compared to others [35]. However other force and moment components should also be checked for their possible significance in terms of the helicopter rotor vibratory loads from Figure 33 and Figure 34.

Reference steady force and moment components can be used in selecting the critical loads so that each 3/rev component can be compared with these reference values and decided about its significance. The most suitable steady force reference can be selected as the aircraft weight which is nearly 20000 N. According to the flight test results of Figure 33 the peak value of the 3/rev vertical (T) hub force was given as and 4593 N. Since gross weight of SA 349/2 Helicopter is nearly 20000 N and vertical 3/rev hub load was found as 4593 N, vertical component was believed to be able to affect the whole body whereas longitudinal and lateral components are negligible with respect to helicopter weight. The 3/rev moment were 145 Nm, 208 Nm, and 431 Nm at peak values according to the Figure 34 and the reference steady moment can be selected as the main rotor steady torque which is approximately 10000 Nm for 145 knots speed. The 3/rev moment components at peak values are all smaller than 5% of the main rotor steady torque therefore none of them was believed to be able to affect the whole fuselage significantly as vertical force component could do. Therefore in this analysis priority was given to the 3/rev vertical hub force in minimizing the fuselage vibrations and other load components of optimum design were checked if there was any significant increase. Figure 35 represents the distribution of 3/rev vertical hub force over the rotor disc for the experimental results and CAMRAD JA model.

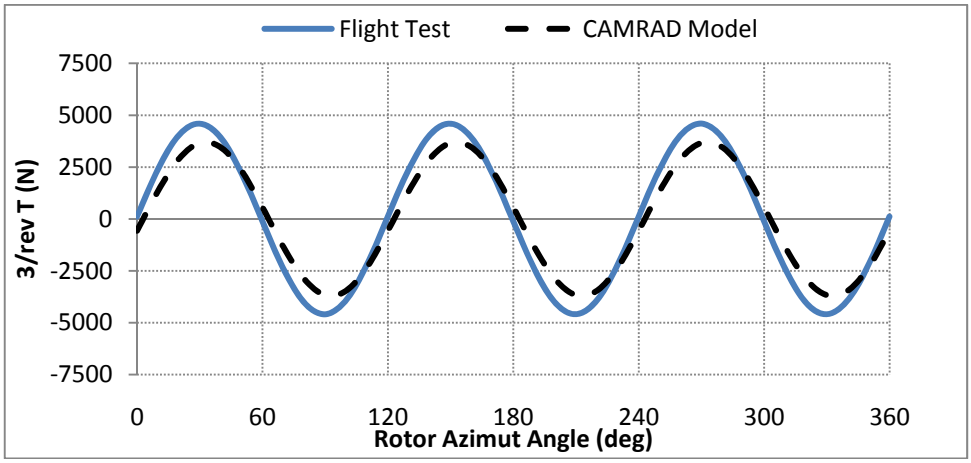


**Figure 35:** Comparison of CAMRAD JA and Experimental 3/rev Vertical Hub Force of SA349/2 Helicopter over the Rotor Azimuth

Figure 35 indicates that every rotor revolution approximately 4500 N amplitude force hits rotor hub 3 times. The objective function is the peak value of the 3/rev vertical load wave plotted in Figure 35 and also given in Equation 22 which was derived from Equation 13.

$$F_{obj} = Max(T(\psi)_{3/rev}) = Max(T_{3,c}\cos N\psi + T_{3,s}\sin N\psi) \ for\ 0^0 \le \psi \le 360^0 \tag{22}$$

CAMRAD JA solves equations of motion by applying modal analysis procedures, therefore system degrees of freedom of are defined by the number of modes of the helicopter [44]-[45]. Blade degrees of freedom ($DOF_{BLADE}$) represent the bending and torsional modes for each blade of a rotor with $N$ blades, hub degree of freedom ($DOF_{HUB}$) represents the gimbal or teeter hinge and fuselage degrees of freedom ($DOF_{BLADE}$) represent the rigid and elastic degrees of freedom of fuselage. CAMRAD provides ten blade bending and five blade torsion modes for the blade motion. One gimbal mode, which provides a ball and socket type of motion, can be implemented at the rotor hub if the hub has an extra degree of freedom with respect to fuselage. For the fuselage six rigid airframe modes and thirty elastic modes can be implemented. Fuselage elastic modes can be included if the mode shapes and natural frequencies of the fuselage are available. Then total number of modes can be calculated by using Equation 23:

$$DOF_{TOTAL} = N \times DOF_{BLADE} + DOF_{HUB} + DOF_{FUSELAGE} \tag{23}$$

The CAMRAD gives possibility to define the numbers of degrees of freedom by selecting the proper blade, hub and fuselage degrees of freedom. For this particular problem, the

fuselage was considered as rigid and there was no gimbal degree of freedom at hub. Total 6 modes, 5 bending modes and 1 torsional mode, were used for the blade because of the aforementioned 6/rev criterion. When the 6 degrees of freedom of the fuselage was also added, total modal degrees of freedom became;

$$DOF_{TOTAL} = 3 \times 6 + 0 + 6 = 24$$

#### 3.2.2.2 Design Variables

In terms of the CAMRAD JA input files, the design variables are the bending stiffness distribution in flapwise and chordwise directions, torsional stiffness distribution and mass distribution. In this analysis these parameters were directly used as the design variables. Since very large mean values of centrifugal and shear loads exist, the inner part of a typical helicopter blade is very stiff and structurally non-linear as compared to outer part in order to accommodate those large loads. Hence, it is not a good idea to modify the inner blade of an existing design without making detailed strength analysis. Therefore, the current optimization analysis only covered the outer part of the blade and the border was taken at r/R=0.30 radial location. After that coordinate, the design variables were equally spaced.

The effect of design variable station number was discussed in 3.1.2.2 chapter while pointing the importance of modal nodal points. A large station number should be selected according to the number of modes interest. In this case, the highest mode was the 3$^{rd}$ flapping mode and at least 6 stations should be used in order to achieve a good resolution of blade dynamics. Then, a higher number of 8 elements were used to resolve the outer blade properties. The mass, flapwise bending stiffness, chordwise bending stiffness and torsion stiffness were defined at these points so that a total of 32 design variables were taken into account. The starting design was taken as that having the initial distributions on the SA349/2 blade. Side constraints were applied to design variables in order to prevent the occurrence of unrealistic results. Based on the original design, the applied side constraints were defined as:

| | |
|---|---|
| [4 kg/m < $m_{c/s}$ < 12 kg/m] | (For sections before tip) |
| [12 kg/m < $m_{c/s}$ < 20 kg/m] | (For Blade Tip) |
| [5000 Nm$^2$ < $EI_F$ < 10000 Nm$^2$] | (For sections before tip) |
| [5000 Nm$^2$ < $EI_F$ < 20000 Nm$^2$] | (For Blade Tip) |

[200000 $Nm^2$ < $EI_C$ < 600000 $Nm^2$] (For sections before tip)

[200000 $Nm^2$ < $EI_C$ < 1000000 $Nm^2$] (For Blade Tip)

[5000 $Nm^2$ < GJ < 17000 $Nm^2$] (For sections before tip)

[5000 $Nm^2$ < GJ < 25000 $Nm^2$] (For Blade Tip)

#### 3.2.2.3 Constraints

Blade mass, blade mass moment of inertia and blade natural frequencies were applied as the constraints for the problem as it was explained in the beginning of CHAPTER 1. Blade mass was chosen by considering the performance. Blade mass moment of inertia was taken by considering auto-rotation such that optimum design did not have lower inertia than the initial value. Blade natural frequencies were defined as constraints such that the natural frequencies and excitation frequencies cannot be closer than a specified interval. In this particular case an offset was chosen as 0.15. This was lower than the interval used in the optimization studies involving natural frequency separation. The reason of selecting larger interval in natural frequency separation analysis was due to the fact that the absence of the aerodynamic model. Hence in that study the interval was decided to be higher for a more conservative approach. Critical blade modes were taken as those modes used previously in Section 3.1.2. These modes were the rigid lag mode, 3rd, 4th and 5th bending modes and first torsional mode whereas first flapping mode was excluded because it was dominated by the centrifugal acceleration as it was discussed in Section 1.2. Table 11 summarizes these constraints.

**Table 11:** Design Constraints of the Optimization Problem for Minimum Vibratory Loads of SA349/2 Helicopter

| Parameter | Constraint |
|---|---|
| Blade Mass (kg) | Blade Mass< 80 kg |
| Blade Inertia ($Nm^2$) | Final Inertia > Initial Inertia |
| Rigid Lag Frequency (n/rev) | 0.15/rev away from n/rev |
| Third Bending Frequency (/rev) | 0.15/rev away from n/rev |
| Forth Bending Frequency (/rev) | 0.15/rev away from n/rev |
| Fifth Bending Frequency (/rev) | 0.15/rev away from n/rev |
| First Torsion Frequency (/rev) | 0.15/rev away from n/rev |

### 3.2.2.4 Results

Figure 36 and Figure 37 show the optimization results for the optimization analysis which was conducted in order to minimize 3/rev vertical hub force.

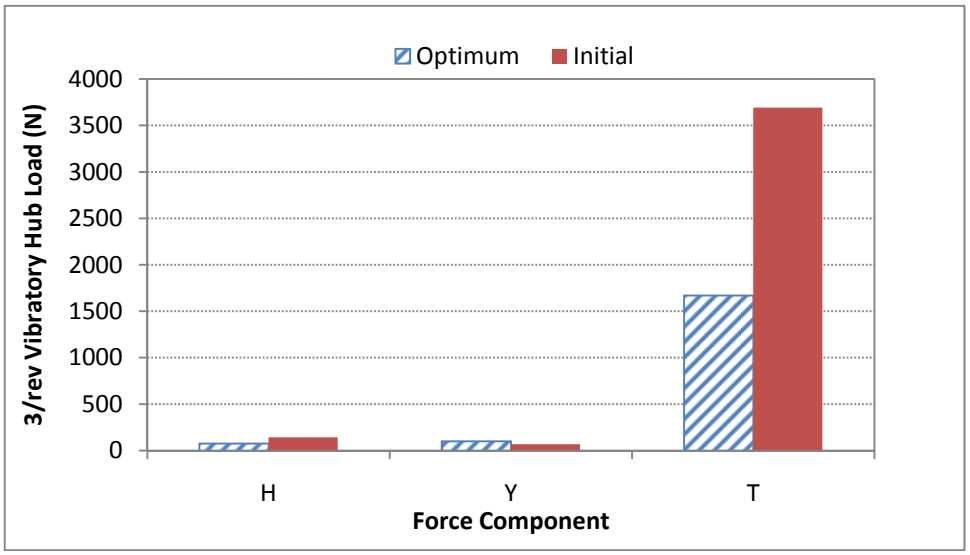


**Figure 36:** Peak Values of 3/rev Hub Forces of Initial and Optimum Designs of SA349/2 Helicopter

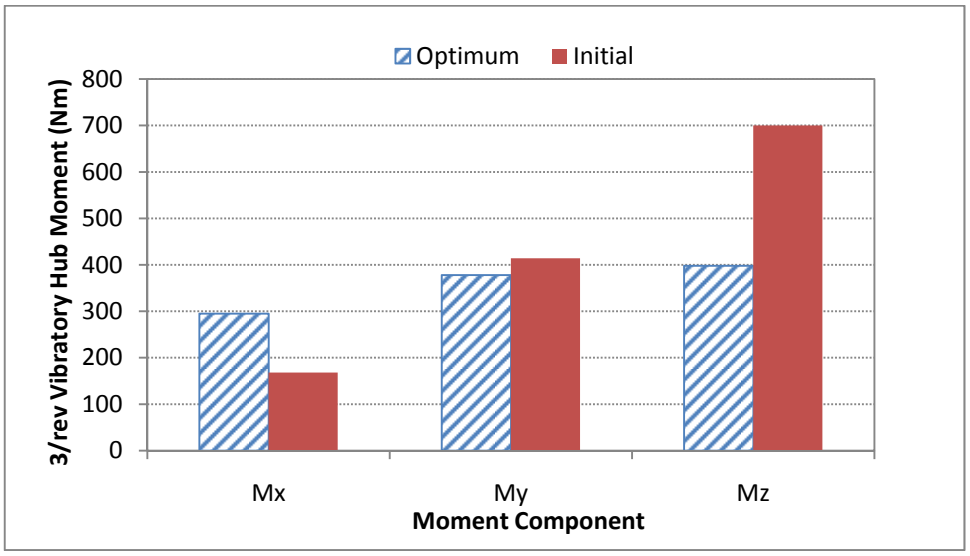


**Figure 37:** Peak Values of 3/rev Hub Moments of Initial and Optimum Designs of SA349/2 Helicopter

There was a significant 55% reduction achievement in the critical vibratory load with approximately 2000 N in amplitude. Due to their lower magnitudes, longitudinal and lateral 3/rev hub forces were ignored compared to vertical load, but it was important to see that their values were still negligible with respect to helicopter weight. Considering the moments, only the 3/rev rolling moment increased, however its value is already small as compared to other moments. The distribution of the vertical 3/rev force over the rotor disc and the improvement in objective function are represented in Figure 38.

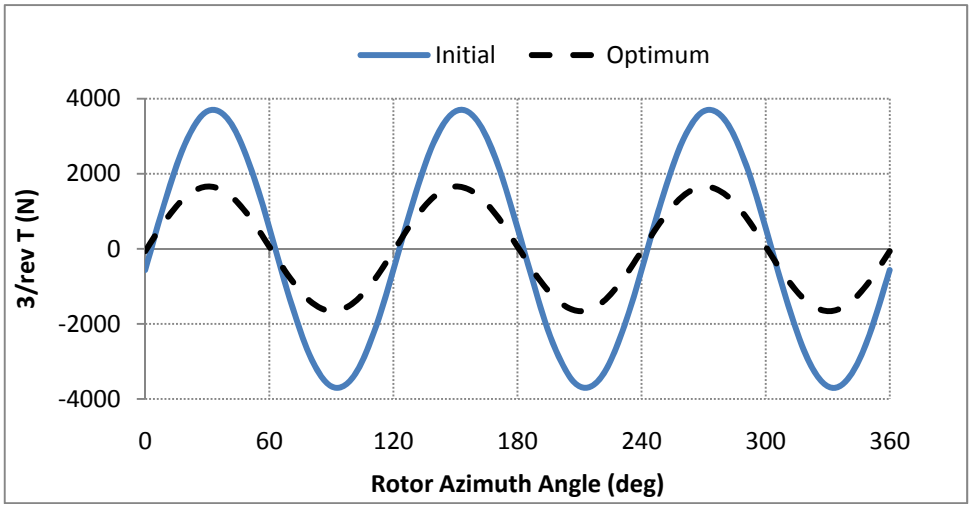


**Figure 38:** 3/rev Vertical Hub Force of Initial and Optimum Designs of SA349/2 Helicopter over Rotor Azimuth

Table 12 gives the initial and optimized values of constraints, together with the constraint limits. The mass increase was only 3 kg hence the increase in total mass reached to 9 kg. There was approximately 90 N increase in static load but 2000 N reduction in vertical vibratory force. Considering the likely improvement in flight comfort, avionics reliability, and increase in maintenance period and material life cycle as well, the increase in mass was acceptable. In addition to blade mass, blade moment of inertia increased and blade natural frequencies did not violate the criteria of 0.15 /rev separation form excitation frequencies as required.

**Table 12:** Constraint Values of Initial and Optimum Designs and Constraints of SA349/2 Helicopter

| Parameter | Initial Design | Optimum Design | Constraint |
|---|---|---|---|
| Blade Mass (kg) | 74.7 | 77.4 | Blade Mass< 80 kg |
| Blade Inertia ($Nm^2$) | 376 | 379 | Inertia > 376 $kgm^2$ |
| Rigid Lag Frequency (/rev) | 0.54 | 0.54 | 0.15/rev away from n/rev |
| Third Bending Frequency (/rev) | 2,74 | 2,53 | 0.15/rev away from n/rev |
| Forth Bending Frequency (/rev) | 4.27 | 4.15 | 0.15/rev away from n/rev |
| Fifth Bending Frequency (/rev) | 5.15 | 4.59 | 0.15/rev away from n/rev |
| First Torsion Frequency (/rev) | 4.78 | 4.47 | 0.15/rev away from n/rev |

The reduction in the 3/rev vibratory load was achieved by the optimum distribution of the design variables. Figure 39 to Figure 42 give the initial and optimized design variables.

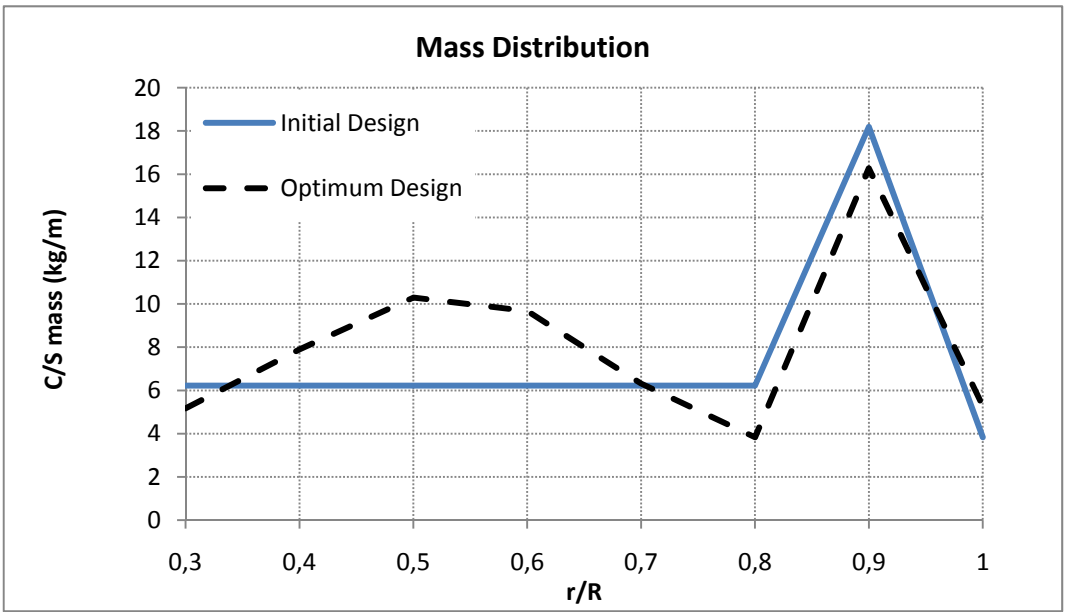


**Figure 39:** Mass Distributions of Initial and Optimum Designs of SA349/2 Helicopter

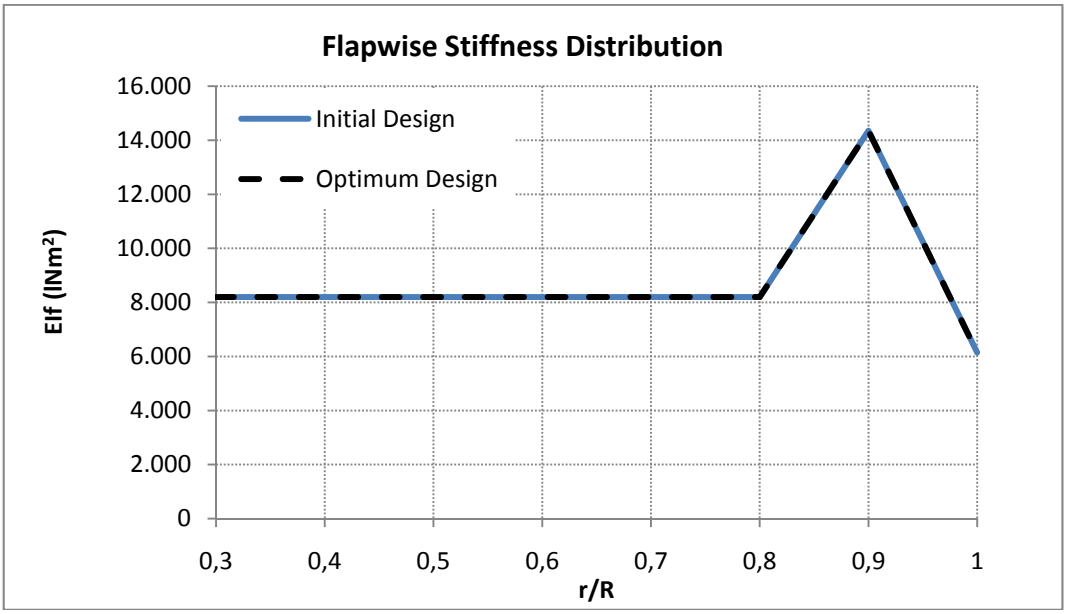


**Figure 40:** Flapwise Stiffness Distributions of Initial and Optimum Designs of SA349/2 Helicopter

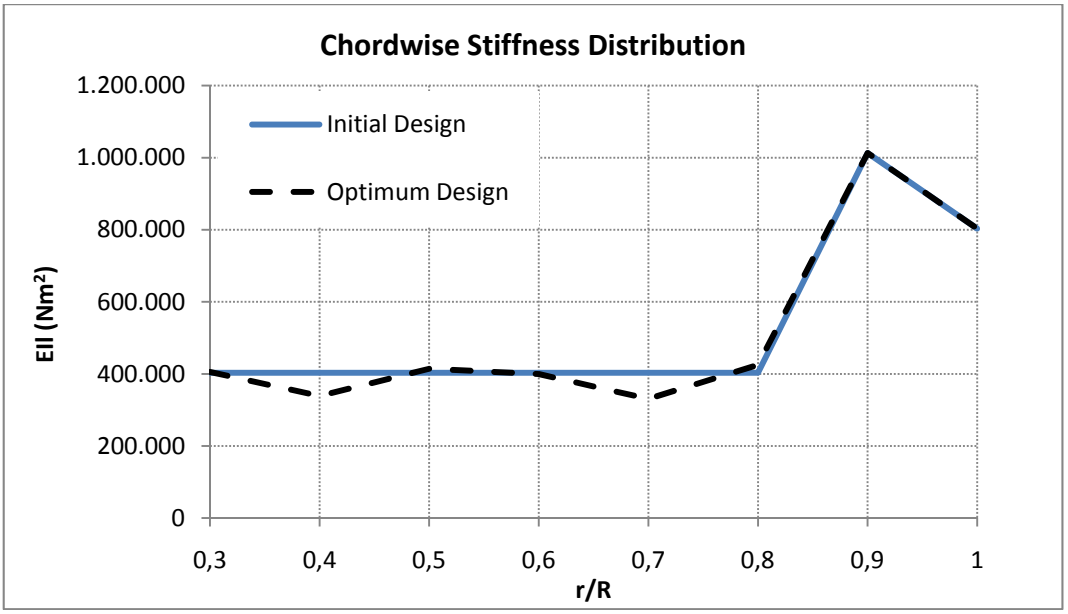


**Figure 41:** Chordwise Stiffness Distributions of Initial and Optimum Designs of SA349/2 Helicopter

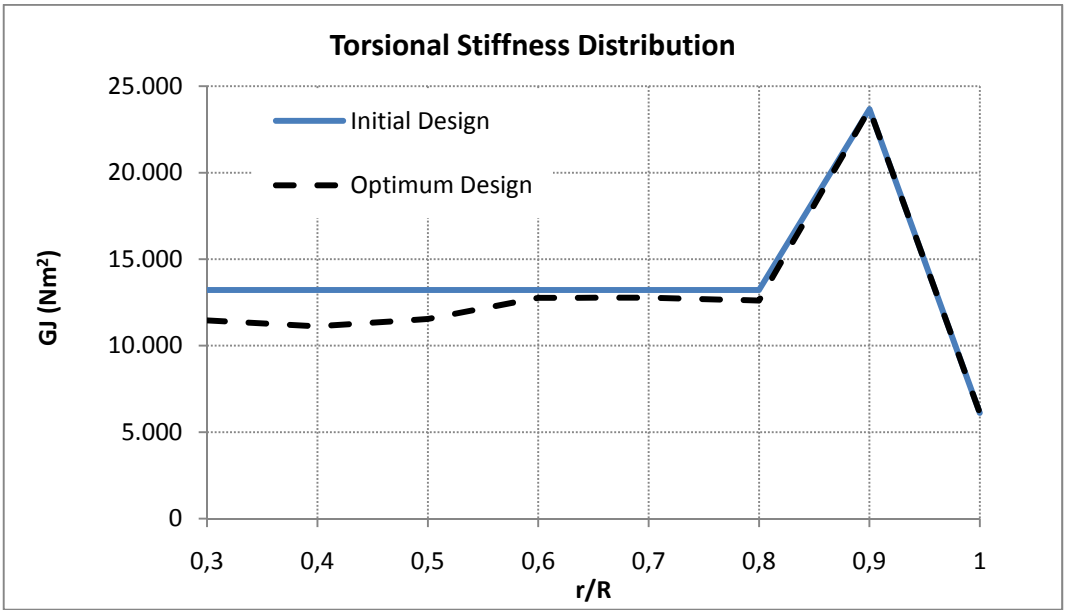


**Figure 42:** Torsion Stiffness Distributions of Initial and Optimum Designs of SA349/2 Helicopter

According to the Figure 39, the cross section mass increase between r/R=0.35 and r/R=0.7 and slightly decreased between r/R=0.7 and r/R=0.95 and slightly increased up to blade tip. The change in mass distribution was believed to reduce the vibratory loads with a favorable blade response. In Figure 40 the flapwise stiffness remained constant whereas Figure 41 shows that there were only slight modifications in chordwise stiffness near r/R=0.4 and r/R=0.7.

The torsion stiffness in Figure 42 decreased significantly until r/R=0.5 and slightly until r/R= 0.8. This reduction in torsional frequency changed the blade elastic twist distribution over the rotor disc. The change in blade elastic twist was believed to cause a more favorable blade angle of attack distribution over the rotor disc which smoothed the aerodynamic loads. The similar result is aimed in active vibration solutions which were explained in Section 1.5.2.

This analysis did not benefit from the dimensions and material properties of a cross section model therefore there was necessity of matching the required optimization in achieving 55% reduction. A sample model that can be used in optimum stiffness matching is presented in Figure 43.

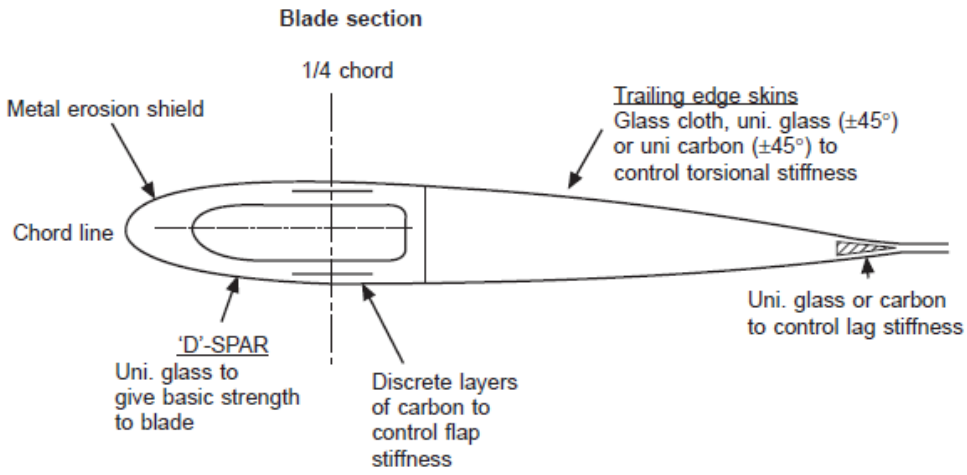


**Figure 43:** A Sample Composite Blade Cross Section Model [8]

In the composite cross section model of Figure 44, the layers of carbon fibre on the upper and lower surfaces of the glass fibre D-spar can be used in adjusting flapwise stiffness without affecting the chordwise and torsional stiffness. It is also possible to adjust chordwise stiffness by designing the carbon fibre at the trailing edge. The necessary torsional stiffness can be achieved by proper selection of fibre type and orientation for the trailing edge skin. In addition to blade stiffness all these modifications and non-structural mass addition contribute to blade cross section mass. Therefore, if the cross section model of Figure 43 was assumed for SA349/2 blade, the optimum distributions can be achieved by proper modifications. According to the Figure 39 to Figure 42, the significantly modified region was between r/R=0.3 and r/R=0.5 where there was nearly 20 % reduction in torsional stiffness. There were no significant changes in flapwise and lagwise bending stiffness distribution. The increase in blade cross section mass between r/R=0.34 and r/R=0.7 can easily be achieved by non-structural mass addition without affecting blade stiffness. Therefore the optimum distributions can possibly be handled with a similar model to the model of Figure 43.

### 3.2.3 SA349/2 Vibratory Hub Load Minimization by Non-Structural Mass Addition

For the same rotor of SA349/2 helicopter, optimization analysis was performed by only including nonstructural mass addition. From previous analysis, Figure 39-Figure 42 showed that the main change was in mass distribution whereas there were only slight changes in

torsion and edgewise bending stiffness distributions and no change in flapwise bending stiffness distribution. Therefore 3/rev vibratory loads were mostly dependent on mass addition meaning it is expected that changing the mass distribution may give satisfactory results.

In this analysis, the goal was to achieve an improved design with non-structural mass addition. The model, complexity and optimization procedure were all same with previous analysis except for the design variable which was explained in relevant chapter.

#### 3.2.3.1 Objective Function

The aim of this optimization analysis was same as previous analysis which was decreasing critical vibratory hub loads. The same analysis model with the same degrees of freedom of Section 3.2.2 was used. The objective function was again amplitude of 3/rev vertical load at 145 knots flight speed as given in Equation 24.

$$F_{obj} = Max(T(\psi)_{3/rev}) = Max(T_{3,c}\cos N\psi + T_{3,s}\sin N\psi) \; for \; 0^0 \le \psi \le 360^0 \tag{24}$$

#### 3.2.3.2 Design Variables

In terms of CAMRAD model, the design variable is the mass distribution of blade for this particular analysis. For the previously mentioned reasons, the inner part of the blade was not included in design variable distribution and the variables were equally distributed after r/R=0.30.

The initial mass distribution included blade structure; therefore non-structural masses were added on top of these mass distributions within the optimization algorithm. Blade stiffness was held constant, added mass was assumed to have no contribution on the blade stiffness. Besides it was assumed that mass was added at center of gravity in order not to include effect of non-structural mass on coupled twisting motion.

Side constraints were applied to design variables in order to avoid the likely occurrences of possible unrealistic results. Although total mass was also controlled by maximum mass

constraint, side constraints were necessary to control the local mass limits. Based on the initial mass distribution of the SA349/2 blade, the side constraint was defined as follows:

[0.0 kg/m < $m_{NS}$ < 5 kg/m] (for the whole blade)

#### 3.2.3.3 Constraints

Blade mass and natural frequencies were applied as the constraints for the problem for the previously mentioned reasons which were discussed previously in Section 3.1 and Section 3.2.2. Blade mass was chosen by considering the performance. Blade fundamental lag, 3rd, 4th, 5th bending and 1st torsional natural frequencies were included in constraints. As opposed to previous analysis blade mass moment of inertia did not need to be taken into account because any mass addition increases blade inertia. Table 13 summarizes the constraints.

**Table 13:** Design Constraints of the Optimization Problem of SA349/2 Helicopter

| Parameter | Constraint |
|---|---|
| Blade Mass (kg) | Blade Mass< 80 kg |
| Rigid Lag frequency (/rev) | 0.15/rev away from n/rev |
| Third Bending Frequency (/rev) | 0.15/rev away from n/rev |
| Forth Bending Frequency (/rev) | 0.15/rev away from n/rev |
| Fifth Bending Frequency (/rev) | 0.15/rev away from n/rev |
| First Torsion Frequency (/rev) | 0.15/rev away from n/rev |

#### 3.2.3.4 Results

Figure 44 and Figure 45 show the results of optimization analysis which was conducted in order to minimize vertical 3/rev hub force.

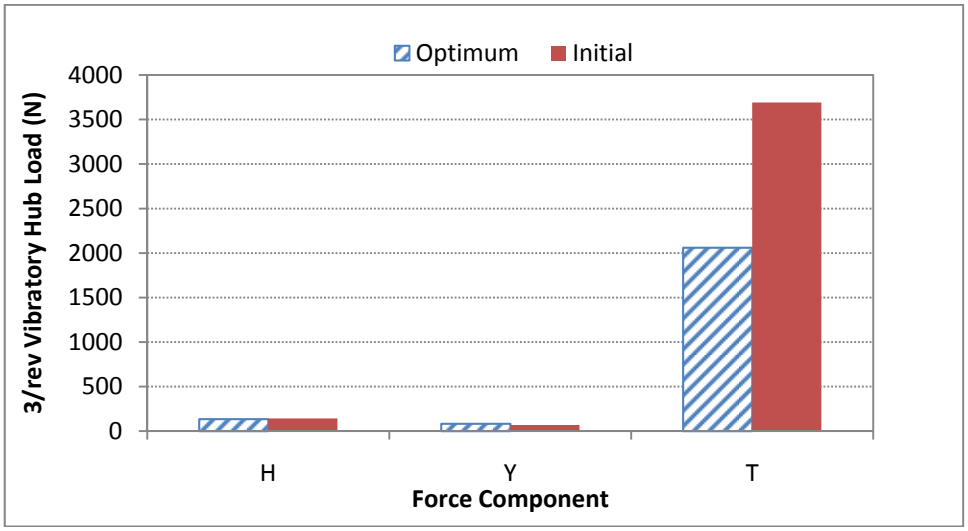


**Figure 44:** Peak Values of the 3/rev Hub Forces of Initial and Optimum Designs of SA349/2 Helicopter

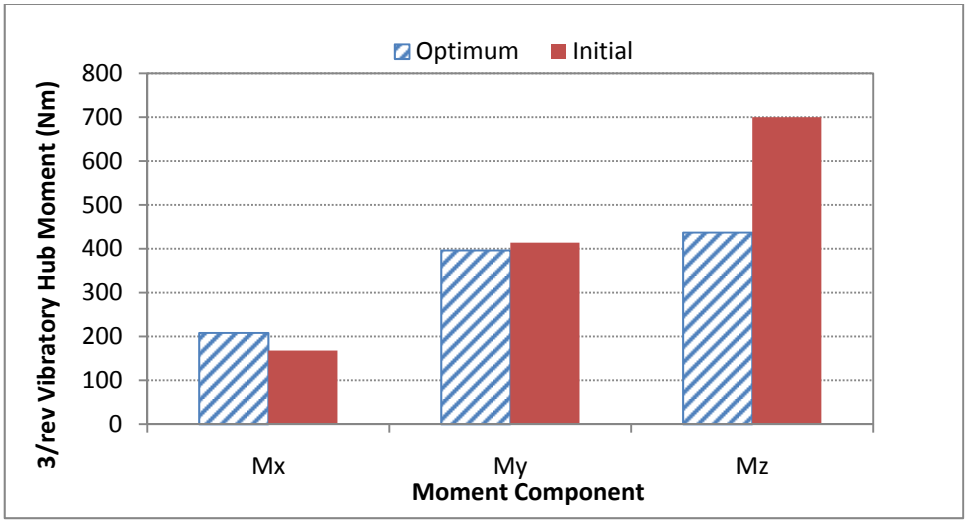


**Figure 45:** Peak Values of the 3/rev Hub Moments of Initial and Optimum Designs of SA349/2 Helicopter

There was a 44% reduction achievement in objective function with approximately 1600 N reduction in amplitude. Due to their lower magnitudes, longitudinal and lateral 3/rev hub loads were ignored compared to vertical load, but it was important to see that their values were still negligible with respect to vertical force. Considering moments only 3/rev rolling moment slightly increased, however its value was already small compared to other moments. The vibratory load reduction over the rotor disc can be observed in Figure 46.

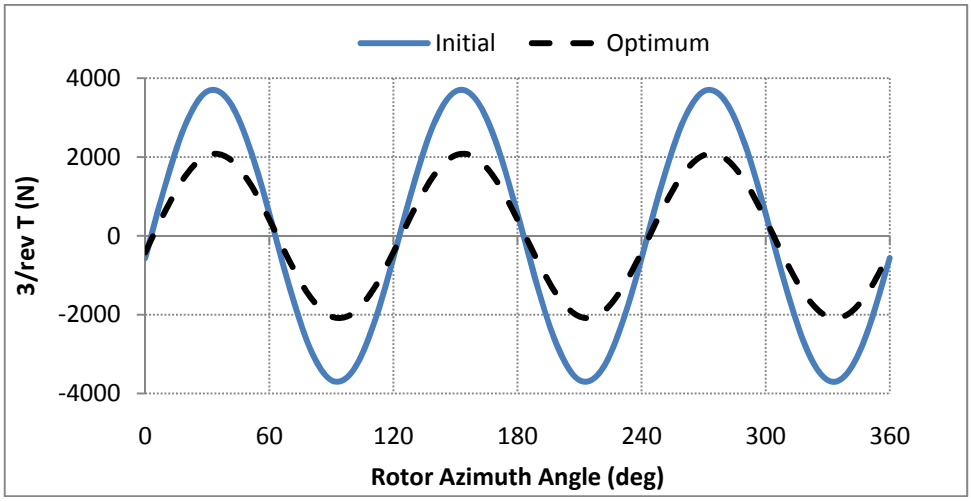


**Figure 46:** 3/rev Vertical Hub Force of Initial and Optimum Designs of SA349/2 Helicopter over Rotor Azimuth

Table 14 gives the initial and optimized values of constraints, together with the constraint limits. The mass increase was 5 kg hence the increase in total mass reached to 15 kg. There was approximately 150 N increase in overall static load but 1600 N reduction in vertical vibratory force. Considering the likely improvement in flight comfort, avionics reliability, and increase in maintenance period and material life cycle as well, the increase in mass was acceptable. In addition to blade mass, blade natural frequencies did not violate the criteria of 0.15 /rev separation form excitation frequencies as required.

**Table 14:** Constraint Values of Initial and Optimum Designs of SA349/2 Helicopter

| | Initial Design | Optimum Design | Constraint |
|---|---|---|---|
| Blade Mass (kg) | 74.7 | 79.7 | Blade Mass< 80 kg |
| Rigid Lag Frequency (/rev) | 0.54 | 0.54 | 0.15/rev away from n/rev |
| Third Bending Frequency (/rev) | 2,74 | 2,55 | 0.15/rev away from n/rev |
| Forth Bending Frequency (/rev) | 4.27 | 4.26 | 0.15/rev away from n/rev |
| Fifth Bending Frequency (/rev) | 5.15 | 4.64 | 0.15/rev away from n/rev |
| First Torsion Frequency (/rev) | 4.78 | 4.78 | 0.15/rev away from n/rev |

According to the constraints of initial and optimum designs given in Table 14, the reduction in the 3/rev vibratory load was achieved while preserving the proposed constraints. Figure 47 gives the initial and optimized cross section mass distribution.

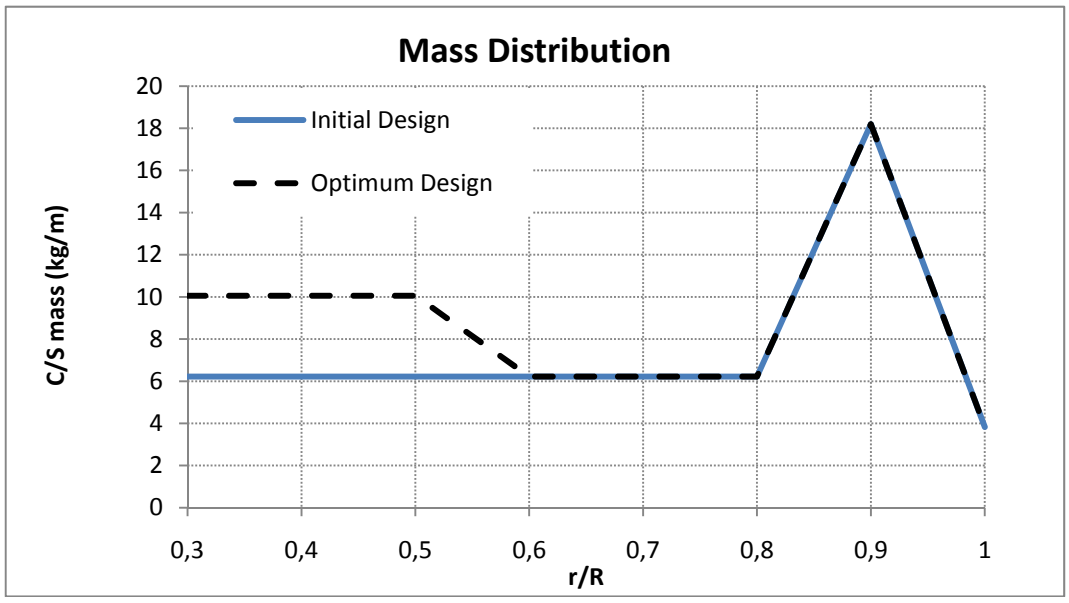


**Figure 47:** Outer Blade Mass Distribution of Initial and Optimum Designs of SA349/2 Helicopter

The optimum mass distribution given in Figure 47 shows that mid-blade region was effective in terms of mass addition whereas tip of the blade was insensitive to critical 3/rev loads. The change in mass distribution was believed to reduce the vibratory loads with a favorable blade response. Similar result is aimed in passive vibration reduction techniques which were discussed in 1.5.1.

### 3.2.4 Conclusion

In this chapter, two different optimization studies were conducted on a three bladed light helicopter. In the first analysis, a full cross section optimization was attempted whereas the second analysis included optimization of a blade by non-structural mass addition. The analyses of both cases yielded satisfactory results. Figure 48 and Figure 49 outline the results of the two analyses.

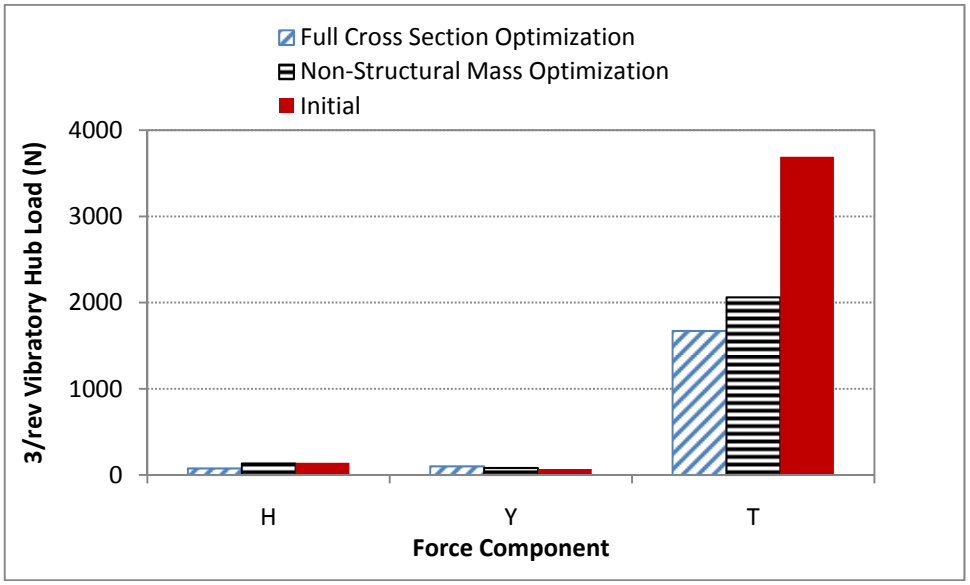


**Figure 48:** Comparison of Initial 3/rev Hub Forces with 3/rev Forces of Full Cross Section Optimization and Non-Structural Mass Optimization of SA349/2 Helicopter

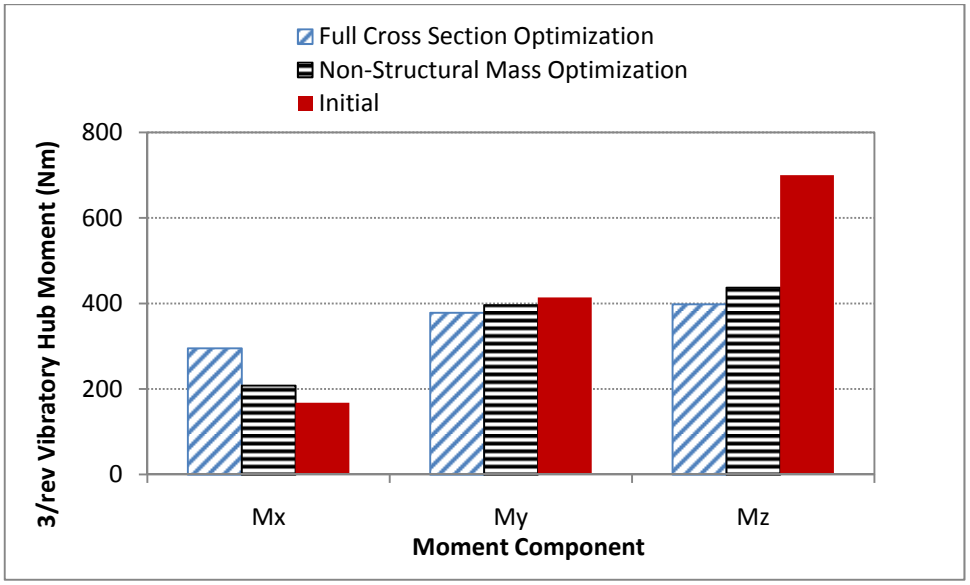


**Figure 49:** Comparison of Initial 3/rev Hub Moments with 3/rev Moments of Full Cross Section Optimization and Non-Structural Mass Optimization of SA349/2 Helicopter

Less reduction in vertical hub force was achieved in non-structural mass optimization analysis though with higher mass penalty. This indicates the benefit of stiffness distribution

optimization as a design variable. The modification in torsional frequency changed the blade elastic twist distribution over the rotor disc. The change in blade elastic twist was believed to cause a more favorable blade angle of attack distribution over the rotor disc hence this smoothes the aerodynamic loads. This provides extra benefit in reducing the 3/rev vertical hub force. The only drawback of the first analysis was higher 3/rev rolling moment but it is still negligible with respect to other moment components

It was determined that the first analysis required a design modification but only non-structural mass is required to be added to the specified locations in the second analysis. The optimum design of the full cross section optimization is more difficult to achieve than that of non-structural mass optimization. While former method includes the post-processing treatment of mass distribution, bending and torsion distributions the latter only required the addition of mass which do not contribute to blade stiffness. Therefore it is logical to decide about the modification and its type not only by considering the reductions in vibratory loads but additional design studies, manufacturing processes and feasibility should also be taken into consideration.

It is important to define design variables according to the required blade modification. If the blade is in design phase, a full cross section analysis can be preferred in order to reach a more efficient design. Therefore the product can benefit from more parameters that affect vibratory loads. However if the blade is in operation or blade cross section model do not allow modifications then the non-structural mass addition can be a better choice. In this case engineers do not have to think about the cross sectional model and the production capabilities. Only necessity is to add the weights at their appropriately calculated locations in the structure.

Finally, it should be mentioned that the vibratory load optimizations were performed for a rotor with equally spaced identical blades, in other words the critical frequencies were *N/rev* where *N* was the blade number. Vibratory loads that are not the multiples of the rotor speed and lower than *N/rev* frequency occur because of non-identical blades or blades out of track. Rotor Balance and tracking procedures must be applied for these type of problems whenever necessary and prior to the optimization analyses [68]. But still, *N/rev* harmonics dominate the vibration produced by helicopter rotors under normal circumstances [1].

# CHAPTER 4

# CONCLUSIONS

## 4.1 General Conclusions

In this thesis, the analyses and design of helicopter rotor blades were conducted for the purpose of reduced vibrational level. The vibrational levels of a helicopter are very critical in terms of safety, crew health, passenger comfort, performance and maintenance cost. In order to prevent undesirable results ranging from reduced comfort to fatal failures, the vibrational levels should be kept as low as possible.

The study presented coupled CAMRAD JA helicopter comprehensive analysis program with CONMIN gradient based optimization algorithm in order to consider the main rotor induced vibration.

The natural frequency separation and the vibratory hub loads reduction approaches were implemented in the thesis. The natural frequency separation method was used in order to separate the natural frequencies of rotor blades from n/rev aerodynamic excitation frequencies. The blade cross section was modeled with a simple box beam and the CAMRAD inputs of blade mass and stiffness distributions were evaluated accordingly. Articulated and hingeless blades were analyzed for natural frequency separation. The minimum difference between the blade natural frequencies and excitation frequency was initially 0.02/rev. The analyses improved these initial resonant conditions. The results showed 0.33/rev and 0.26/rev minimum differences between the blade natural frequencies and the excitation frequencies.

The vibratory hub loads reduction method was applied on a SA 349/2 helicopter rotor for N/rev vertical vibratory shear force. The initial N/rev vertical shear was on the order of 20% of the total helicopter weight at high speed cruise flight. 55% and 44% reductions were achieved with the full cross section optimization and the non-structural mass optimizations respectively.

The studied procedure of helicopter vibration reduction was found to be effective and successful in reducing the main rotor induced vibration levels. Application of this procedure to the rotor blade design and modification activities are expected to lead low vibration designs. The procedure is not only suitable for the vibration reduction of conventional helicopters but it can also be applied for optimizing the blades of conventional, tandem, tilt-rotor and co-axial rotorcraft configurations for improved performance, stability and noise characteristic.

## 4.2 Recommendations for Future Work

This thesis included the vibration reduction of helicopter rotor blades for reduced vibration level by coupling CAMRAD JA rotorcraft comprehensive analyses tool and CONMIN gradient based optimization algorithm. The same procedure can also be used for increased performance by weight reduction, increased thrust and decreased power required. It is also possible to reduce the rotor induced noise and increase helicopter and rotor stability. Furthermore all the vibration, performance, noise and stability considerations can be integrated and evaluated within a design procedure by using the proposed procedure.

Other rotorcraft analysis tool can be replaced with CAMRAD JA so that improved models can lead to more accurate results if the licenses of these tools are available. CAMRAD II, FlightLab and DYMORE which have better structural dynamics models than that of CAMRAD JA are the examples for the possible replacements of CAMRAD JA. Besides, the aerodynamic calculations can be improved by using CFD analysis.

Finding local maxima rather than absolute maxima, inability to solve non-differentiable and discontinuous problems and ineffectiveness in parallel computing are the main drawbacks of

a gradient based optimization algorithm [54]. Hence, CONMIN can be replaced with more recent optimization techniques like genetic algorithm or neural networks.

Detailed isotropic or composite blade cross section models can be used which enables better calculation of cross section elastic and inertial properties. The accurate representation of the cross section model yields to more precise results. In addition to the blade models, the modes of an elastic fuselage can be added to CAMRAD JA model so that the effect of rotor fuselage interference can be taken into account and even vibration response of a specific point on the fuselage can be reduced by defining the acceleration of that point as the objective function.

Blade stiffness and mass distributions were analyzed as the design variables. Blade aerodynamic properties such as chord and twist distribution, tip sweep angle and airfoil profiles also affect rotor vibration characteristics and can be included within the design variables. In this case constraints on helicopter performance such as maximum flight speed, main rotor thrust and main rotor power required should be constrained.

# REFERENCES


[1] Johnson, W., "Helicopter Theory," Dover Publications, Inc., 1994

[2] Watkinson, J., "The Art of the Helicopter," Elsevier, 2004

[3] Bielawa, R.L., "Rotary Wing Structural Dynamics and Aeroelasticity," AIAA Education Series, 2005

[4] Leishmann J.G., "Principles of Helicopter Aerodynamics," Cambridge Aerospace Series, 2006

[5] Plamen Antonov's Personal Web-Page, http://pantonov.com/galleries/aircraft-close-by.php , last visited on 01 August 2011

[6] Hodges D.H., "Aeromechanical Stability of Helicopters with a Bearingless Main Rotor – Part 1: Equations of Motion," NASA Technical Memorandum No. 78459, 1978,

[7] Arnold, L., "Aerodynamics of the Helicoper," Frederick Ungar Publishing Co., 1985

[8] Bramwell, A.R.S., Done, G., Balmford, D., "Bramwell's Helicopter Dynamics," Butterworth-Heinemann, 2001

[9] Brentner, K.S., Farassat, F., "Modeling Aerodynamically Generated Sound of Helicopter Rotors," Progress in Aerospace Sciences, Vol.39, 2003, pp.83-120

[10] Veca, A.C., "Vibration Effects on Helicopter Reliability and Maintainability," USAAMRDL Technical Report No.73-11, 1973

[11] "Helicopter Fatigue Design Guide," General Editor F.P. Liard, AGARDograph No.292, 1983

[12] Mansfield N.J., "Human Response to Vibration," CRC Press LLC, 2005, pp.14-16

[13] Harrer, K., Yniguez, D., Majar, M., Ellenbecker, D., Estrada, N., Geiger, M., "Whole Body Vibration Exposure for MH-60S Pilots," 43th SAFE Association Symposium, Utah, 2005

[14] Auffret, R., Delahaye, R.P., Metges, P.J., Vicens, "Vertebral Pain in Helicopter Pilots," NASA Technical Memorandum No.75792, 1978

[15] Straub, F.K., Byrns, E.V., "Application of Higher Harmonic Blade Feathering on the OH-6A Helicopter for Vibration Reduction," NASA Contractor Report, 1986

[16] Inman, D.J., "Vibration with Control," John Wiley and Sons Ltd, 2006, pp.145-148

[17] Harris, C.M., Piersol, A.G., “Harris’ Shock and Vibration Handbook,” McGraw-Hill, 2002, pp.30.1

[18] Pierce, G.A., Hamouda M.N.H., “Helicopter Vibration Suppression Using Simple Pendulum Absorbers on the Rotor Blade”, NASA Contractor Report, 1982

[19] Bauchao O.A., Rodriguez J., “Modeling the Bifilar Pendulum Using Non-Linear, Flexible Multibody Dynamics,” Journal of the American Helicopter Society, No 1, 2003, pp.53-62

[20] Nguyen, K.Q., “Higher Harmonic Control Analysis for Vibration Reduction of Helicopter Systems,” NASA Technical Memorandum No.103855, 1994, pp.2-11

[21] Jacklin, S.A., Haber, A. , Simone, G., Norman, T.R., Kitaplioglu C., Shinoda, P., “Full-Scale Wind Tunnel Test of an Individual Blade Control System for a UH-60 Helicopter,”, American Helicopter Society, 2002

[22] Millott, T.A., Friedmann, P.P., “Vibration Reduction in Helicopter Rotors Using an Actively Controlled Partial Span Trailing Edge Flap Located on the Blade,” NASA Contractor Report No. 4611, 1994

[23] Shen, J., “Vomprehensive Aeroelastic Analysis of Helicopter Rotor with Trailing-Edge Flap for Primary Control and Vibration Control,” PhD Dissertation, University of Maryland-Collage Park Maryland, 2003

[24] “Smart Structures Technology: Innovations and Applications to Rotorcraft Systems,” General Editor I. Chopra, University of-Maryland Collage Park, Maryland, 1997, pp.8-9

[25] Doman, G.S., “Research Requirements for the Reduction of Helicopter Vibration,” NASA Contractor Report No.145116, 1976

[26] Ko, T.W.H., “Design of Helicopter Rotor Blades for Optimum Dynamic Characteristics”, PhD Dissertation, Washington University Sever Institute of Technology, Washington, 1984

[27] Friedmann, P.P., Celi, R. ”Structural Optimization of Rotor Blades with Straight and Swept Tips Subject to Aeroelastic Constraints,“ Recent Advances in Multidisciplinary Analysis and Optimization, NASA Conference Publication, Part1, 1989,pp.145-162

[28] Peters, D.A., Cheng Y.P., ”Optimization of Rotor Blades for Combined Structural, Performance, and Aeroelastic Characteristics,“ Recent Advances in Multidisciplinary Analysis and Optimization, NASA Conference Publication, Part1, 1989, pp.163-180

[29] Lim, J.W., Chopra, I. ”Efficient Sensitivity Analysis and Optimization of a Helicopter Rotor,“ Recent Advances in Multidisciplinary Analysis and Optimization, NASA Conference Publication, Part1, 1989, pp.195-208

[30] Chattopadhyay A., Walsh J.L., ”Structural Optimization of Rotor Blades with Integrated Dynamics and Aerodynamcis,“ Recent Advances in Multidisciplinary Analysis and Optimization, NASA Conference Publication, Part1, 1989, pp.145-162

[31] Chattopadhyay, A., Walsh, L.W., Riley, F., “Integrated Aerodynamic/Dynamic Optimization of Helicopter rotor Blades,” NASA Technical Memorandum No.101553, 1989

[32] Chattopadhyay A., Chiu Y.D., “An Enhanced Integrated Aerodynamic Load/Dynamic Optimization Procedure for Helicopter Rotor Blades,” NASA Contractor Report No.4326, 1990

[33] Adelman, H. M., Mantay, W.R., “Integrated Multidisciplinary Optimization of Rotorcraft,” NASA Technical Memorandum No. 101642, 1989

[34] Walsh J.L., LaMarsh II, W.J., Adelman, H.M., “Fully Integrated Aerodynamic/Dynamic Optimization of Helicopter Rotor Blades,” NASA Technical Memorandum No. 104226, 1992

[35] Pritchard, J.I., Adelman, H.M., Walsh, J.L., Wilbur, M.L., “Optimization Tuning Masses for Helicopter Rotor Blade Vibration Reduction Including Computed Airloads and Comparison with Test Data,” NASA Technical Memorandum No. 104194, 1992

[36] Lee, J., Hajela, P., “Parallel Genetic Algorithm Implmentation in Multidisciplinary Rotor Blade Design,” AHS Technical Specialists’ Meeting on Rotorcraft Structures, Williamsburg, 1995

[37] Ganguli, R., “Optimum Design of a Helicopter Rotor for Low Vibration Using Aeroelastic Analysis and Response Surface Methods,” Journal of Sound and Vibration Vol. 258, Issue 2,2002, pp,327-344

[38] Bhadra, S., Ganguli, R., “Aeroelastic Optimization of a Helicopter Rotor Using Orthogonal Array Based Metamodels,” AIAA Journal Vol. 44 No. 9, 2006, pp.1941-1951

[39] Murugan, S., Ganguli, R., Harursampath, D., “Robust Aeroelastic Optimization of Composite Helicopter Rotor,” International Conference on Engineering Optimization, Rio De Janerio, 2008

[40] Glaz, B., Geol, T., Liu, L., Friedmann, P.P., Haftka, R. T., “Multiple-Surrogate Approach to Helicopter Rotor Blade Vibration Reduction,” AIAA Journal Vol. 47 No. 1, 2009, pp.271-282

[41] Viswamurthy, S.R., Ganguli, R., “An Optimization Approach to Vibration Reduction in Helicopter Rotors with Multiple Active Trailing Edge Flaps,” Aerospace Science and Technology Vol. 8 Issue 3,2004, pp.185-194

[42] Kvaternik, R.G., Murthy, T.S., “Airframe Structural Dynamic Considerations in Rotor Design Optimization,” NASA Aeroelasticity Handbook Vol.2 Part 2,pp.13.1-13.3

[43] Harrison R., Hansford, B., “BERP IV The Design Development and Testing of an Advanced Rotor Blade”, AHS 64th Forum, Montreal, 2008

[44] Johnson, W., “CAMRAD JA A Comprehensive Analytical Model of Rotorcraft Aerodynamics and Dynamics Volume I: Theory Manual,” Johnson Aeronautics, 1988

[45] Johnson, W., “CAMRAD JA A Comprehensive Analytical Model of Rotorcraft Aerodynamics and Dynamics Volume I: User’s Manual,” Johnson Aeronautics, 1988

[46] Houbolt, J.C., Brooks, G., “Differential Equations of Motion for Combined Flapwise Bending, Chordwise Bending, And Torsion of Twisted Non-Uniform Rotor Blades,” NACA Technical Note No. 3905, 1957

[47] Hodges, D.H., Dowell E.H., “Nonlinear Equations of Motion for the Elastic Bending and Torsion of Twisted Nonuniform Rotor Blades,” NASA Technical Note No. 7818, 1974

[48] Ozturk, D., “Development of a Myklestad’s Rotor Blade Dynamic Analysis code for Application to JANRAD”, MSc Dissertation, Naval Postgraduate School, Monterey California, 2002

[49] Bir, G.S., Chopra, I., Kim, K.C., Wang, J., Smith, E., Vellaichamy, S., Ganguli, R., Nixon, M., Torok, S., “University of Maryland Advanced Rotorcraft Code (UMARC) Theory Manual,” Aero Report No.94-18, University of Maryland-Collage Park, Maryland, 1994

[50] Johnson, W., “CAMRAD II Comprehensive Analytical Model of Rotorcraft Aerodynamics and Dynamics,” Newslatter Issue 14, Johnson Aeronautics, 2008d

[51] Advanced Rotorcraft Technology Inc., http://www.flightlab.com/flightlab.html , last visited on 01 August 2011

[52] Bauchau, O.A., “Dymore User’s Manual,” School of Aerospace Engineering Georgia Institute of Technology, Atlanta, 2007

[53] Johnson, W., “Airloads, Wakes, and Aeroelasticity,” NASA Contractor Report No. 177551, 1990

[54] Onwubolu, G.C., Babu, B.V., “New Optimization Techniques in Engineering,” , Springer, 2004

[55] Rao, S.S. “Engineering Optimization,” John Wiley % Sons, Inc., 1996

[56] Vanderplaats, G.N., “CONMIN – A Fortran Program for Constrained Function Minimization User’s Manual,” NASA Technical Memorandum No. 62282, 1973

[57] CONMIN Source Code, Manual, Sample Problems and License, http://www.eng.buffalo.edu/Research/MODEL/mdo.test.orig/CONMIN/ , last visited on 01 August 2011

[58] Vanderplaats Research & Development Inc., http://www.vrand.com/education.html, last visited on August 2011

[59] Filippone, A., “The Flight Performance of Fixed and Rotary Wing Aircraft,” Elsevier, 2006

[60] Yamauchi, G.K., Heffernan, R.M., “Structural and Aerodynamic Loads and Performance Measurements of an SA 349/2 Helicopter with an Advanced Geometry Rotor,” NASA Technical Memorandum No.88370, 1986

[61] Lau, B.H., Louie, A. W., Griffiths, N., Sotiriou, C.P., “Performance and Rotor Loads Measurements of the Lynx XZ170 Helicopter with Rectangular Blades,” NASA Technical Memorandum 104000, 1993

[62] Seddon, J., “Basic Helicopter Aerodynamics,” BSP Professional Books, 1990

[63] Padfield, G.D., “Helicopter Flight Dynamics,” Blackwell Publishing, 2007

[64] Cugnon, F., Eberhard, A., “Aeroelastic Modeling of the Hub and Blade Rotor System of the Nicetrip Tilt-Rotor Aircraft Using Finite Element Multibody Approach,” Multibody Dynamics 2011 ECCOMAS Thematic Conference, Brussels, 2011

[65] Yamauchi, G.K., Heffernan, R.M., “Hub and Blade Structural Load Measurements of an SA 349/2 Helicopter,” NASA Technical Memorandum No.101040,1988

[66] Endres, G., Gething, M., “Jane’s Aircraft Recognition Guide,” Harper Collins, 2002

[67] Airplane Pictures, http://www.airplane-pictures.net/image50845.html , last visited on 01 August 2011

[68] Renzi, M.J., “An Assessment of Modern Methods for Rotor Track and Balance,” MSc Dissertation, Air Force Institute of Technology, Ohio, 2004

# APPENDIX A

# CAMRAD JA COMPREHENSIVE ANALYSIS

Figure 50 represents the computation tasks and problems solved by CAMRAD JA [44].

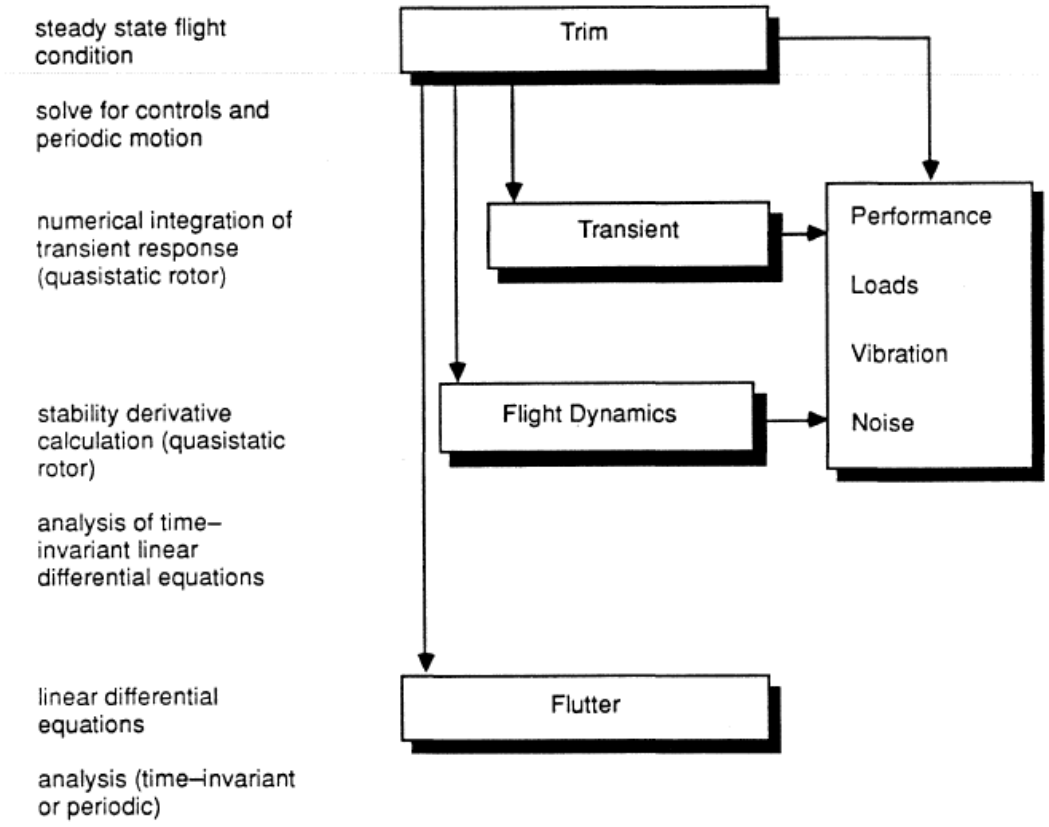


**Figure 50:** CAMRAD JA Computation Scheme

According to the Figure 50, initially the trim analysis is performed and other tasks start from the trimmed structure. Trim analysis refers to calculating periodic rotor motion and finding

the required trim variables. Rotor collective and cyclic control angles, pilot controls and aircraft Euler Angles are trim variables which are defined according to the problem. If trim solution is converged; loads, performance, vibration and noise evaluated can be performed. Trim analysis can only be skipped if the trim variables are exactly known.

CAMRAD JA has the capability of analyzing rotorcrafts that has two rotors or isolated rotor by using above computation scheme. Among the rotorcraft configurations conventional, tandem, tilt-rotor and coaxial rotorcraft can be analyzed.

Trim calculation can be defined as the condition at which the sum of the forces and moments on the fuselage center of gravity is zero. Trim analysis that defines the operation state of rotorcraft or isolated rotor. Operation state refers to the required values of rotor control angles, pilot controls and aircraft Euler Angles for the prescribed flight condition. The flight condition and trim variables are selected according to the complexity or the assumptions related to the problem.

Comprehensive analysis is strictly dependent on operating conditions. Flight speed, rotor angular speed, aerodynamic environment and ground interaction are input parameters which define operation condition. These parameters are followed by aircraft description. Number of rotors distinguishes isolated rotor analysis from helicopter analysis. The engine state defines the operation which can be normal operation, autorotation and no engine analysis. Helicopter motion calculations depend on degrees of freedom and provided as modes. There are 10 bending, 5 torsion and 1 gimbal for rotors, 6 rigid and 30 elastic for fuselage and 6 for drive train. When a mode is zero its contribution to motion is excluded from calculations.

Bending modes of blade include coupled flapwise and edgewise bending. Modes can be calculated by CAMRAD or mode shapes with natural frequencies can be explicitly provided. First torsion mode comes from control link flexibility and the rest comes from elastic blade. There is an extra degree of freedom at hub for gimbaled rotors which are common in two-bladed rotors and tilt-rotors. Six rigid fuselage modes can be implicitly included in trim analysis whereas elastic modes must be supplied for fuselage vibrational response analysis.

Trim analysis can be performed for a two rotor configuration or an isolated rotor. Trim variables are the setting that is necessary to achieve a trimmed flight. The analysis starts from the initial trim variables and iterates the analysis until the motion and loads converges within a prescribed tolerance based on prescribed target. A two rotor configuration can be analyzed in free flight meaning that the helicopter is free from any supports. Analysis capacity allows six degree of freedom motion. For the prescribed description and flight condition, trimmed flight can be achieved by main rotor collective and cyclic angles, tail rotor collective angle and Aircraft Euler angles. Some of these can be eliminated if the flight is known to be symmetric. For the isolated rotor case, wind tunnel trim analyses are performed. In this case since there is no fuselage with weight and inertia, targets should be defined which include lift, drag, thrust and tip path plane angles.

The rotor description includes configuration, rotor blade connection model and blade structural dynamic properties and aerodynamic parameters. Rotor configuration includes fundamental features of the rotor such as number of blades, rotor angular speed, blade hinge offsets. All the blades are assumed to be identical and equally spaced.

Aerodynamic model consists of characteristics of aerodynamic surfaces and the model parameters. The aerodynamic surfaces are the rotor blades and they are characterized by airfoil distribution, airfoil lift, drag, moment coefficients, root cut-out and blade section characteristics. Chord length, twist, aerodynamic center, sweep angle distributions over blade are considered as blade section characteristics. Aerodynamic model parameters include Mach number and Reynolds number corrections, inflow type and wake properties and stall model. Besides compressibility effects, aerodynamic stall and vortex loads are included in CAMRAD which have significant effects on vibratory loads depending on the rotor configuration and flight conditions.

Dynamic model of the rotor models the motion of hub. The most important parameter is the blade hub connection. CAMRAD can apply hinged and cantilever connections which can model articulated, hingeless, teetering and gimballed rotors. Single load path is assumed and structures with multiple load paths like bearingless rotors cannot be modeled. Other dynamic parameters include spring and damper constants, hinge offsets, pitch-bending coupling angles and control system stiffness values.

Blade is defined by inertial and structural parameters which include distributions of mass, flapwise bending stiffness, edgewise bending stiffness, torsional stiffness, offsets of center of gravity and tension center, polar radius of gyration and moment of inertia about elastic axis. For load analysis the most significant parameters are mass and stiffness distribution whereas others have minor contribution to loads. Structural damping of blades in bending and torsion modes can be included in the analysis. CAMRAD uses these parameters in calculating the rotating blade modes therefore mode shape and natural frequencies of the blades can also be provided explicitly.

Load calculation involves airframe vibratory response, rotor aerodynamic loads, blade section aerodynamic loads, hub and control loads and blade section loads. Throughout this thesis, hub loads analyses were performed. For the rotor, there are three force and 3 moment components which can be calculated at rotating and non-rotating frames. Rotating frame loads are evaluated at prescribed blade sections and all load harmonics exist. The integration of rotating frame loads for all blades gives the non-rotating frame loads. In this case only N/rev frequency loads are transferred to non-rotating frame because other frequencies are canceled. As it was previously discussed in Section 2.2.2, the frequencies at (N+1)/rev, N/rev, (N-1)/rev rotating fame loads are transferred as N/rev non rotating load. Therefore for a vibratory load analysis the number of harmonic should be defined at least N+1 in order to see all the blade load comports at the rotor hub.